

IO, AN ALFVEN-WAVE GENERATOR

by

Edward J. Schmahl

B.S. University of Santa Clara, 1963

M.A. University of Illinois, 1965

A thesis submitted to the Faculty of the Graduate School  
of the University of Colorado in partial fulfillment  
of the requirements for the degree of

Doctor of Philosophy

Department of Astro-Geophysics

1970

This Thesis for the Doctor of Philosophy Degree by  
Edward J. Schmahl  
has been approved for the  
Department of  
Astro-Geophysics  
by

*James W. Warwick*

---

James W. Warwick

*Edward R. Benton*

---

Edward R. Benton

Date July 28, 1970

Schmahl, Edward Joseph (Ph.D., Astro-Geophysics)

Io, an Alfven-Wave Generator

Thesis directed by Professor J. W. Warwick

Io, the nearest of Jupiter's four large satellites, controls the emission probability of about half of Jupiter's decametric radiation. Io can excite hydromagnetic waves and/or particle streams in various ways. One of the most efficient of these mechanisms is the dipole radiation of Alfven waves. Induction effects cause Io to have a sizeable dipole moment. Its magnitude and direction depend on Io's core conductivity and the amplitude of variation of Jupiter's magnetic field as seen by Io. A reasonable estimate of this moment is  $10^{22}$  gauss  $\text{cm}^3$ . A low frequency solution of Maxwell's equations coupled to the linearized Vlasov equation indicates that shear Alfven waves will be radiated with a power on the order of  $8 \times 10^9$  watts. It is suggested that these waves, which are largely unattenuated, are the means of interaction between Io and the ionosphere of Jupiter.

This abstract is approved as to form and content. I recommend its publication.

Signed James W. Warwick  
Faculty member in charge of dissertation

## ACKNOWLEDGEMENTS

The ever-patient advice of Drs. George Dulk and Jim Warwick has guided my efforts for the past three years in learning about Jupiter's radiation and in writing this thesis. I am very grateful to them for their help. Drs. Ted Speiser and Peter Gilman have given very useful counseling in the development of my ideas on the Io-effect. Dr. Ed Walbridge has cheerfully spent many hours of his time discussing the physics of this and related problems with me, as well as asking many thought-provoking questions. I thank all these men for serving on my thesis committee; I am also grateful to Dr. Keith MacLane for serving on the committee on such short notice. I thank Dr. Dick Aamodt for his help in the early stages of preparing this thesis. Without his assistance I might have wandered down many a blind alley before finding the right track. I wish to thank the many others who contributed useful ideas and productive discussions, particularly Joseph Blank, Joe Romig, and Daniel Vasicek.

I heartfully thank Barbara Villarreal for her careful and uncomplaining typing of the first draft, despite many last-minute alterations of heiroglyphic-like symbol arrays. I especially thank Susan Haxo for her encouragement and for her meticulous preparation of graphs and figure captions.

## TABLE OF CONTENTS

### CHAPTER I INTRODUCTION

1.1	Decametric Emission	1
1.2	The Io Effect	2
1.3	The Other Satellites	4
1.4	Source Size	5
1.5	Io-Effect Theories	6

### CHAPTER II JUPITER'S MAGNETOSPHERE

2.1	Magnetic Field Properties from DIM	8
2.2	Magnetic Field Properties from DAM	11
2.3	Extent of the Magnetosphere	12
2.4	Co-Rotation	14
2.5	Plasma Density	16
2.6	Plasma Temperature	19

### CHAPTER III THE MINIMUM HYPOTHESIS AND THE ASSUMED PARAMETERS

3.1	A Moon-Like Io	21
3.2	Assumed Properties of the Magnetosphere	22
3.3	Available Energy	23
3.4	Nonlinear vs Linear	24

CHAPTER IV  
IO AS AN ELECTROMAGNETIC SOURCE

4.1	Io's Wake	26
4.2	Moments of the Source	28
4.3	The Mathematics of Dipole Sources	33

CHAPTER V  
EQUATIONS DESCRIBING A COLLISIONLESS,  
MAGNETOACTIVE PLASMA

5.1	The Collisionless Regime	36
5.2	Equations for a Collisionless Plasma	38
5.3	Formal Solution	42
5.4	The Hydromagnetic Modes	44
5.5	The Alfvén Wave Fields	46

CHAPTER VI  
GENERATION OF SHEAR ALFVÉN WAVES

6.1	The Wave Equation	48
6.2	Waves from a Finite Source	50
6.3	Energy Flux	52

CHAPTER VII  
AN INDUCED DIPOLE MOMENT IN IO

7.1	Large-Source Effects	57
7.2	Magnetic Field Seen by Io	57
7.3	Induction Effects in Io	60
7.4	Application to Io	62

CHAPTER VIII  
TRANSPORT ALONG FIELD LINES

8.1	Damping of High Wavenumbers	65
8.2	Field Curvature	68
8.3	Density Effects	70
8.4	Rotational Effects	71

CHAPTER IX  
DISCUSSION

9.1	Alfven Waves into Electromagnetic Waves	74
9.2	Model-Testing and Observations	75
9.3	Limitations of the Model	79
9.4	Other Satellite Effects?	82
9.5	Conclusions	84

APPENDICES

I.	The Dielectric Tensor for a Magnetoactive Plasma	93
II	Inversion of the Wave Operator	100
III	Fried and Gould Modes	102
IV	Shear Alfven Mode in the Frequency Domain	105
V	Shear Alfven Mode in Time and Space	108
VI	Conversion from Infinitesimal to Finite Sources	111
VII	Power Transported by the Shear Alfven Waves	113
VIII	Magnetic Field of a Tilted, Displaced Dipole	119
IX	Critical Frequency for Alfven Waves in a Curved Field	123

## LIST OF TABLES AND FIGURES

	<u>Page</u>
TABLE I Masses, radii, periods, and orbital radii of the Galilean satellites.	4a
TABLE II Properties of earth's moon and Io.	21a
FIGURE 1 Radio spectrum of Jupiter from 3 to $10^5$ MHz. (Carr and Gulkis, 1969 and Dickel et al., 1970.)	1a
FIGURE 2 Probability of DAM emission as a function of Jupiter's central meridian longitude for the years 1961-1968. (Warwick and Dulk, 1968.)	2a
FIGURE 3 Probability of DAM emission as a function of Io's orbital position. (Warwick and Dulk, 1968.)	3a
FIGURE 4 Joint probability of DAM emission as a function of both Io's orbital position and Jupiter's central meridian longitude. (Warwick and Dulk, 1968.)	3b
FIGURE 5 Two models of magnetization density and associated induction currents in the core of Io.	54a
FIGURE 6 Contours of constant peak Alfven power from Io for a range of field strength and electron density in Io's vicinity. The downturns and upturns of the curves are due, respectively, to the Alfven speed approaching the speed of light and the speed of Io.	56a
FIGURE 7 The ratio of the induced to the inducing field for core conductivities from $10^{-4}$ to $10^2$ mho/m. This figure was taken from Sill and Blank (1969) with the horizontal axis altered to show explicit values of conductivity. Io's core radius was set equal to 1700 km and the period of the inducing field was taken to be 6 hours.	61a
FIGURE 8 Comparison curves of radiated Alfven power for different positions of Jupiter's tilted dipole along the rotation axis. The power peaks strongly when Jupiter's north pole tilts toward Io if the dipole displacement is southward.	63a

## CHAPTER I INTRODUCTION

### 1.1 DECAMETRIC EMISSION

The planet Jupiter is a strong source of radio waves at frequencies below 40 MHz. Burke and Franklin (1955) discovered this decametric (DAM) emission at 22 MHz while testing the Carnegie Mills Cross array in early 1955. Study of Sydney records (Shain, 1956) showed that radio bursts from Jupiter had been recorded but not recognized as early as 1950. The DAM radiation has a flux density as high as and higher than a million flux units (one f.u. =  $10^{-26}$  watt  $m^{-2}$   $Hz^{-1}$ ) and is therefore much more easily observed than the thermal radiation at centimeter wavelengths discovered by Mayer et al. (1958) or the non-thermal, decimetric (DIM) radiation discovered by Sloanaker (1959). Figure 1, a composite of figures from the excellent review article on Jupiter's magnetosphere by Carr and Gulkis, (1969), and the review of Jupiter's microwave spectrum by Dickel et al (1970), gives the flux density of Jupiter's radio emission as a function of wavelength.

Shain (1956) first showed the dependence of the DAM emission probability on Jupiter's central meridian longitude (CML), and later results indicated that there were at least three distinct sources. (Carr and Gulkis call these A, B, and C; Douglas (1964) calls them 2, 1, and 3,

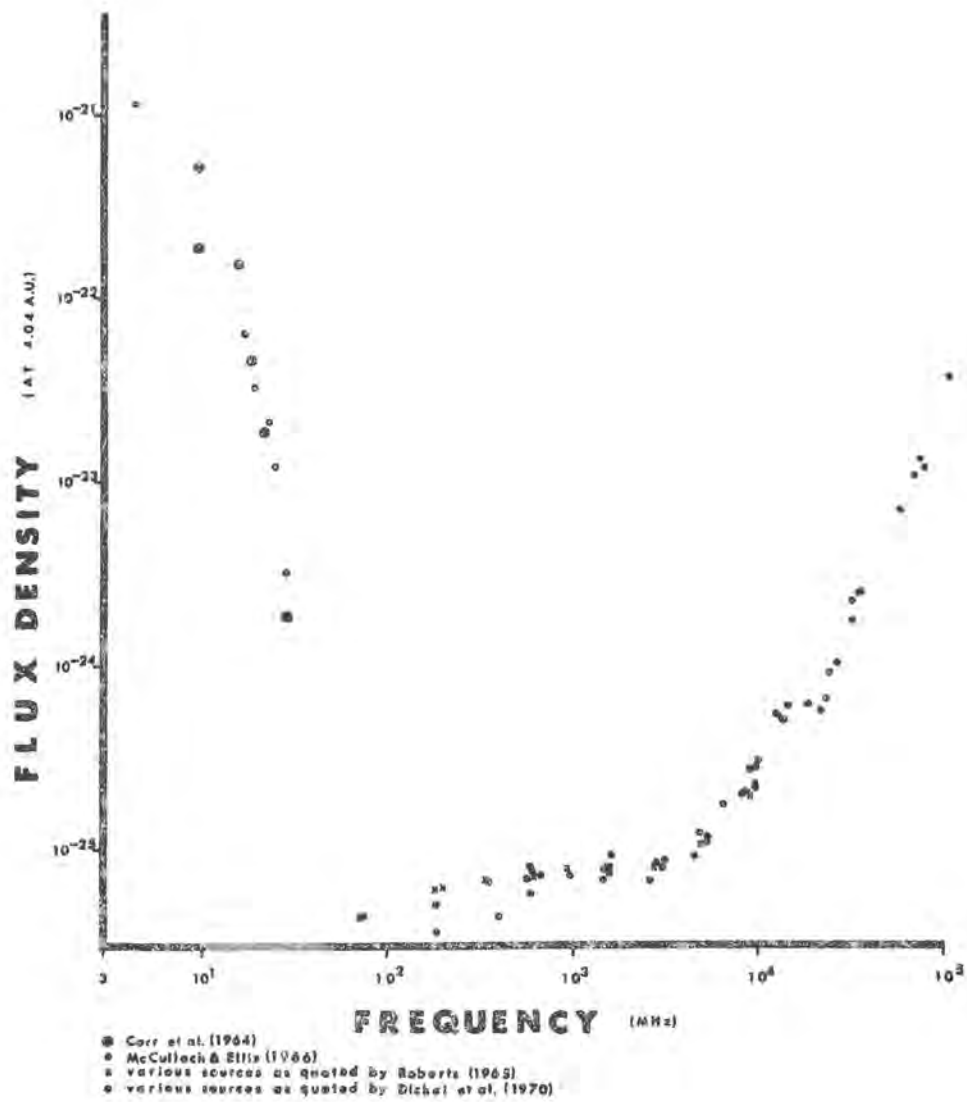


Figure 1

Radio spectrum of Jupiter in the frequency range 3 to  $10^5$  MHz. This is a composite of figures from Carr and Gulkis, 1969 and Dickel et al., 1970.

respectively, and Dulk (1965a, b) labels them as main, early, and third.) Figure 2 (Warwick and Dulk, 1968) shows the modulation of DAM radiation by the rotation of Jupiter in the years 1960 to 1964. Warwick (1963) describes a fourth source which does not appear in this Figure.

Franklin and Burke (1955) first demonstrated that the radio emission was elliptically polarized, suggesting that Jupiter had a magnetic field. This polarization is predominantly right-handed for all longitudes at frequencies greater than 18 MHz (Barrow, 1964a, Sherrill 1965). Warwick and Dulk (1964) showed that the orientation of the major axis of the polarization ellipse may be perpendicular to Jupiter's axis of rotation.

Some of the foregoing characteristics lead to surmises concerning Jupiter's magnetic field and magnetosphere. The properties of Jupiter's field and its environment will be discussed in Chapter II. Several review articles discuss the radiation from Jupiter in great detail: Douglas (1964), Ellis (1965), Warwick (1967), and Carr and Gulkis (1969).

## 1.2 THE IO-EFFECT

Nearly a decade of Jupiter radio observations passed before E. K. Bigg (1964) discovered the strong correlation between DAM radiation and the position of Io, the nearest of the four Galilean satellites. The effect

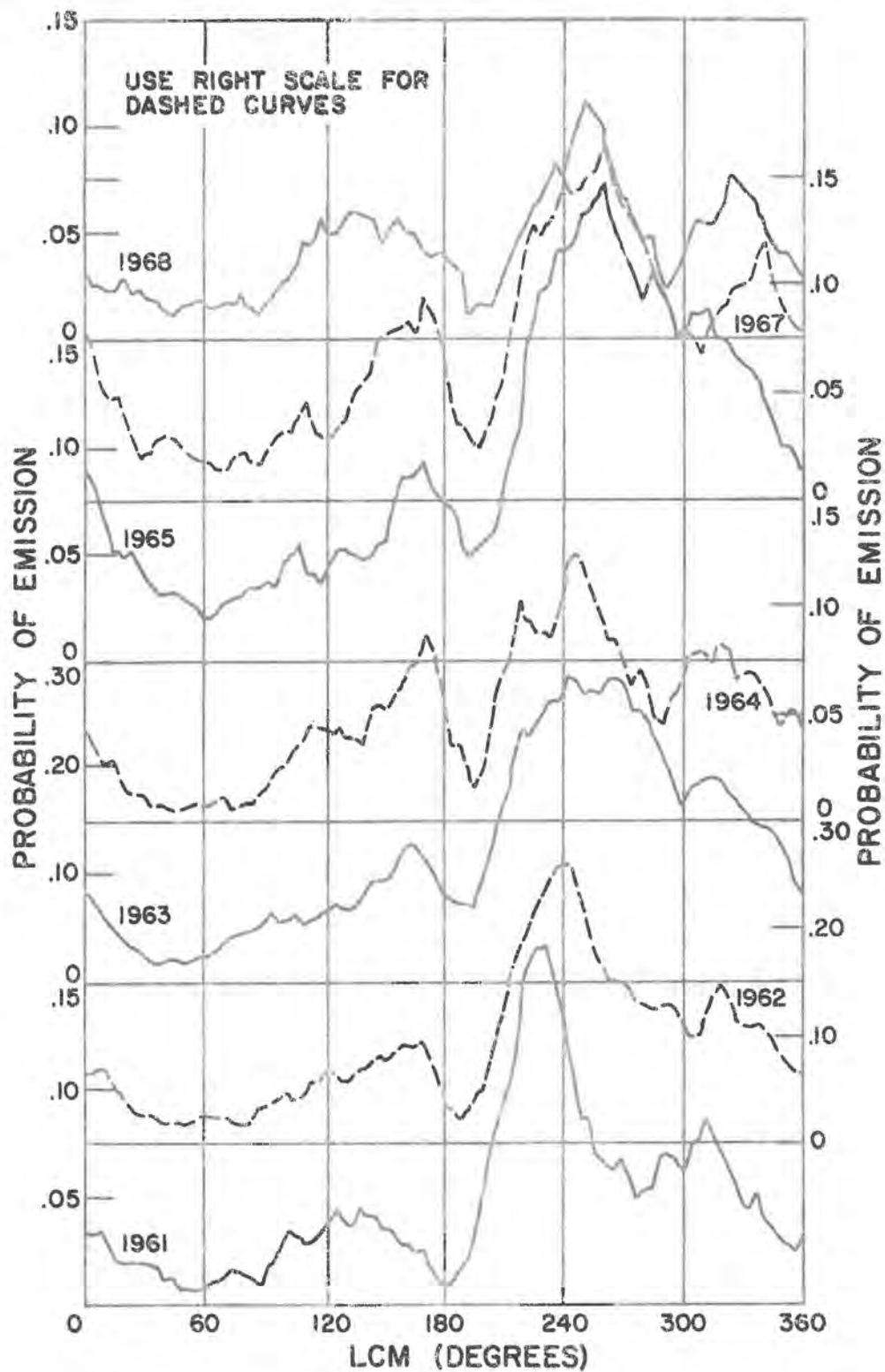


Figure 2

Probability of DAM emission for the years 1961-1968 plotted against the longitude of Jupiter's central meridian. (Warwick and Dulk, 1968)

of the control which Io exerts on the radio emission is illustrated by Figure 3 (Warwick and Dulk, 1968) in which strength of the DAM radio emission is plotted against departure of Io from superior geocentric conjunction (hereafter designated by  $\phi_{Io}$ ). All frequencies in Warwick's catalogue for the years 1961-1963 were included in this plot, but if only frequencies above 30 MHz are included, the control is even more striking. George Dulk continued the analysis of the Io-control, and came to several conclusions, (Dulk, 1965a):

1. Io induces nearly 50 percent of Jupiter's radio emission.
2. The emission probability approaches 1.0 when Io's position and Jupiter's longitude are simultaneously favorable.
3. Io induces early source and fourth source emission when  $\phi_{Io} \approx 90^\circ$  and it enhances the main source and third source probability when  $\phi_{Io} \approx 240^\circ$ .
4. The spectral character of many radio events is determined not only by Jupiter's LCM but also Io's position.

Figure 4 shows the dual modulation of DAM emission by Jupiter's rotation and Io's orbital motion. Contours of equal probability of emission are plotted against  $\phi_{Io}$  and Jupiter's LCM.

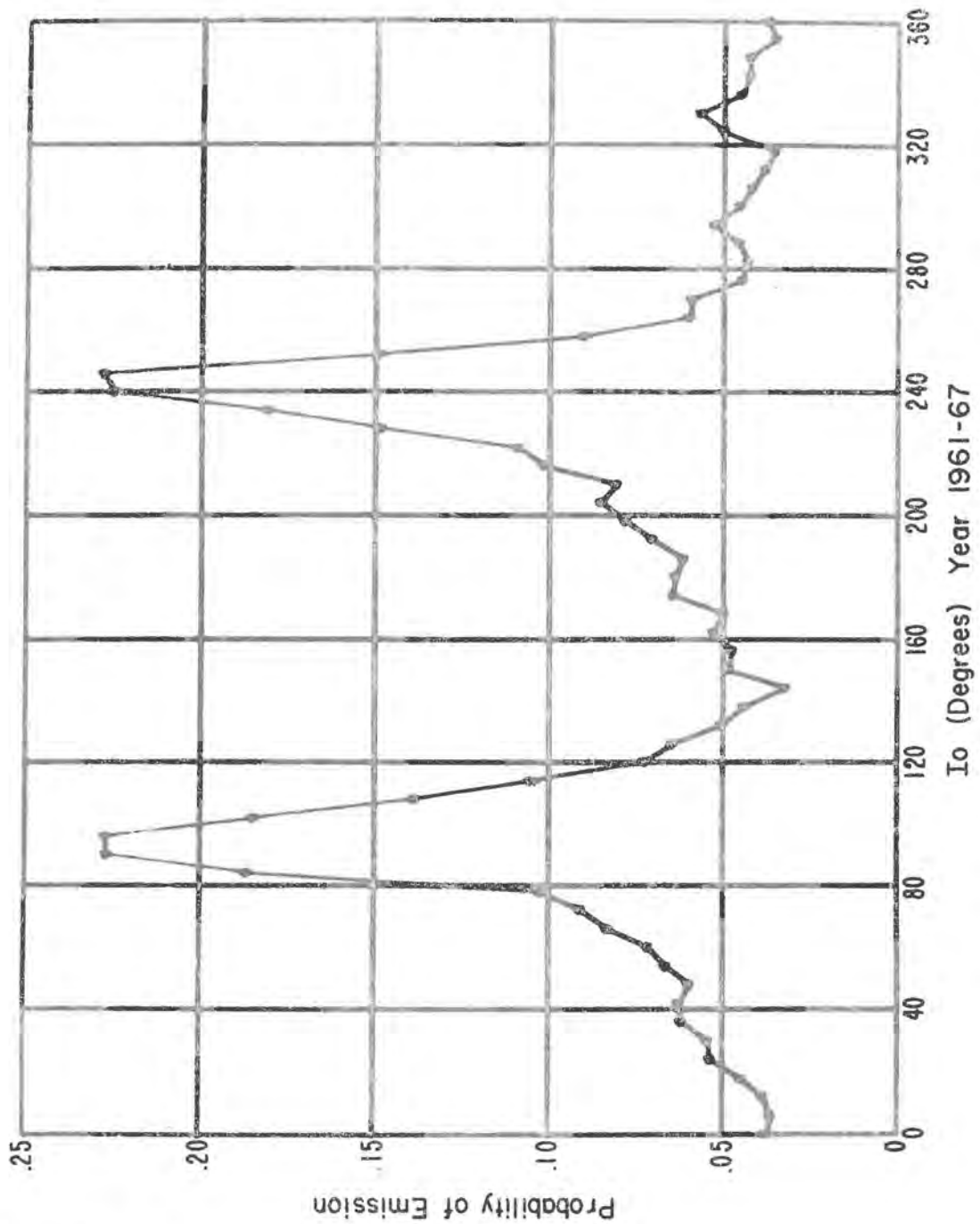


Figure 3

Probability of DAM emission plotted against departure of Io from geocentric conjunction. The data of the University of Colorado radio telescope for the years 1961-67 were used in this diagram. This is very similar to the figure Bigg (1964) used to support his discovery of the Io control. (Warwick and Dulk, 1968)

Io, LCM PROBABILITY CONTOUR MAP FOR COMBINED  
DATA OF 1961-68, CONTOUR INTERVAL .10

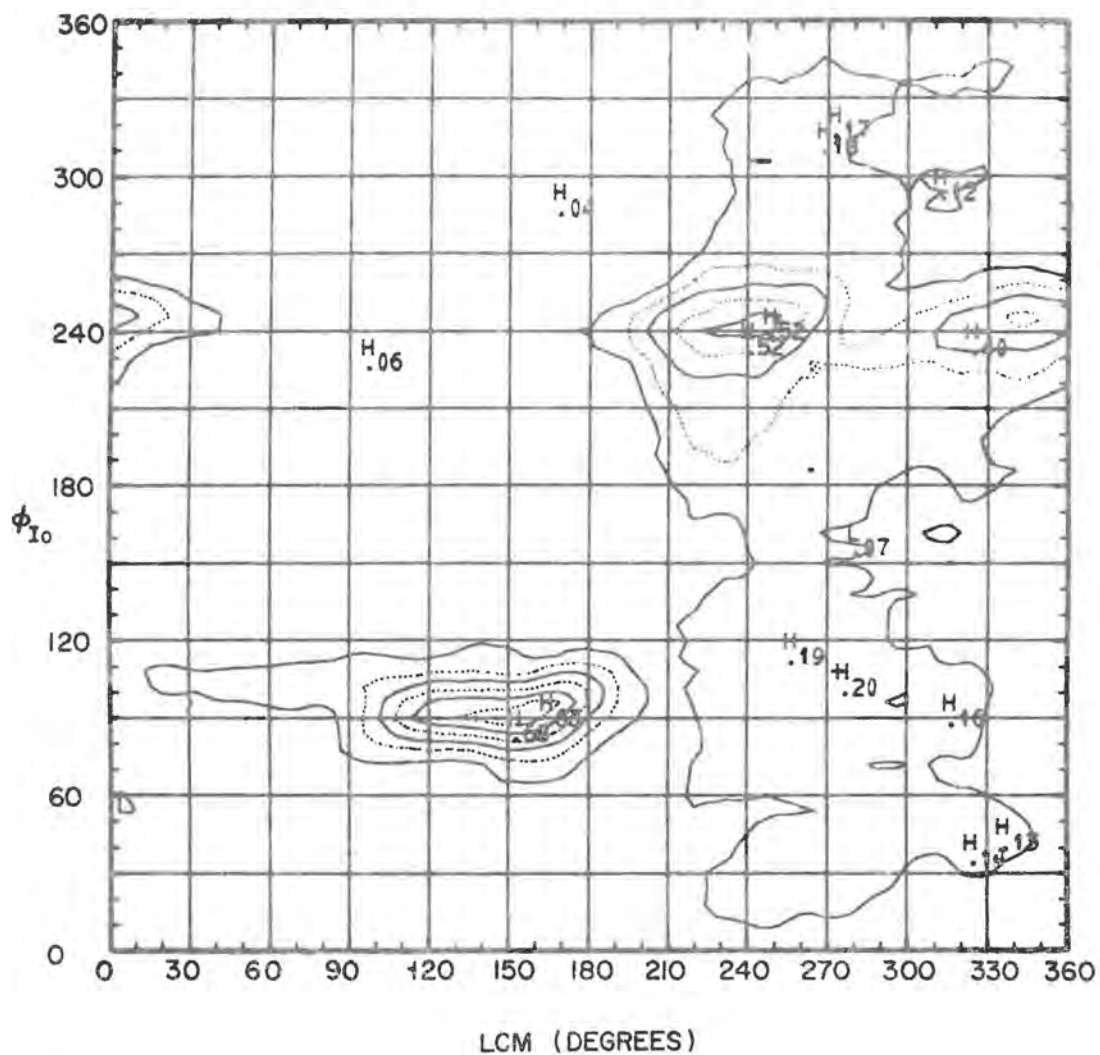


Figure 4

Contours of equal probability of DAM emission plotted against  $\phi_{Io}$  (the departure of Io from geocentric conjunction) and LCM (the longitude of Jupiter's central meridian). (Warwick and Dulk, 1968)

### 1.3 THE OTHER SATELLITES

Io is about the size of earth's moon. Its apparent angular diameter at opposition is about 0.9 seconds of arc, so estimates of its true diameter are severely limited by seeing conditions. Koylovskaja (1963) has tabulated 28 measurements of the diameters of the Galilean satellites made between 1827 and 1954. (The weighted mean diameter for Io is 3470 km. This could easily be off by  $\pm 100$  km.) The other satellites have comparable sizes, but their distances are greater (see Table I).

The orbital periods of the Galilean satellites are roughly in the ratios 1:2:4:8, so that several years of radio records are necessary to determine whether Europa, Callisto, and Ganymede cause effects like that of Io. In addition to these approximate resonances, there is an important resonance which is exact on a time-average. It is expressed parametrically by J. Kovalevsky (1967) in terms of the longitudes  $L_1$ ,  $L_2$ ,  $L_3$  of the inner Galilean satellites:

$$L_1 = (4-k)t$$

$$L_2 = (2-k)t + 180^\circ$$

$$L_3 = (1-k)t$$

The quantity  $k = d(L_2 - L_3)/dt$ .

This resonance was discovered by Laplace (1805). Callisto causes perturbations on this relationship (Brouwer and Clemence 1961), and the periodic variations from the zero-order system are described by de Sitter (1931) in

TABLE I

Satellite	Radius (km)*	Mass ( $\times 10^{-5} M_J$ )**	Mass ( $\times 10^{25} g$ )***	Orbital Radius ( $\times 10^3$ Km)	Sidereal Period (days)
Io	1735 $\pm$ 25	2.60 4.497 3.80 3.81	7.22	421.8	1.77
Europa	1550 $\pm$ 30	2.31 2.536 2.54 2.48	4.70	671.4	3.55
Ganymede	2500 $\pm$ 38	8.04 7.988 8.20 8.17	15.5	1,071	7.15
Callisto	2350 $\pm$ 38	4.248 4.504 4.52 5.09	9.62	1,884	16.69

\*Kozlovskaya (1963): weighted mean of 28 measurements between 1824 and 1954.

\*\*Kozlovskaya (1963): four determinations by Sampson and deSitter.

\*\*\*Brouwer and Clemence (1961).

his theory for the motions and mass determinations of the Galilean satellites (Marsden, 1966). Unfortunately such calculations serve only imprecisely to determine Io's mass, which may lie somewhere in the range  $2.6$  to  $3.8 \times 10^{-5}$  the mass of Jupiter (see Table I). According to Marsden (1966), this uncertainty could have been lowered had careful observations of the satellite positions been made after de Sitter's last study in 1931. In any case, the mass, radius, and density of Io are roughly comparable to the mass, radius, and density of earth's moon.

Searches have been made for DAM effects caused by other satellites. When careful account is taken of the near commensurability of the satellite periods, only Io proves to have a direct association with DAM radiation. (Lebo, et al., 1965a; Duncan, 1966; Dulk, 1965a; Warwick and Dulk, 1966; Wilson, et al. 1968).

#### 1.4 SOURCE SIZE

The dimensions of the region which gives rise to the Io-related DAM emission can be estimated, in principle, by radio interferometry. As Dulk (1970) points out, neither phase nor intensity interferometry alone will determine the size of a coherent source, but a time history analysis of interferometric records will give the size of the lobe produced by such a source, and therefore the source size. Interferometry will, on the other hand, determine the size of a totally incoherent source

either by fringe visibility or intensity correlations. Even the size of an incoherent source which is jumping from place to place can be found by intensity interferometry. (The jumping causes only phase variations and does not affect intensity.)

On the basis of radio interferometry on a baseline between Boulder and Arecibo (487,000 wavelengths apart) and also between Boulder and Clark Lake, California (120,000 wavelengths apart), Dulk (1970) concludes that an incoherent source must be less than 400 km in size and a coherent source must be less than 4000 km in size. These correspond to 1/180 and 1/18 of Jupiter's diameter, respectively.

If the source were incoherent, individual particles would have to have energies greater than  $10^{13}$  ev (Warwick 1967). Furthermore, the apparent beaming of the radiation, either in narrow cones (Warwick 1963a) or thin sheets (Dulk 1967), suggests a coherent mechanism. So the source is probably coherent, and its smallness suggests that Io excites a small region of Jupiter's ionosphere or magnetosphere to radiate.

#### 1.5 IO-EFFECT THEORIES

It is remarkable that such a relatively small body as Io could influence the environment of its parent planet so strongly as it does. Nonetheless it does, and so theories of the Io-Jupiter interaction have proliferated. All of the theories invoke the magnetic field in

one way or another as part of the means of generation of waves or currents which propagate from Io down toward Jupiter. J. D. G. Rather and J. M. Witting (unpublished, reported by Warwick, 1967) and Witting (1966) suggested satellite sweeping of trapped particles. Warwick (1967) argued that a finitely conducting satellite should thrust field lines aside, generating Alfvén waves. Marshall and Libby (1967) suggested the stimulation of MHD waves by a plasma wake following Io. J. A. Burns (1968) considered trapping of charged particles around a magnetic or highly permeable satellite. Piddington and Drake (1968) suggested that the conducting interior of Io would trap its local flux tube, dragging it behind the other field lines co-rotating with Jupiter. Goldreich and Lynden-Bell (1969) argued similarly, saying that Io would act as a unipolar generator, driving currents into the ionosphere of Jupiter along the magnetic field lines. Dulk (1965a) suggested that a magnetic wake with a neutral point might form behind Io, in which particles could be accelerated. Ellis (1965) discussed the possible Cerenkov generation of an Alfvén wave by super-Alfvénic motion of Io.

It is the purpose of this thesis to give a general mathematical formulation of some ways in which a satellite can excite hydromagnetic waves in its vicinity. Most of the foregoing theories can be categorized within this formulation. A new mechanism for generating hydromagnetic waves will be discussed and calculated in detail.

CHAPTER II  
JUPITER'S MAGNETOSPHERE

A variety of techniques can be used to infer the properties of the magnetosphere of Jupiter. Since a knowledge of the medium through which the Galilean satellites travel is essential to any theory of their interaction with their parent planet, a brief summary of some of the derived parameters of Jupiter's environment is in order.

2.1 MAGNETIC FIELD PROPERTIES FROM DIM

Roberts and Komesaroff (1965) demonstrated that a knowledge of the pitch angle distribution of the synchrotron radiating electrons in Jupiter's Van Allen belts plus a good measurement of the degree of circular polarization would, in principle, yield an unequivocal value for the magnetic field of the belts. Unfortunately the pitch angle distributions are unknown, and the polarization is poorly known, so the value of this method is limited. Nonetheless, Berge (1966) estimated that the field of the belts was on the order of 0.1 to 1 gauss. Legg and Westfold (1968) say this may be an overestimate.

The time  $T$  for an ultrarelativistic electron to radiate half its energy is given by Ginzberg and Syrovatskii (1965). According to Carr and Gulbis (1969),

$$T = \text{const} \times B^{-3/2} v_m^{-1/2}, \quad (2.1)$$

where  $B$  is the belt field strength and  $\nu_m$  is the frequency of maximum synchrotron intensity. The time over which appreciable variations occur cannot be smaller than  $T$ , and in fact the DIM variations are small over a period of at least three years (Komesaroff and McCulloch 1967). Thus either  $T > 3$  years or the source of the synchrotron-radiating electrons is constant in time. According to Carr and Gulkis  $T = 0.7$  yr. when  $B = 1$  gauss. Thus lifetime effects do not place stringent limits on the magnetic field strength. However if  $B$  is extremely high, no conceivable source of electrons could maintain the synchrotron emission.

The peak frequency  $\nu_m$  of synchrotron emission depends on the electron energy  $E$  and the belt magnetic field  $B$ . If  $\nu_m = 850$  MHz Carr and Gulkis (1969) show that

$$BE^2 \approx 4 \times 10^{-11} \text{ cm}^{-3} \text{ gauss erg}^2. \quad (2.2)$$

Equations 2.1 and 2.2 do not determine the field or particle energy, but if the requirement of stable trapping is given, a lower limit on  $B$  and upper limits on  $E$  and  $N_e$  can be derived. Ginzburg and Syrovatskii (1969) show that the diamagnetic effect of ultrarelativistic electrons will be small only if

$$EN \ll 6 B^2/8\pi. \quad (2.3)$$

Equations 2.1, 2.2, and 2.3 can be combined to yield the inequalities:

$$B \gg 5 \times 10^{-4} \text{ Gauss}, E \ll 600 \text{ Mev}, N \ll 9 \times 10^{-5} \text{ cm}^{-3}$$

Again, the limit on the field is not strong. However for more reasonable energies like 20 Mev (and corresponding density of  $3 \times 10^{-6}$ ), the first equation yields a field of 0.5 gauss in the belts. This would imply an equatorial surface field of 4 gauss, assuming that the belts maximize at two Jupiter radii from the center.

Spatial information on DIM radio brightness has been obtained by Roberts (1965), Roberts and Komesaroff (1965), Barber (1966), Branson (1968). Asymmetries in the data have suggested (Warwick, 1964) that the magnetic field of Jupiter is not centered, but displaced along its axis such that the surface field is stronger in the southern hemisphere. The field may be nearly axisymmetric (Warwick 1967) and is almost dipolar. Branson's (1968) contours of constant DIM radio brightness may suggest a small displacement of Jupiter's dipole in the geomagnetic equatorial plane. Roberts and Ekers (1966) claim to have shown that the centroid of DIM emission lies within  $\pm 0.3$  radius in declination and  $\pm 0.1$  radius in right ascension.

Morris and Berge (1962) discovered that the polarization is nearly linear and rocks  $\approx 10^\circ$  with respect to the equatorial plane of Jupiter. Roberts and Komesaroff (1965) confirm this, and it is easily seen in Branson's data. Their interpretation is that Jupiter's magnetic moment is inclined at  $10.0^\circ \pm 0.3^\circ$  (Roberts and Komesaroff, 1965) to the rotation axis. The longitude of the pole in the northern hemisphere is near  $\lambda_{III} 200^\circ$

(with an uncertainty of  $\approx 5^\circ$ ; Roberts and Ekers 1968). Warwick (1967) points out that this analysis accounts only for the first harmonic of the data, where the fundamental frequency is that of Jupiter's rotation. The amplitude of the second harmonic is about 20 percent that of the first. Warwick (1964a) suggested that vignetting by the planet could produce the second harmonic term, but vignetting may be insufficient (Warwick 1967). Roberts and Komesaroff offer only the suggestion of asymmetries for the second term, but strangely enough, re-analysis of Roberts (1965) data by Warwick (1967) suggests that the field is axisymmetric. The problem remains unresolved.

Berge (1965) found a small degree of left-hand circular polarization when the pole in the northern hemisphere is tilted toward earth. This indicates that the magnetic moment of Jupiter is directed from south to north, just the opposite of earth's moment. Earlier, Warwick (1963b) concluded the same in a theory of DAM emission.

## 2.2 MAGNETIC FIELD PROPERTIES FROM DAM

The decametric emission from Jupiter is less well understood than the decimetric radiation. The source of the emission is as yet unsettled, but it is very probably close to the planet, either in the ionosphere or just above it. Warwick (1963a, 1967) argues that the narrowband dynamic spectral features of DAM emission could not occur

repeatedly and precisely at the same longitudes unless the source regions are connected to the planet. Warwick also argued that the stability of the dynamic spectrum strongly suggests that emission is at or near the electron gyrofrequency. If this is so, then the peak DAM frequency of 39.5 MHz probably originates in a source region of field strength having the corresponding gyrofrequency. This field strength would be 14 gauss.

Warwick and Gordon (1965a) found that the "Y-one" Faraday effect occurred infrequently in their DAM records, but on one occasion they obtained a measure of the field strength equal to 14 gauss. This effect involves the interference of the two base modes, producing alternating circular polarization at the gyrofrequency. (See also Gordon and Warwick, 1967, and Gordon 1966).

### 2.3 EXTENT OF THE MAGNETOSPHERE

If we assume a field strength  $B_0$  equal to 10 gauss at the equatorial surface of Jupiter and assume a dipole field, the distance to the sunward surface of the zenomagnetic cavity can be calculated. McDonough and Brice (1970) assert that the termination of the solar wind (where interstellar gas pressure balances solar wind pressure) is at a distance on the order of 100 A.U., and therefore beyond Jupiter. At a point where the magnetic field of Jupiter is small enough that magnetic pressure equals the solar wind pressure, the zenomagnetic cavity will end.

The distance  $R_C$  to this point (in the sunward direction) is given by:

$$R_C = R_J \left( \frac{2 B_o^2}{4\pi N m V^2} \right)^{1/6},$$

where  $N$  is the solar wind number density,  $m$  is the proton mass,  $V$  is the solar wind velocity, and  $R_J$  is Jupiter's equatorial radius. Brice and Ioannidis (1970) take  $N = 0.26 \text{ cm}^{-3}$  and  $V = 400 \text{ km/s}$ , yielding  $R_C = 53 R_J$ . (If  $B_o$  is 1 gauss,  $R_C$  is about half this value.) Thus the magnetosphere includes all of the Galilean satellites.

The shape of the magnetosphere is independent of solar wind pressure in Williams' and Mead's model (1965). One would expect that the shape of earth's and Jupiter's magnetospheres are about the same. Brice and Ioannidis estimate the effect of convection patterns in the zero-magnetic cavity. If the internal field lines co-rotate with Jupiter, their motion is very rapid near the boundary of the magnetosphere; their velocity near the magnetopause would be 640 km/s (for  $R_C = 53 R_J$ ). The co-rotation electric fields then would be about 4 volt/km. Brice and Ioannidis use both Axford's (1964) model and the Dungey-Petschek (Petschek 1966, Dungey 1961) model to calculate the expected convective electric fields, which turn out to be about 0.1 volt/km and 0.2 volt/km, respectively. Since these values are small compared to the co-rotation field values, the convection patterns are restricted to the vicinity of Jupiter's magnetopause,

and a few radii inside, the fields are largely unaffected by boundary effects.

#### 2.4 CO-ROTATION

The magnetosphere of Jupiter should co-rotate with the planet provided that its density is neither too high nor too low. Gledhill (1967) has given a discussion of this problem. If the ionosphere of Jupiter is a good conductor, the field lines passing through it will be "frozen in." Now if the field lines are perfect conductors, the electric field along them must vanish. The electrostatic potential  $\phi$  is determined by these two conditions. The first condition gives the gradient of  $\phi$  at the ionosphere, since

$$\bar{E} = -\text{grad } \phi = -\frac{\bar{V}}{c} \times \bar{B} \quad (2.4)$$

in a good conductor; and the second condition implies that

$$\bar{E} \cdot \bar{B} = (\text{grad } \phi + \dot{\bar{A}}) \cdot \text{curl } \bar{A} = 0 \quad (2.5)$$

where  $A$  is the magnetic vector potential.

Hones and Bergeson (1965) solved for  $\phi$  explicitly for the case of a tilted, centered dipole field. The electrostatic field is exactly such that the  $E \times B$  first order drift is the co-rotation velocity. The field is set up by a very small amount of charge separation throughout the magnetosphere. Melrose (1967) estimates that this electrostatic potential requires an excess charge density of only about  $10^{-14}$  electrons/cm<sup>3</sup>. Clearly if the overall

density is this low, equation 2.4 cannot be satisfied. At very low densities equation 2.5 cannot be satisfied either. Gledhill also remarks that if the density is so high that the conductivity perpendicular to the field lines is large, then the field lines need not be equipotentials and equation 2.5 breaks down.

Chapman (1964) gives the ratio of the longitudinal to the transverse conductivity as:

$$\frac{k_L}{k_T} = 1 + \frac{\Omega_e}{\nu_e} \frac{\Omega_i}{\nu_i} \quad (2.6)$$

where  $\Omega_e$  and  $\Omega_i$  are the electron and ion gyrofrequencies, and  $\nu_e$  and  $\nu_i$  are the collision frequencies of electrons with electrons and ions with electrons, respectively.

Ginzberg (1964) shows that  $\nu_e = \nu_i$ , approximately, and gives the mean value of  $\nu_i$  (averaged over velocities) as:

$$\nu_i = 5.5 N T^{-3/2} \ln (220 T N^{-1/3}) \quad (2.7)$$

If the transverse conductivity is to be much less than the longitudinal conductivity, then

$$\nu_i \ll \Omega_e \Omega_i \approx 43 \Omega_i \quad (2.8)$$

For a surface equatorial field of 10 gauss, the ion gyrofrequency at Io's orbit ( $5.9 R_J$ ) is  $500 \text{ sec}^{-1}$ . A plasma of temperature  $10^4 \text{ }^\circ\text{K}$  would have to have a density there on the order of  $10^8 \text{ cm}^{-3}$  in order to violate inequality 2.8. However, the inequality must be great, or else the co-rotation charge distribution will

be shorted out, and the magnetosphere will not co-rotate. There are good reasons to believe that the density is, in fact, very small, so that 2.8 is very well satisfied.

## 2.5 PLASMA DENSITY

Carr and Gulkis (1969) give a survey of ideas about the number density of the zenomagnetic cavity. Brice (1968) argues that photoelectrons alone will populate the zenomagnetic cavity to a density  $0.1 \text{ cm}^{-3}$ . (Ioannidis (1970) and Ioannidis and Brice (1970) consider this and related problems in more detail.)

Warwick and Dulk (1964), Warwick (1967), and Parker, Dulk, and Warwick (1969) have looked for Faraday rotation in Jupiter's DAM radiation. The observed rotation occurs almost entirely in earth's ionosphere. The radiation is probably penetrated in the extraordinary mode. If mode coupling occurs in Jupiter's plasmasphere, then its density must be less than  $10 \text{ cm}^{-3}$  at  $2 R_J$ . This would be about two orders of magnitude down from the density of the earth's magnetosphere.

Brice and Ioannidis (1970) quote Axford (1964) to the effect that on the order of 1 percent of the energetic particles incident from the solar wind on the magnetosphere of the earth are deposited in it. If the same ratio holds for Jupiter, and if the solar wind continues out beyond Jupiter, the total flux deposited into the polar regions of Jupiter's magnetosphere could

be larger. On the other hand, the convective electric fields would be less efficient in injecting plasma through the boundary of the geomagnetic cavity. So the plasma density around Jupiter may or may not be comparable to that around the earth.

The variation of density with radius is restricted to lie between two limits determined by interchange instabilities. If the density falls off too fast, then an instability like the Rayleigh-Taylor instability, except that centrifugal force replaces gravitational force, will tend to decrease the gradient by replacing inner, denser flux tubes by outer, less dense flux tubes. Melrose writes the condition that this instability not arise as:

$$-\frac{1}{N} \frac{dN}{dr} < \frac{\beta^2 \gamma (\gamma - 1)}{r (b r^2 - \frac{1}{r} + \beta \gamma / a)}, \quad (2.9)$$

where  $\beta$  is 1 plus the exponent in the radial dependence of magnetic field ( $\beta = 4$  for a dipole field);  $\gamma$  is the ratio of specific heats;  $a$  and  $b$  are dimensionless ratios which Melrose gives as 35 and .086, respectively;  $r$  is radius divided by  $R_J$ .

At the point  $r = 2.3$ ,  $b r^2 - 1/r = 0$ , and gravitational force just balances centrifugal force. At this radius 2.9 implies that the density gradient cannot fall off faster than:

$$N \propto r^{-\beta(\gamma-1)} \approx r^{-4}. \quad (2.10)$$

However, at very large distances, a smaller density gradient is required. In fact, for  $r > 10$ , equation 2.9 implies that the maximum stable gradient corresponds to the profile:

$$N \propto \exp \frac{\beta^2 r(r-1)}{2 a b} \frac{1}{r^2} \approx \text{const.} \quad (2.11)$$

The outer magnetosphere then should be of roughly constant density at large distances. This whole analysis, of course, neglects external sources of plasma, which would change the stability criteria.

Piddington (1967) calculates the maximum plasma density that Jupiter's magnetosphere can hold. In a curved field, electrons and protons execute drift motions perpendicular to both the field and the radius of curvature. The result in a dipole field is a ring current which tends to decrease the field inside and increase it outside. The body force on the plasma,  $\vec{j} \times \vec{B}$ , is exactly equal and opposite to the centrifugal force. The current density is given by:

$$j = \frac{\Omega N M r^4 R_J}{2 B_0} , \quad (2.12)$$

where  $\Omega$  is the rotational velocity of Jupiter,  $N$  is the particle density,  $M$  is the proton mass, and  $B_0$  is the surface field. Piddington makes an order of magnitude estimate for stability against the diamagnetic effects of the current by requiring that the current density  $\times 4_\pi$  must be less than the radial derivative of the magnetic dipole field. He obtains:

$$N < \frac{3 B_o^2}{2\pi\Omega^2 r^8 R_J^2 M} \quad (2.13)$$

At  $r = 6$ , the density must be less than  $10^7 \text{ cm}^{-3}$ .

Equation 2.13 is rewritten by Piddington in terms of the rotational velocity  $V_R$  and the Alfvén velocity  $V_A$ :

$$V_R < \sqrt{3} V_A \quad (2.14)$$

Thus in a stable magnetosphere, the Alfvén speed cannot be smaller than a limit determined only by the speed of rotation at any given point.

## 2.6 PLASMA TEMPERATURE

The outer magnetosphere of the earth seems to include two energy components (Cole, 1966), but the experimental data are scanty. Patel (1964) infers a temperature of about 1 eV from data of Gringauz, et al. (1962) in the outer magnetosphere. Sagalyn and Smiddy (1965) find a positive ion density of  $1 \text{ cm}^{-3}$  with an average ion energy of 350 eV. Liemohn and Scarf (1962) find a temperature of 30 eV from nose-whistler data, but Guthart (1964) claims an upper limit of 2 eV. The variation in measurements may be due to the difference between quiet and disturbed conditions. Bengt Hultquist (1966) says that when the magnetosphere is disturbed, a temperature of 10 eV is not unreasonable.

Particles energized by resonance with convective electric fields in Jupiter's magnetosphere would have

about 200 times the energy of such particles in earth's magnetosphere (Brice and Ioannidis 1970). If the thermal component of the plasma results from cooling of this particular high energy component, then one would expect the energy of the thermal plasma to be higher in Jupiter's magnetosphere than in earth's.

CHAPTER III  
THE MINIMUM HYPOTHESIS  
AND THE ASSUMED PARAMETERS

3.1 A MOON-LIKE IO

As has been shown in Chapter II, the exact values of Io's mass, Jupiter's magnetic field, plasma density profile, etc. are not known very well. In considering ways in which Io can excite a plasma disturbance, some range of values of each of the relevant parameters must be assumed. Although the actual mechanism by which Io influences Jupiter may in fact involve some unexpected or unusual datum (such as large permeability in Io or non-synchronous rotation) it would be wiser to assume a more unimaginative family of parameters characterizing Io. This thesis makes the assumption that Io is not unlike earth's moon in size, rotation, density, conductivity, permeability, and permittivity. In other details it will differ, for example: temperature, atmosphere, and velocity. (Surprisingly enough, in spite of the assumption of moon-like characteristics for Io, the mathematical description of Io's wake will be general enough to include the two "unexpected" characteristics mentioned above: large permeability, and non-synchronous rotation.)

Table II lists the estimated conductivity, permeability, permittivity, the density, radius, and mass of earth's moon. Io's surface temperature as determined by infrared measurements, its velocity through

TABLE II

Properties of Earth's Moon

<u>Parameter</u>	<u>Value</u>	<u>Source</u>
Conductivity (surface)	$10^{-12}$ to $10^{-10}$ (MKS)	Ward, 1969
(interior)		
young, cold moon	$10^{-2}$	England et al. 1968
old, hot moon	$10^2$	"
Permeability (surface)	$1.026 < K_m < 1.7$	Ward, 1969
(=free space value)		
Permittivity		
(=free space value)		
(Homogeneous moon)	$2.8 \pm 0.7$	"
(concentric layers)	1.8 above 5-10m	"
	5 below 5-10m	"
(local variations)	1.8-20	"
Density (surface)	$3.1 \pm 0.1$ g cm <sup>3</sup>	Solomon and
(core)	$3.6 \pm 0.1$	Toksöz, 1968
(mean)	3.34	
Radius	1738 km	
Mass	$7.34 \times 10^{25}$ g	
<u>Temperature of Io</u>		
Observed brightness of Io at inferior geocentric conjunction:	135°K	Murray et al. 1964
Average brightness temperature	101°K	Binder and Cruikshank 1964
Minimum theoretical temperature at I.G.C. (without atmosphere)	145°K	Richardson and Shum, 1966
Minimum theoretical average temperature (without atmosphere)	~100°K	
<u>Velocity of Io</u>		
Relative to field lines:	56 km/s	
inertial:	17 km/s	

the magnetosphere relative to an inertial frame and relative to a co-rotating magnetosphere are also listed.

### 3.2 ASSUMED PROPERTIES OF THE MAGNETOSPHERE

The density of Io's environment is probably sufficiently low, and the thermal energy sufficiently high, that the plasma is nearly collisionless. The restrictions which this puts on the possible range of density and temperature are very weak, and will be discussed in Chapter V. If the Magnetic field is sufficiently large, then low frequency phenomena will be of more importance than high frequency phenomena. This is because, (Warwick, 1967) the base frequency associated with the motion of Io will be the rate at which plasma flows by Io. This is about one cycle per minute for a speed of 56 km/s relative to the co-rotating field lines (which move faster than Io) and a diameter of 3400 km. This frequency is much lower than the ion gyrofrequency or the plasma frequency, and thus resonance effects will probably be negligible.

The magnetic pressure is certainly larger than the thermal pressure, or else the plasma could not be contained for long. The ratio of thermal to magnetic pressure (called  $\beta$ ) will be assumed  $\ll 1$ . As a consequence of this, it is clear that magnetic forces will dominate pressure gradient forces, and so we will consider only electromagnetic sources of hydromagnetic waves

and neglect pressure or density sources. The meaning of this statement will be clarified in Chapter IV.

### 3.3 AVAILABLE ENERGY

On the basis of the DAM energy received at earth, and the narrow beaming effects referred to in Section 1.4, Warwick (1963a, 1967) infers that the power output in a single DAM event is about  $2 \times 10^7$  to  $10^8$  watts. If all of this energy comes ultimately from Io with an efficiency of 1 percent, will the supply of energy at Io be depleted rapidly? First of all, suppose it comes from the kinetic energy of Io, which amounts to about  $4 \times 10^{31}$  joules. In one century it would lose only about  $10^{-12}$  of its energy. The corresponding change on its orbital period would therefore be only about  $10^{-7}$  seconds, which would be undetectable. In view of the strong resonance Io has with the other satellites, their energy might be available as well.

Suppose that some fraction of the magnetic energy through which Io passes is converted into waves or currents which propagate down to the surface of Jupiter, where they are converted into electromagnetic waves.

This power would equal

$$P_{\text{Mag}} = f V_I \left( \frac{B_I^2}{8\pi} \right) \pi R_I^2 \quad (3.1)$$

For a ten gauss surface equatorial field, the field  $B_I$  at Io is about 0.05 gauss,  $V_I = 55$  km/s,  $R_I = 1650$  km, and so

$$P_{\text{Mag}} = f \times 4 \times 10^{20} \text{ watts.}$$

All that is necessary is that  $f \gtrsim 10^{-11}$  to get a reasonable amount of power at Io. If the thermal energy were so converted, the maximum power available would be lower by a factor of  $\beta$ . For a plasma density of  $1/\text{cm}^3$  and a temperature of 10 eV,  $\beta = 2 \times 10^{-7}$ , and so the process would have to be very efficient to rival the source of magnetic energy.

### 3.4 NON-LINEAR VS. LINEAR

If the energy needed to power the Io-associated radiation were too high, then the currents and/or waves generated by Io might have to be large in amplitude, which would mean that the problem is inherently non-linear. This thesis will show, however, that a large class of disturbances which Io could generate are of sufficiently small amplitude that they are at least approximately linear and yet can transport as much as a few orders of magnitude more power toward Jupiter than is inferred to exist in the Io-related emission. The actual disturbance may in fact involve nonlinear motions or fields, but the point here is that it is not necessary to assume ab initio that the motions are non-linear in order to get a reasonable amount of radiated hydro-magnetic power from Io.

One good reason for looking at linear disturbances first is that they are better understood than nonlinear

ones, and can be calculated more accurately. The nonlinear disturbances postulated by Goldreich and Lynden-Bell (1969) or Piddington and Drake (1968), for example, are not intuitively obvious solutions of the system of equations which describes a magnetoactive medium. Whether they are or they are not, of course, would likely be difficult to demonstrate. Such models would be much more convincing if the motions in the disturbance could be shown to be the large amplitude limit of a family of small amplitude linear disturbances. For this reason only linear wave motions will be studied in this thesis.

CHAPTER IV  
IO AS AN ELECTROMAGNETIC SOURCE

4.1 IO'S WAKE

An analytical solution to the general problem of Io's wake in Jupiter's magnetosphere is not likely to be found except in some sort of approximate or asymptotic form. Even if the problem were governed by the equations of compressible, magnetofluid dynamics (and Chapter V will show it is not), the nonlinearity of the equations makes an analytic solution improbable. A numerical solution may eventually be possible, but present-day electronic computers are barely adequate for three-dimensional hydrodynamic problems at low Reynolds numbers, let alone magnetohydrodynamic problems at high magnetic Reynolds numbers. Laboratory simulation is impossible because all of the relevant dimensionless ratios cannot be duplicated simultaneously in a laboratory-sized plasma chamber (Kristofesson, 1969).

Analytical solutions have been obtained for the linear problem of compressible, collision-dominated, magneto-gas-dynamic flow around a two-dimensional, slender obstacle. See for example, Sears and Resler (1958), Sears (1960), McCune and Resler (1960). Extension to the case of a three-dimensional, thin obstacle is probably possible. However, such solutions would not have much relevance to the case of a blunt

(spherical) obstacle, which would produce a nonlinear disturbance.

The problem of the wake of an earth satellite moving in a collisionless, low  $\beta$  medium has been studied by Ja. Al'Pert., et al. (1963), Ja. Al'Pert (1965), K. Chopra (1961), Drell, et al. (1965), Liu (1969), Gurevich, et al. (1969) and many others. Some of the ideas presented by these authors are disputed, and a good deal of work remains to be done in this field. Perhaps the question of Io's wake is more closely related to the earth satellite wake problem than to the lunar wake problem--another unsettled issue--since earth's moon, during most of its orbit, moves through the interplanetary medium, which has  $\beta$  comparable to unity (Ness, et al., 1968), rather than very small. On the other hand, the ratios of body size to gyro-radii and Debye length are not scaled well in the earth satellite problem and one does not expect Cowling times to be as large for an artificial satellite as for the moon or Io.

If the problems of earth satellite wakes and the lunar wake are still unresolved, then how much faith can be put in theories of the wake of Io whose nature and environment are so uncertain? This leads one to search for a more general approach to the problem of wave generation by a moving satellite than the more rigorous technique of solving for all features of the wake. The answer lies in the standard approaches of Lighthill

(1958) and Kuperus (1965) to the problem of hydromagnetic radiation. If the equations of a system can be linearized, then it is a standard technique to take the nonlinear terms and--rather than throw them out--put them on the right hand side of the equations as source terms. Then one makes estimates of these terms on the right hand side and calculates the response of the system by obtaining the particular solution for those source terms. This technique works well for hyperbolic equations, because then the nonlinear terms do not feed back onto the system, but cause waves which are radiated away. The solution is then good only at large distances from the source of waves, and not applicable near the region where the nonlinear terms are large. The great advantage of the technique is that one may solve a good fraction of the problem by obtaining the waves first for quite general source terms, leaving an accurate calculation of the source amplitude for later, and merely making estimates of their strength in the initial stage.

#### 4.1 MOMENTS OF THE SOURCE

Whatever the nature of the flow patterns and current systems around  $I_0$ , it is clear that if they are to cause significantly large waves, they must be simply correlated over dimensions of a few  $I_0$  radii. This implies that the dipole and quadrupole moments of the disturbance ought to cause the largest waves at great

distances. Now whether these lower moments will predominate in the actual disturbance is not immediately obvious, but a few examples should illustrate that this is normally true for a wide variety of disturbances.

#### Magnetic dipole examples

1. Burns (1968) suggested that Io might have a finite dipole moment, presumably due to ferromagnetism.

2. A more likely possibility is that Io would have a small but significant dipole moment if it contained only as much magnetite as the Surveyor satellites seem to have found on the lunar surface (Ward, 1969).

3. If the field lines "cleave around" Io, as Warwick (1967) has suggested, then currents inside Io or on its surface must exist to cancel the field inside, and Io would have a correspondingly strong magnetic dipole moment.

4. One system of flow patterns and field disturbances suggested by Dulk (1965) requires corresponding dipole current loops in the plasma around Io.

5. This thesis will suggest that inductive effects caused by the slightly varying field seen by Io will also produce a magnetic moment.

#### Magnetic quadrupole

1. A quadrupole can be thought of as the juxtaposition of two opposing dipoles. If any of the systems mentioned above, for example, tended to cancel one

another, the leading moment would be a quadrupole (unless the symmetry were so strong that the quadrupole moment also vanished, leaving an octupole).

2. A conceivable way in which Io might induce a quadrupole moment in itself, is by rotating non-synchronously. (Observations suggest synchronous rotation: Dollfus, 1961). As an example, consider rotation about an axis parallel to the ambient field. If the interior of Io is slightly conducting, the local flux tube would be twisted, with maximum twist at Io's equator. This is equivalent to the sum of a uniform field plus a toroidal field in Io's northern hemisphere plus the opposite toroidal field in the other hemisphere. Clearly this is the field produced by a cylindrically symmetric, toroidal solenoid, with windings in meridional planes, and characterizes the quadrupole moment that Io would have in that case.

#### Electric monopole

It has been observed that earth satellites in the ionosphere tend to become charged to a potential of a few volts because of the higher flux of electrons onto their surface or other effects (Al'Pert, 1965). However, such charging cannot be significantly large for a natural satellite like Io, because the Debye length is so small compared to its dimensions. Charge neutrality is not likely to be violated over a scale length much greater

than a Debye length. (Besides which, charge is conserved, so that whenever there is negative change someplace, positive change exists elsewhere, hence a dipole is more likely than a monopole.)

#### Electric dipole

1. Because of the co-rotation electric field in Jupiter's magnetosphere, Goldreich and Lynden-Bell (1969) argued that Io would have a potential across it in the direction perpendicular to its motion and to the ambient magnetic field. Gurevich, et al. (1969) discusses such an effect for earth satellites in the ionosphere. Whether currents flow or not in response to this potential is debatable. The crust of earth's moon (which Chapter III takes as a model for Io) has a D.C. conductivity on the order of  $10^{-10}$  to  $10^{-12}$  mho/m (Ward, 1969), which is five to seven powers of ten lower than the value used by Goldreich and Lynden-Bell for Io. If there are no currents, then Io has an electric dipole moment. If there is current flow, then the electric dipole moment will be decreased. The current distribution has to be a localized one to apply the method of moments, and in fact, if there are large currents along the field lines, the mathematical techniques (to be developed in Chapter V) do not apply.

2. Because of the different mean thermal velocities of ions and electrons, the region behind a satellite will have a gradient in charge density which is a very

complicated (and unknown) function of the satellite speed, the temperature, the field strength, and the distance behind the body. If the satellite is moving rapidly with respect to the ions, but slowly with respect to the electrons, shadowing will cause the ions to be slightly depleted immediately downstream. The difference in charge will be made up elsewhere around the satellite. The result is a charge distribution which has a dipole moment parallel to the stream velocity. Higher moments will also exist. Charge neutrality cannot be violated over a dimension much larger than a Debye length, but the latter is inversely proportional to the square root of density, and so may be relatively large in the close wake. The strength of this dipole moment may be estimated by the condition that the electrostatic energy of the charge distribution must be of the order of the thermal energy in that same volume, since the kinetic energy of the individual particle determines the amount of charge gradient and a large charge gradient will alter this kinetic energy to destroy itself. Not even an approximate solution of this problem has been achieved for the case of a low  $\beta$ , collisionless plasma with strong magnetic field (Gurevich, et al., 1969).

## 4.3 THE MATHEMATICS OF DIPOLE SOURCES

Magnetic dipoles

A macroscopic dipole field is representable as a super-position of microscopic dipoles. Let  $\bar{M}(\bar{x})$  be magnetization as a function of position  $\bar{x}$ . The macroscopic and microscopic magnetic fields  $\bar{H}$  and  $\bar{B}$  are related by the equation:

$$\bar{B} = \bar{H} + 4 \pi \bar{M} \quad (4.1)$$

(Gaussian units are used throughout.)

The current density of any steady system of currents can be represented by some function  $\bar{M}(\bar{x})$  through the relation:

$$\bar{j} = c \text{ curl } \bar{M} \quad (4.2)$$

Consider a singular magnetization density given by

$$\bar{M}(\bar{x}; \bar{x}') = m \hat{e} \delta(\bar{x} - \bar{x}'), \quad (4.3)$$

where  $\hat{e}$  is a unit vector and  $\delta(\bar{x})$  is the three-dimensional Dirac delta function, and  $m$  is the magnetic moment. Similarly, let  $\bar{j}'$  be the corresponding current density:

$$\bar{j}'(\bar{x}; \bar{x}') = c \text{ curl } \bar{M}'(\bar{x}; \bar{x}') \quad (4.4)$$

Then it is clear that an arbitrary steady current density is a linear combination of such currents because of the identity:

$$j_i(\bar{x}) = \frac{1}{m} \int d^3 x' M_i(\bar{x}') e_j j'_j(\bar{x}; \bar{x}'), \quad (4.5)$$

where the summation convention on the component indices is assumed. It is easy to show that  $\vec{j}'(\bar{x}; \bar{x}')$  represents an infinitesimal dipole (Jackson 1963), so it follows that any steady system of currents can be represented as a superposition of infinitesimal dipole current loops. As a consequence, we need only to study the effect of infinitesimal dipoles to determine the effects of finite dipoles in a linear system.

The solution to the equation

$$\text{curl } \vec{B} = \frac{4\pi}{c} \vec{j}'(\bar{x}, \bar{x}') = -4\pi \hat{e} \times \text{grad } \delta(\bar{x} - \bar{x}') \quad (4.6)$$

is the dipole field centered at  $\bar{x} = \bar{x}'$  :

$$\vec{B} = (3\hat{n}(\hat{n} \cdot \hat{e}) - \hat{e})/R^3 \quad (4.7)$$

where  $R$  is the distance from  $\bar{x}$  to  $\bar{x}'$  and  $\hat{n}$  is the unit vector in that direction.

#### Electric dipoles

An electric dipole source has the charge density:

$$q = p \hat{e} \cdot \text{grad } \delta(\bar{x} - \bar{x}'), \quad (4.8)$$

where  $p$  is the dipole moment and is related to the current density by the continuity equation:

$$\text{div } \vec{j} + \frac{\partial q}{\partial t} = 0 \quad (4.9)$$

The current density is clearly given by:

$$\vec{j} = -\hat{e} \frac{\partial p}{\partial t} \delta(\bar{x} - \bar{x}') \quad (4.10)$$

Thus the current density due to electric and magnetic dipole sources is:

$$\vec{j} = -\vec{M}\vec{C} \times \text{grad } \delta(\vec{x}-\vec{x}') - \frac{\partial \vec{p}}{\partial t} \delta(\vec{x} - \vec{x}''), \quad (4.11)$$

where  $\vec{M}$  and  $\vec{p}$  are the vectorial magnetic and electric dipole moments, located at  $\vec{x} = \vec{x}'$  and  $\vec{x} = \vec{x}''$ , respectively.

#### Moving and stationary dipoles

It is easy to see that a constant but linearly moving dipole is a linear combination of stationary but oscillating dipoles stationed along the axis of the linear motion. Let

$$\vec{M}(\vec{x}, t) = \vec{M} \delta(x - vt) \delta(y) \delta(z) \quad (4.12)$$

Then frequency analyze this equation, to obtain

$$\vec{M}(\vec{x}, t) = \int_{-\infty}^{\infty} d\omega \frac{\vec{M}}{2\pi v} \delta(y) \delta(z) e^{-i\omega x/v} e^{i\omega t} \quad (4.13)$$

Therefore  $M$  is manifestly a linear combination of dipoles of frequency  $\omega$  and amplitude

$$\frac{\vec{M}}{2\pi v} \delta(y) \delta(z) e^{-i\omega x/v} \quad (4.14)$$

The linear combination of equation 4.13 holds for transformation of source terms, so it holds for the corresponding fields caused by the sources, or for any system of quantities which are linearly related to such sources. This fact will be used implicitly in discussions of later chapters.

CHAPTER V  
EQUATIONS DESCRIBING A COLLISIONLESS,  
MAGNETOACTIVE PLASMA

5.1 THE COLLISIONLESS REGIME

Bernstein and Trehan (1960) divide plasma collisions into three classes. First are those in which the impact parameter  $b$  is less than that for  $90^\circ$  scattering,  $b_{90}$ . Second are those collisions in which the impact parameter is larger than  $b_{90}$  but less than the Debye length,  $D$ . The third class includes impact parameters greater than  $D$ . These are many body collisions when the number of particles in a Debye sphere is large. This sort of scattering is a collective effect described by Maxwell's equations.

The impact parameter for  $90^\circ$  scattering comes from the Rutherford formula:

$$b = (Z_1 Z_2 e^2 / m \langle v^2 \rangle) \cot \theta/2 \quad (5.1)$$

where  $Z_1$  and  $Z_2$  are the charge numbers,  $m$  is the reduced mass and  $v$  is the relative velocity of the particles. For electron-proton and electron-electron scattering  $b$  is lower by  $1.8 \times 10^3$ . For thermal energies of about 10 eV, the former is about  $2 \times 10^{-8}$  cm.

The Debye length  $D$  is given by

$$D = (m \langle v^2 \rangle / 12 \pi N_e^2)^{1/2}, \quad (5.2)$$

where  $m$  is the electron mass.

For  $kT = 10$  ev, and  $N = 1 \text{ cm}^{-3}$ ,  $D = 2 \times 10^3$  cm.

The number of particles  $g$  in a Debye sphere is

$$g = \frac{4\pi}{3} ND^3 \quad (5.3)$$

For the same values of  $T$  and  $N$ ,  $g = 3 \times 10^{10}$ .

The time  $T_c$  between  $90^\circ$  deflections (Bernstein and Trehan, 1960) is

$$T_c = \sqrt{\frac{m}{2\pi kT}} \frac{3(kT)^2}{2N_e^4 \ln(g/9)} \quad (5.4)$$

This is simply a more exact formulation of the approximate formula:

$$T_c = 1/N\pi b^2 \langle v \rangle,$$

where  $\langle v \rangle$  is a mean relative velocity.

Equation 5.4 yields  $T_c \sim 6 \times 10^5$  sec for the temperature and density used previously.

One may conclude that at densities of  $1 \text{ cm}^{-3}$  and temperatures of 10 ev, any process which has a period less than  $10^5$  sec may be regarded as collisionless. For frequencies on the order of  $10^{-1}$ , and a temperature of 10 ev, equation 5.4 implies that the density may be as high as  $10^5$  and the process will still be collisionless. For higher temperatures the densities could still be higher and yet the medium will be collisionless at this frequency.

These estimates imply that the Vlasov equation plus Maxwell's equations form the relevant system for Jupiter's magnetosphere.

## 5.2 EQUATIONS FOR A COLLISIONLESS PLASMA

The fields generated by an arbitrary system of currents in a vacuum are governed by the equations

$$\text{curl curl } \bar{E}(\bar{x}, t) + \frac{1}{c^2} \frac{\partial^2 \bar{E}}{\partial t^2}(\bar{x}, t) = \frac{4\pi}{c} \frac{\partial \bar{J}}{\partial t}(\bar{x}, t) \quad (5.5)$$

$$\frac{\partial \bar{B}}{\partial t} = -c \text{ curl } \bar{E} \quad (5.6)$$

Equation 5.5 is the wave equation for the electric field, and equation 5.6 is Faraday's law, which determines the magnetic field in terms of the electric field. The function  $\bar{J}$  on the right hand side of 5.5 may include polarization currents  $j_p$  as well as source currents  $j_s$ . The effect of a plasma may be included in the current density in the following way (Stepanov 1958):

$$\begin{aligned} \text{curl curl } \bar{E} + \frac{1}{c^2} \frac{\partial^2 \bar{E}}{\partial t^2} = & - \frac{4\pi e}{c^2} \frac{\partial}{\partial t} \int d^3v \left( f_i(\bar{v}) - f_e \right) (\bar{v}) \bar{v} \\ & - \frac{4\pi}{c} \frac{\partial \bar{J}}{\partial t} \quad s \end{aligned} \quad (5.7)$$

The first term on the right hand side of 5.7 is due to the polarization current  $j_p$  caused by differential motions of the plasma ions and electrons. The second term is an arbitrary source function. The quantities  $f_i$  and  $f_e$  are the distribution functions for ions and electrons, normalized such that their integrals over

velocity space are each unity.

The Vlasov equation determines the distribution functions:

$$\frac{\partial f}{\partial t} + \bar{v} \cdot \frac{\partial}{\partial \bar{x}} f + \frac{e}{m} (\bar{E} + \frac{\bar{v}}{c} \times \bar{B}) \cdot \frac{\partial}{\partial \bar{v}} f = 0, \quad (5.8)$$

where  $f$  may be  $f_i$  or  $f_e$ ,  $e$  is ion or electron charge, and  $m$  is ion or electron mass.

Up to this point, the only approximations have been the neglect of collisions and the assumption of non-relativistic motions. At this point, it is necessary to make further approximations. Equation 5.8 must be linearized. This requires the following assumptions:

1. The "zero order" electric field in the plasma frame vanishes.
2. The "zero order" magnetic field is parallel to the  $Z$  axis and homogeneous.
3. The "zero order" velocity distributions are independent of position and time, and are "gyrotropic."
4. "Second order" terms are negligible.

The first three assumptions imply that this formalism is valid for wave motions in a non-homogeneous medium only on a scale small enough that variations in the zero order quantities are negligible. This limitation will be discussed in Chapter VII. Assumption (3) implies that the zero-order velocity distributions are functions only of the velocity components  $V_r$  and  $V_z$ ,

perpendicular and parallel to the field. Such a function satisfies the "zero-order" Vlasov equation, which is the "gyrotropic" condition:

$$\frac{\bar{v}}{c} \times \bar{B}_0 \cdot \frac{\partial}{\partial \bar{v}} f_0(\bar{v}) = 0 \quad (5.9)$$

Zero subscripts indicate zero order. All functions that remain in the theory will be first order. It is convenient to Fourier analyze 5.8 using the transform:

$$f(\bar{k}, \omega) = \frac{1}{(2\pi)^2} \int d^3x \int dt e^{i\bar{k} \cdot \bar{x} + i\omega t} f(x, t). \quad (5.10)$$

The Vlasov equation then becomes (Stepanov, 1958):

$$\left[ i(\omega - \bar{v} \cdot \bar{k}) + \frac{eB_0}{mc} \frac{\partial}{\partial \phi} \right] f(\bar{k}, \omega) = \frac{e}{m} \bar{E}(k, \omega) \cdot \frac{\partial f_0}{\partial \bar{v}}(\bar{v}). \quad (5.11)$$

The quantity  $\phi$  is the azimuth angle of velocity. Let  $\Omega = eB_0/mc$ , with subscripts  $e$  or  $i$  for each species, and let  $\alpha$  be the azimuth angle for  $\bar{k}$ . Then equation 5.11 has the solution for  $f$  in terms of  $E$ :

$$f(\bar{k}, \omega) = \frac{c}{B_0} e^{is(\phi)} \bar{E} \cdot \int_{-\phi}^{\phi} \frac{\partial f_0}{\partial \bar{v}} e^{-is(\phi')} d\phi' \quad (5.12)$$

$$\text{where } s(\phi) \equiv \left( (\omega - v_t k_z) \phi - v_r k_r \sin(\phi - \alpha) \right) / \Omega$$

Equation 5.12 gives an order of magnitude estimate relating  $E$  and  $f_e$  or  $f_i$ .

$$\frac{E}{B_0} \sim \frac{v_t}{c} \frac{f}{f_0} \sim \frac{v_{re}}{c} \frac{f_e}{f_{oe}} \sim \frac{v_{ri}}{c} \frac{f_i}{f_{oi}} \quad (5.13)$$

(The latter estimates follow from 5.18. The plasma currents must be "first order.") Thus for linearization to be valid, we must have the following inequalities:

$$\begin{aligned} f_e/f_{oe} &<<1 \\ f_i/f_{oi} &<<1 \\ E/B_0 &<< v_i/c \end{aligned} \quad (5.14)$$

Since linearization has been assumed, there must be a linear relation between  $\bar{J}$  and  $\bar{E}$ , and this is put into the form 5.15 (Stix, 1962), with  $\bar{K}$  denoting the "dielectric tensor."

$$\bar{J}(\bar{k}, \omega) = \frac{\omega}{4\pi i} \left\{ \bar{K}(\bar{k}, \omega) - \bar{I} \right\} \cdot \bar{E}(\bar{k}, \omega) \quad (5.15)$$

The tensor  $\bar{K}$  may be determined by taking equation 5.11 for ions and for electrons, subtracting them, obtaining the resulting current density and equating coefficients of electric field components in equations 5.12 and 5.15.

$$\bar{J}(\bar{k}, \omega) = \frac{ec}{B_0} \sum z \int d^3 v \int_{\phi}^{\phi} d\phi' \bar{v} \bar{E} \cdot \frac{\partial f_0}{\partial \bar{v}} \exp[i(s(\phi) - s(\phi'))] \quad (5.16)$$

The sum is over species, and  $z = \pm 1$  for ions and  $-1$  for electrons.

Stepanov (1958), Stix (1962), and Tajiri (1967) (for slightly different assumptions), have evaluated  $\bar{K}$  by going through the process mentioned above after taking  $f_0$  to be a Maxwellian distribution function. The most general form was taken by Stix who allowed the temperature to be different for ions and electrons, permitted

anisotropy with respect to radial and longitudinal velocities, and introduced an arbitrary drift velocity parallel to the magnetic field. The elements of the dielectric tensor can be written as definite integrals which are not reducible to simple closed functions (Stepanov, 1958), or as infinite series of Bessel functions and plasma dispersion functions (Stix, 1962). An entirely equivalent, though different analysis was carried through by Barnes (1968) in the formalism of Chandrasekhar, Kaufman, and Watson (1956). The tensor elements are displayed in Appendix I.

The Fourier transform of 5.7 coupled to 5.17 yields the wave equation for collective oscillations of a plasma:

$$\bar{k} \times \bar{k} \times \bar{E}(\bar{k}, \omega) + \frac{\omega^2}{c^2} \bar{K}(\bar{k}, \omega) \cdot \bar{E}(\bar{k}, \omega) = -\frac{4\pi i \omega}{c} \bar{J}_s(\bar{k}, \omega) \quad (5.17)$$

### 5.3 FORMAL SOLUTION

The current density  $j_s$  on the right hand side of this equation is a source current for the electric field  $\bar{E}$ . It is specified in advance and  $\bar{E}$  is calculated.  $\bar{B}$  follows from Faraday's law. The matrix operator acting on  $\bar{E}$  may be inverted to obtain a formal solution for  $\bar{E}$  in terms of  $\bar{J}_s$ . The general form of the matrix operator, in component form, is:

$$L_{ij} = (n_i n_j - n^2 \delta_{ij} + K_{ij}) \quad (5.18)$$

where  $n_i = k_i c/\omega$  is the vector index of refraction.

Thus the formal solution to (2.13) is given by:

$$\bar{E}(\bar{k}, \omega) = \frac{-4\pi ic}{\omega} \bar{L}^{-1}(\bar{k}, \omega) \cdot \bar{J}_s(\bar{k}, \omega). \quad (5.19)$$

For any source term, in principle, we may do the inverse Fourier transform in  $\bar{k}$  and  $\omega$  to find the "response"  $\bar{E}(\bar{x}, t)$ . We may choose a real  $\bar{k}$  vector and let  $\omega$  be complex. The frequency transform is a contour integral containing the poles of the right hand side of 5.19. If  $|L|$  has zeroes in the upper half  $\omega$  plane, the system will be unstable. Much of the plasma physics involves searching for these instabilities. Among them are the loss-cone and two-stream instabilities, which depend on the distribution functions, the firehose instability which depends on a species temperature anisotropy, and various instabilities depending on density gradients, etc. As discussed in Chapter III, we will not look into the difficult (but interesting) problem of ways in which sources can excite such instabilities, but will assume that all of the zeroes of  $|L|$  are in the lower half  $\omega$  plane. Tajiri (1967) has shown that this is true in the low frequency range ( $\omega \ll \Omega_i$ ), which is the regime we are interested in.

## 5.4 THE HYDROMAGNETIC MODES

In the low-frequency limit the explicit form of  $\bar{\bar{L}}^{-1}$  is very simple. Appendix II derives the appropriate form as a limiting case of the general expression for  $\bar{\bar{K}}$ . Since  $\bar{\bar{L}}$  is a tensor function of the vector  $\bar{k}$ , it can be expressed in terms of products of rotation matrices and its value when  $\bar{k}$  is restricted to (say) the xz plane. Thus:

$$\bar{\bar{L}}(k_x, k_z, \alpha; \omega) = \bar{\bar{R}}(-\alpha) \bar{\bar{L}}(k_x, k_z, 0; \omega) \bar{\bar{R}}(\alpha), \quad (5.20)$$

Where  $\alpha$  is the azimuth angle of the wave vector  $\bar{k}$ , and  $\bar{\bar{R}}$  is a rotation matrix. For simplicity we look at  $\bar{\bar{L}}_0$ , the  $\alpha=0$  expression of  $\bar{\bar{L}}$ ;  $\bar{k}$  is therefore in the xz plane. Equation 5.20 will be used to obtain the general expression for  $\bar{\bar{L}}$ .

From appendix II,

$$\bar{\bar{L}}_0^{-1} = \begin{bmatrix} \frac{1}{K_{11} - n_z^2} & 0 & \frac{-n_x n_z}{K_{33}(K_{11} - n_z^2)} \\ 0 & \frac{1}{K_{11} - n^2} & 0 \\ \frac{-n_x n_z}{K_{33}(K_{11} - n_z^2)} & 0 & \frac{1}{K_{33}} \end{bmatrix} \quad (5.21)$$

The dispersion relation in this approximation is simply

$$\det L_0 = (K_{11} - n_z^2) (K_{11} - n^2) K_{33} = 0 \quad (5.22)$$

Note that terms of order  $1/K_{33}$  have been neglected. This is an essential part of the approximation, which is justified at low frequencies and long wavelengths. Barnes (1966) and Tajiri, (1967) derive the same dispersion relation for low frequency and low  $\beta$ . The three factors correspond to three sets of modes.  $K_{11} - n_z^2 = 0$  for the shear Alfvén mode. It involves only the wave vector component in the field direction, therefore travels along the magnetic field.  $K_{11} - n^2 = 0$  for the compressional Alfvén mode, which is neither purely transverse nor longitudinal. At low  $\beta$  it involves only the magnitude of the wave vector, and therefore propagates spherically outward from its source. These two modes are essentially the same as the two fastest modes of low  $\beta$  MHD (Denisse and Delcroix, 1963) or of quasi-hydrodynamics (Chew, Goldberger and Low, 1956). The main virtue of this formulation is that equation 5.22 can be embellished to include collisionless damping effects.

The third factor yields modes given by  $K_{33}=0$ . These were first discussed by Fried and Gould (1961). There are an infinity of roots to  $K_{33}=0$ , all of them in the lower half  $\omega$  plane. These "Fried and Gould" waves are simply longitudinal plasma oscillations which damp out in at most one wavelength by Landau damping effects. Appendix III estimates their total amplitude for a simply source current and demonstrates explicitly that their effect is negligible compared to that of the Alfvén

waves at low frequencies.

### 5.5 THE ALFVEN WAVE FIELDS

Since the compressional Alfvén waves propagate out nearly radially from the source, they are geometrically attenuated as the inverse square of the radius. The Fried and Gould waves are heavily damped. Thus only the shear Alfvén modes remain. These modes are slightly damped by collisionless processes. Chapter VIII discusses this. The electric and magnetic fields of the shear Alfvén mode can be calculated by extracting the appropriate terms from  $\bar{L}^{-1}$ . We call this tensor  $\bar{S}$ . Appendix IV shows that the shear Alfvén electric field is formally given by:

$$\bar{E}_A(\bar{k}, \omega) = \frac{4\pi ic}{\omega} \bar{S} \cdot \bar{j}_s(\bar{k}, \omega)$$

where  $\bar{S} = \frac{1}{(K_{11} - n_z^2) k_r^2} \begin{pmatrix} k_x^2 & k_x k_y & 0 \\ k_x k_y & k_y^2 & 0 \\ 0 & 0 & 0 \end{pmatrix}$

(5.23)

The electric field in time and space can be evaluated by inverse Fourier-transforming equation 5.23 according to the methods described by Briggs (1964). Small damping terms must be introduced in that case, in order to make the transforms meaningful. An alternative method is to convert 5.23 into a partial differential equation. This is the method to be adopted and carried

through in Chapter VI.

The collisionless damping terms, though very small at low frequencies, produce significant "global" effects in the Alfvén waves. If the temperature is allowed to vanish in the expression for the dielectric tensor, and then the frequency is made very small, the results are qualitatively different than if the reverse procedure is followed. The limits  $T \rightarrow 0$  and  $\omega \rightarrow 0$  do not commute. For this reason, the results of A.K. Sundaram (1969) or Arbel and Felsen (1963) for the effects of point sources in a cold plasma are inapplicable to our problem. These matters will be discussed in Chapter VII.

CHAPTER VI  
GENERATION OF SHEAR ALFVEN WAVES

6.1 THE WAVE EQUATION

The formal solution 5.23 for shear Alfven waves produced by an arbitrary current source may be written in the vector form:

$$\left(\frac{\omega^2}{c^2} K_{11} - k_z^2\right) k_r^2 \bar{E}_A(\bar{k}, \omega) = -4\pi i \frac{\omega \bar{k}_r}{c^2} \bar{k}_r j_s(\bar{k}, \omega) \quad (6.1)$$

The inverse Fourier transform of this equation yields the partial differential equation

$$\left(\frac{K_{11}}{c^2} \frac{\partial^2}{\partial t^2} - \frac{\partial^2}{\partial z^2}\right) \nabla_T^2 \bar{E}_A = \frac{4\pi}{c^2} \nabla_T \cdot \nabla_T \frac{\partial \bar{j}_s}{\partial t} \quad (6.2)$$

where the subscript T designates that the differentiation is transverse to the z (magnetic field) direction.

According to equation (4.6) the current associated with a magnetic dipole source is:

$$\bar{j}_s(\bar{x}, t) = c\bar{m} \times \text{grad } \delta(\bar{x} - \bar{v}t), \quad (6.3)$$

where  $\bar{x}'$  has been set equal to  $\bar{v}t$ . Equation 6.3 gives the current of a dipole source moving with velocity  $\bar{v}$ . An interesting result follows immediately from equations 6.2 and 6.3. If the magnetic moment  $\bar{m}$  of the source is parallel to the z axis, the right hand of 6.2 vanishes. This means that a magnetic dipole parallel to the external magnetic field does not excite shear Alfven waves.

Equation 6.2 can be simplified by observing that

$\vec{j}_s$  is solenoidal, so that its transverse divergence equals minus the  $z$  derivative of its  $z$  component. Since the right hand side of 6.2 is a two-dimensional divergence,  $\vec{E}_A$  is a two-dimensional gradient.

$$\text{Let } \vec{E}_A = \nabla_T \frac{\partial \phi}{\partial t}. \quad (6.4)$$

Then

$$\left( \frac{\kappa_{11}}{c^2} \frac{\partial^2}{\partial t^2} - \frac{\partial^2}{\partial z^2} \right) \nabla_T^2 \phi = \frac{4\pi}{c} \frac{\partial}{\partial z} \left( -m_x \frac{\partial}{\partial y} + m_y \frac{\partial}{\partial x} \right) \delta(\vec{x} - \vec{v}t). \quad (6.5)$$

Equation 6.4 shows that  $\nabla_T \phi$  is proportional to a vector potential, since in the absence of longitudinal electric fields, the electric field may be written:

$$\vec{E} = - \frac{1}{c} \frac{\partial \vec{A}}{\partial t}. \quad (6.6)$$

Thus the vector potential is  $-c\nabla_T \phi$  plus an arbitrary gradient. We choose the gauge in which

$$\vec{A} = c \frac{\partial \phi}{\partial z} \hat{z}, \quad (6.7)$$

and the magnetic field of the Alfvén wave is given by:

$$\vec{B}_A = \text{curl } \vec{A} = c \hat{z} \times \nabla_T \frac{\partial \phi}{\partial z}. \quad (6.8)$$

Equations 6.4 and 6.8 show that the fields of the wave are transverse to the ambient magnetic field, as expected. Appendix V derives the explicit solution of 6.5 for velocity directed along the  $x$  axis:

$$\phi(\vec{x}, t) = \frac{1}{c} \text{sgn}(z) \frac{-m_x y + m_y (x - vt + v|z|/u)}{(x - vt + v|z|/u)^2 + y^2} \quad (6.9)$$

where  $u = c/\sqrt{K_{11}}$  is the Alfvén speed.

The electric and magnetic fields are therefore (for  $z > 0$ ):

$$\begin{aligned}\bar{E}_A &= -v \nabla_T \frac{\partial \phi}{\partial x} = \frac{-u}{c} \nabla_T A \\ \bar{B}_A &= \frac{vc}{u} \hat{z} \times \nabla_T \frac{\partial \phi}{\partial x} = \sqrt{K_{11}} \bar{E}_A \times \hat{z}\end{aligned}\quad (6.10)$$

The flux of energy is given by the Poynting vector since the waves are non-dispersive, and this is clearly parallel to the  $z$  axis and proportional to  $E_A^2$ . However, the integral over an area transverse to the flux does not converge because of the singularity in  $\phi$  at  $x-vt+v|z|/u=0$  and  $y=0$ . The infinity must be treated by going over from an infinitesimal to a finite source.

## 6.2 WAVES FROM A FINITE SOURCE

Since the equations are linear, one may take linear combinations of the sources and the same linear combinations of the fields to find the waves produced by any source whatsoever. For example, if the source current is given by equation 4.2 with an arbitrary magnetization density  $M = M(\bar{x} - \bar{v}t)$ , then the electric field  $\bar{E}_F$  for a finite source is given in terms of the field  $\bar{E}_A$  for an infinitesimal source by:

$$\bar{E}_F(\bar{x}, t) = \frac{\int d^3x' M(\bar{x}') \bar{E}_A(\bar{x} - \bar{x}', t)}{\int d^3x' M(\bar{x}')} \quad (6.13)$$

Note that if  $M(\bar{x}) = \delta(\bar{x})$ ,  $\bar{E}_F = \bar{E}_A$  as desired.

The above integral, for reasonable functions  $M(x)$ , "smears out" the singularity in  $E_A$  such that  $E_F$  produces a finite energy flux. The vector potential  $A_F$  for a finite source is obtained from the potential  $A$  for the infinitesimal source in precisely the same way as the fields are. In obtaining  $A_F$ , it is convenient to modify the form of  $A$ . Equation 6.7 and 6.9 yield the result (for  $z > 0$ ):

Let  $X = x - vt + v|z|/u$  and  $X' = x' + v z'/u$ .

$$\begin{aligned} A &= c \frac{\partial \Phi}{\partial z} = \frac{vc}{u} \frac{\partial \Phi}{\partial x} = \frac{v}{u} \frac{\partial}{\partial x} \left\{ \frac{-m_x y + m_y X}{X^2 + y^2} \right\} \\ &= \frac{v}{u} \left( -m_x \frac{\partial}{\partial y} + m_y \frac{\partial}{\partial x} \right) \left\{ \frac{X}{X^2 + y^2} \right\} \end{aligned} \quad (6.14)$$

Thus  $A$  assumes the form (for  $z > R$  so  $|z - z'| = z - z'$ ):

$$A_F = \frac{v}{u} \left( -m_x \frac{\partial}{\partial y} + m_y \frac{\partial}{\partial x} \right) \frac{\int d^3 x' M(\bar{x}') \frac{X - X'}{(X - X')^2 + (y - y')^2}}{\int M d^3 x} \quad (6.15)$$

The integration is over a sphere of radius  $R$ .

When the source speed  $v$  is small compared to the Alfvén speed  $u$ , and  $M(\bar{x})$  is a function of radius only, then  $A_F$  can be written in a simpler form.

Appendix VI shows that for  $z > R$ ,

$$A_F = \frac{v}{u} \left( -m_x \frac{\partial}{\partial y} + m_y \frac{\partial}{\partial x} \right) \left\{ \frac{X}{X^2 + y^2} G(r) \right\} \quad (6.16)$$

$$\text{where } G(r) = \begin{cases} 1 - \frac{\int_0^R \frac{M(s)s \sqrt{s^2 - r^2} ds}{R M(s)s^2 ds} & , r \leq R \\ 0 & \\ 1 & , r \geq R \end{cases}$$

and  $r \equiv \sqrt{x^2 + y^2}$ .

### 6.3 ENERGY FLUX

For sufficiently "smooth" functions  $M(s)$ ,  $G(r)$  is a continuous, differentiable function, in terms of which one may write the radiated Alfvén power. The Poynting vector may be written as:

$$\bar{S} = \frac{c}{4\pi} \bar{E} \times \bar{B} = \frac{u}{4\pi} |\nabla_{\mathbf{T}} A|^2 \hat{z} \quad (6.17)$$

So the power radiated in Alfvén waves along one flux tube emanating from the source is:

$$P = \frac{u}{4\pi} \int dx \int dy |\nabla_{\mathbf{T}} A|^2 \quad (6.18)$$

Appendix VII shows that 6.16 and 6.18 may be combined into the form:

$$P = \frac{1}{16} \frac{v^2}{u} \frac{3m^2}{R^4} \frac{y^2 + m^2 x^2}{R^4} \int_0^\infty s \left\{ 3 \left[ \left( \frac{G(s)}{s} \right)' \right]^2 + \left[ \left( \frac{G(s)}{s} \right)'' \right]^2 s^2 \right\} ds \quad (6.19)$$

The expression inside the integral is a dimensionless function dependent on the shape of  $M(r)$ : Since  $G(s)$  is known for  $s > 1$ , the integral may be evaluated for the range  $(1, \infty)$ , and it turns out to be 12. The portion of the integral between 0 and 1 requires an assumption

about the form of  $M$ . However we may apply the calculus of variations to find a minimum value of this integral. We require that  $G(s)$  and its first derivative be continuous at  $S = 1$ , and that  $G(s)$  be bounded at the origin. Solving the relevant Euler equation (see Appendix VII) and evaluating the integral for the minimizing function leads to the value 4. Thus we may put a lower limit on the radiated Alfvén power:

$$P > P_{\min} = \frac{v^2}{u} \frac{3m_y^2 + m_x^2}{R^4} \quad (6.20)$$

It is of interest to investigate the extent to which this inequality is exceeded for reasonable functions  $M(r)$ . The shape of  $M(r)$  is roughly dictated by the requirement that the induction currents should maximize near the surface of the core of  $I_0$  at  $r = R$ . The simplest function for  $M$  would be  $M = 1$  for  $r < R$  and  $M = 0$  for  $r > R$ . By equation 4.2, this would be equivalent to a delta function surface current at  $r = R$ . This would be produced by a perfectly conducting sphere of radius  $R$ . It follows easily that  $G(s) = (1 - (1 - s^2)^{3/2})/s$ . But the second derivative of this function contains the term  $(1 - s^2)^{-1/2}$  and the integral in 6.19 would diverge. Perhaps this is not surprising for a perfect conductor. If in fact the conductivity is finite, there will be a finite slope to  $M(r)$  at  $r = R$ . We therefore try simple functions for  $M$  which maximize at  $r = 0$  and fall monotonically to zero at  $r = R$ . A class

of such functions is given by

$$M(r) = \begin{cases} M_p \left[ 1 - (r^2/R^2)^p \right] & , r < R \\ 0 & , r > R \end{cases}$$

(Note that this class of functions tends to the function  $M = 1, r < R; M = 0, r > R$  as  $p$  tends to infinity.)

For simplicity we choose the functions given by  $p = 1$  and  $p = 3$ . These functions and their derivatives (proportional to the associated current densities) are plotted in figure 5. For  $p = 1$ , the induction current rises linearly from zero at the center to a maximum at  $r = R$ . For  $p = 3$ , the current density rises as  $r^5$  from the center, peaking sharply at  $r = R$ .

The functions  $G(s)$  and its derivatives are written out in Appendix VII. Numerical integration of the integrals in 6.19 yield the result that  $P(p=1)$  and  $P(p=3)$  exceed the minimum value of  $P$  by the ratios:

$$P(p=1)/P_{\min} = 2.54$$

$$P(p=3)/P_{\min} = 1.38$$

Thus the power radiated in Alfvén waves is of the order of:

$$P = 2 \frac{v^2}{u} \frac{3m_y^2 + m_x^2}{R^4} \quad (6.21)$$

From the earlier chapters, we have the values

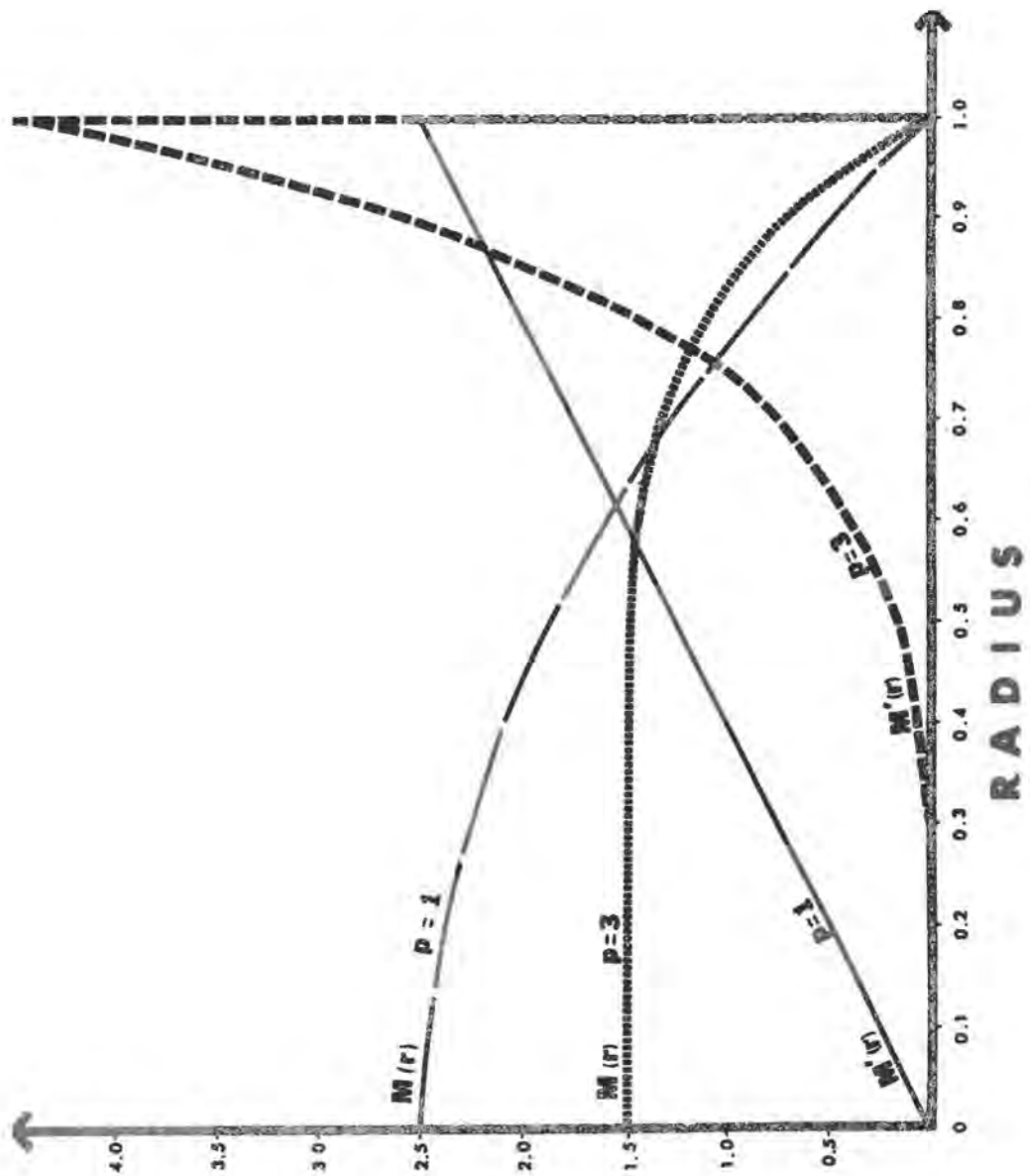


Figure 5

Two model profiles of effective magnetization density  $M(r)$  and their associated current densities.  $M(r) = A(1 - (r^2/R^2))$ , where the constant  $A$  is determined by normalization. The current is given by  $\vec{j} = c\hat{\phi} \sin \theta M'(r)$ , where  $\hat{\phi}$  is a unit vector in the azimuthal direction and  $\theta$  is co-latitude measured from the direction of magnetization.

$v$  = speed of  $I_0$  relative to field lines = 56 km/s

$u$  = Alfven speed  $\approx 10^{10}$  cm/s

$B_0$  = ambient field  $\approx 0.05$  G

$R$  =  $I_0$  radius  $\approx 1700$  km

We may assume that  $m \sim (\delta B_0) R^3$  where  $\delta B_0$  is the perturbation magnetic field. If this is 25 percent of the ambient field, then inserting the above values,

$$P \sim 8 \times 10^9 \text{ watt}$$

The form of equation 6.21 for the radiated Alfven power can be derived qualitatively. First consider the total energy of a magnetic dipole of moment  $m$  and radius  $R$ . This is  $m^2/R^3$ , as may be shown by integrating the magnetic field energy over all space. Next consider the rate at which this magnetic energy passes through the medium. This is  $V/R$ . Thus the power radiated must be some dimensionless quantity times  $(m^2/R^3)(V/R)$ . One expects the Alfven speed  $u$  to enter, and the only dimensionless ratio that may be constructed from  $m$ ,  $R$ ,  $v$ , and  $u$  is  $v/u$  to some power. Reasoning from analogy with the radiation from electric and magnetic dipoles in vacuo, (see Jackson 1962) one expects  $P$  to be proportional to  $v^2$  when  $v$  is small compared to the signal speed  $u$ . Thus the power of  $v/u$  must be one and  $P \sim (v/u)(v/R)(m^2/R^2)$ , which is equation 6.21. (When  $v$  approaches  $u$ , the derivation of 6.21 breaks down, and another dimensionless function of  $v/u$  enters, but this

must be determined by a complicated integration which we have not attempted.)

Figure 6 uses equation 6.21 and the approximation  $m = (\delta B_0) R^3$  to plot the Alfvén power against the magnetic field strength and the particle density at Io's orbit. (The boundaries to the diagram indicate some of the weak constraints on  $B_0$  and  $N$  calculated in Chapter II. Also indicated are the limits of the collisionless regime and the large Alfvén speed approximation.) The horizontal and vertical dotted lines indicate the working estimates of  $B_0$  and  $N$  used in this thesis.

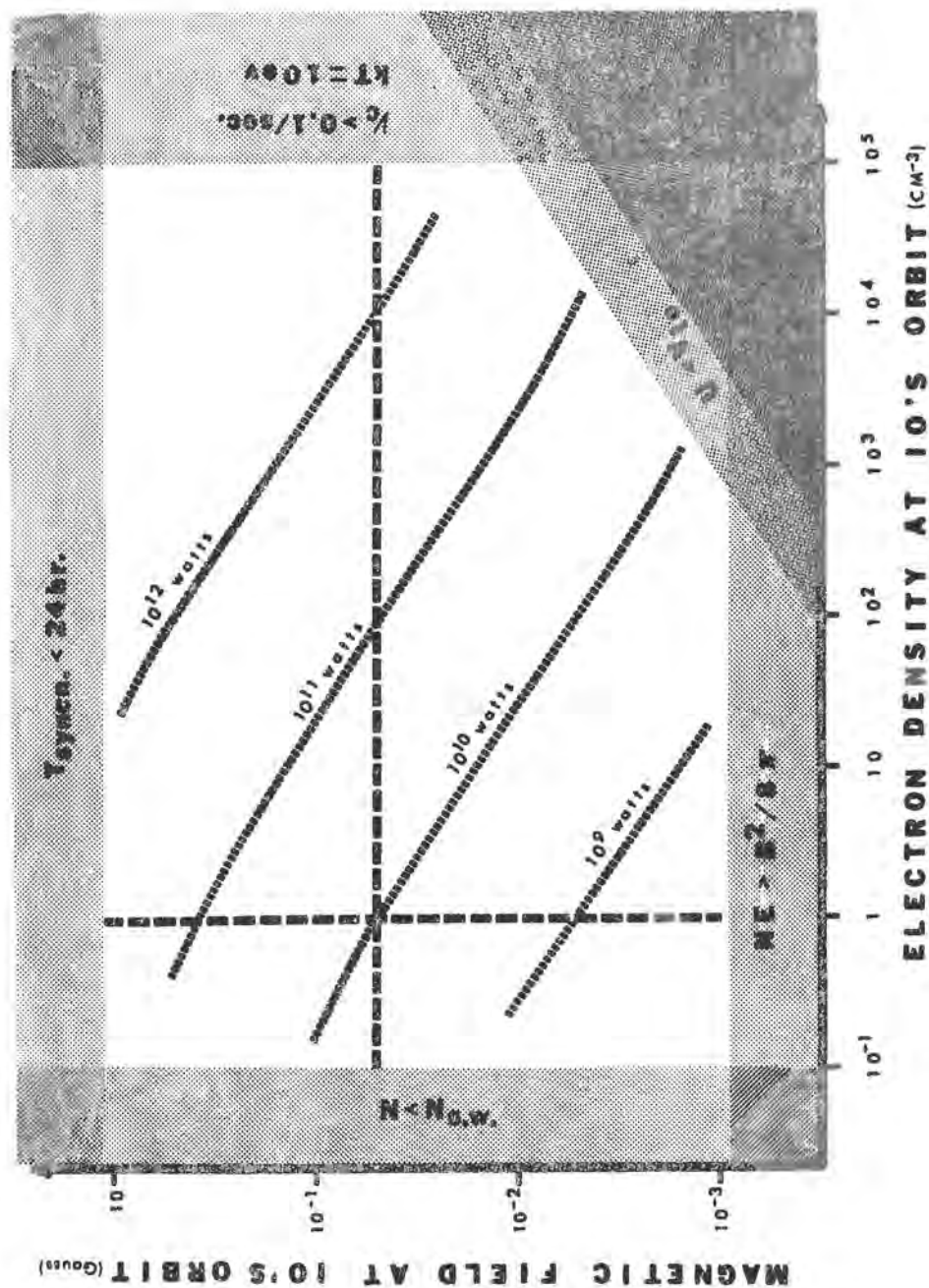


Figure 6

Isopleths of peak Alfvén power from Io for a centered Jovian dipole tilted at 10°. (See chap. VII.) The borders indicate limits discussed in sections 2.1, 2.2, 6.2, and 5.1. The straight dashed lines give the field strength and maximum density estimates of sections 2.2 and 2.5.

CHAPTER VII  
AN INDUCED DIPOLE MOMENT IN IO

7.1 LARGE-SOURCE EFFECTS

The last chapter derived an expression for the Alfvén power generated by a moving magnetic dipole. This derivation is strictly correct only for a dipole sufficiently small that the flow passes undisturbed by collisions with the body itself, or by fields generated by other effects. The method of derivation is good only for source currents which lie in the plasma itself, or for "point" sources. However, the formulas of chapter VI are certainly good to within some dimensionless factor multiplying the source terms in the equations for fields or for power. Such a factor would contain the effects of geometry and "current imaging" between the large magnetic source and the surrounding plasma. The factor cannot be calculated without going into the nonlinear equations describing the local flow and currents, so no attempt will be made to estimate it.

7.2 MAGNETIC FIELD SEEN BY IO

Since the field of Jupiter is not cylindrically symmetric with respect to its rotation axis, Io will see a time varying field as it goes around its orbit. The inclination of Io's orbit to Jupiter's equatorial plane is about  $0.03^\circ$  and the orbit's eccentricity is less than

.001 (de Sitter, 1931). If Jupiter's field is purely a centered dipole tilted at  $10^\circ$ , then Io will see fluctuations of  $\pm 26$  per cent in the ambient field. The period of these variations is half the time for Jupiter to rotate beneath Io, or six hours.

There is evidence that the field of Jupiter's southern hemisphere is stronger (Warwick, 1967), which might mean that Jupiter's dipole is shifted toward the south from the center, or that there are higher multipole moments of the field causing this. In order to illustrate the effects of displacement of the dipole in addition to a tilt, we have calculated the field seen by Io for an arbitrary displacement along the rotation ( $z$ ) axis. Following Warwick (1963), let the dipole lie in the  $xz$  plane, a height  $z = z_N$  above Io's orbit. The co-latitude of Io remains constant at the angle  $\beta = \arctan (-z_N/R_I)$ . This quantity is less than  $\arctan (1/6) = 9.5^\circ$ . Let the tilt angle of Jupiter's dipole be  $\alpha = 10^\circ$ . Appendix VII derives the following approximate equations for the magnetic field at azimuth  $\phi$  measured from the  $xz$  plane:

$$\begin{aligned}
 B_x &= \frac{3M}{R_I^3} \cos \phi (\sin \beta + \cos \phi \sin \alpha) \\
 B_y &= \frac{3M}{R_I^3} \sin \phi (\sin \beta + \cos \phi \sin \alpha) \quad (7.1) \\
 B_z &= \frac{-M}{R_I^3}
 \end{aligned}$$

Terms of order  $\alpha^2$  or  $\beta^2$  have been neglected. When these fields are averaged over azimuth, one gets the mean field seen by Io. If these mean components are subtracted from the above, one obtains the fluctuating parts of the field:

$$\begin{aligned} B_x - \langle B_x \rangle &= \frac{3M}{R_I^3} (\sin \beta \cos \phi + \frac{1}{2} \sin \alpha \cos 2 \phi) \\ B_y - \langle B_y \rangle &= \frac{3M}{R_I^3} (\sin \beta \sin \phi + \frac{1}{2} \sin \alpha \sin 2 \phi) \\ B_z - \langle B_z \rangle &= 0 \end{aligned} \quad (7.2)$$

Again second order terms have been neglected. A probable upper limit to  $\beta$  is given by the data of Roberts and Ekers (1966) who determined that the centroid of DIM emission lay within two seconds of arc in right ascension and ten seconds of arc in declination from Jupiter's center (Warwick, 1967). In terms of Jupiter radii these are .10 and .52, respectively. Thus  $\beta$  is probably less than  $\arctan (.52/6) = 5.0^\circ$ . For  $\alpha = 10^\circ$ , the amplitude of the "displacement" terms in equations 7.2 to the "tilt" terms therefore satisfies:

$$\frac{2 \sin \beta}{\sin \alpha} \lesssim 2 \frac{.087}{.174} = 1.0 \quad (7.3)$$

Note that the "tilt" terms in 7.2 have twice the frequency of the "displacement" terms. This means that the displacement will cause an enhancement of the field

when Io is closest to one end of Jupiter's dipole, and a partial cancellation when Io is closest to the other end.

If the ratio of the two effects is one, as in 7.3, the peak-to-peak variation of Jupiter's field at Io's orbit would be 72 percent of the mean field. If there are quadrupole components to the field or equatorial displacements of the field center, Io will see additional variations in the field. The DIM data of Branson (1968) seem to show a small degree of asymmetry in the radial direction, which Carr and Gulkis (1969) interpret as a field enhancement of  $\lambda_{III} 190^\circ$ , which is only a few degrees from the longitude of the northern end of the dipole. This would increase the variation field at Io by an unknown, but perhaps appreciable, amount.

### 7.3 INDUCTION EFFECTS IN IO

In the reference frame of Io, the magnetic field will vary with periods of 6 or 12 hours. If the interior conductivity of Io is sufficiently large, eddy currents will develop inside in such a way as to cancel the time varying components of the field. These currents will cause Io to act as a very slowly time-varying dipole moving through the plasma. The amplitude of the currents depends on the amplitude of the variation field and the interior conductivity.

A very similar effect for the case of earth's moon moving in the time-varying interplanetary field was

calculated by Sill and Blank (1969). The core conductivities are based on thermal models of the moon by England, et al. (1968). The maximum conductivity in the lunar interior for a young, cold moon is  $10^{-2}$  mho/m, and for the old, hot moon with partial melting it is  $10^2$  mho/m.

The relevant parameter for the problem of diffusion of a magnetic field into a conductor is the Cowling time. The longest time of decay of a magnetic field in a uniform sphere of radius  $a$  is  $\mu\sigma a^2/\pi^2$ , (Cowling, 1957), where the quantities are expressed in MKS units. For a radius of 1700 km, the conductivities above yield Cowling times in the range of 3 hours to 4 years. These times are of the same order as, or much larger than, the periods of variations of Jupiter's field as seen by Io.

Sill and Blank compute the reflection coefficient  $R$ , which is the ratio of the induced (polar) dipole field to the external uniform field.  $R$  is proportional to the magnetic moment  $M$ .

$$\vec{M} = \hat{z} R \frac{B_o a^3}{2} \quad (7.4)$$

$$0 \leq |M| \leq B_o a^3 / 2 \quad (7.5)$$

Figure 7 shows the magnitude and phase of  $R$  against conductivity, for  $a = 1700$  km and period = six hours. If the conductivity is greater than 0.1 mho/m,  $|R|$  is greater than one-half and the magnetic moment is comparable to the maximum value that it can be. If the

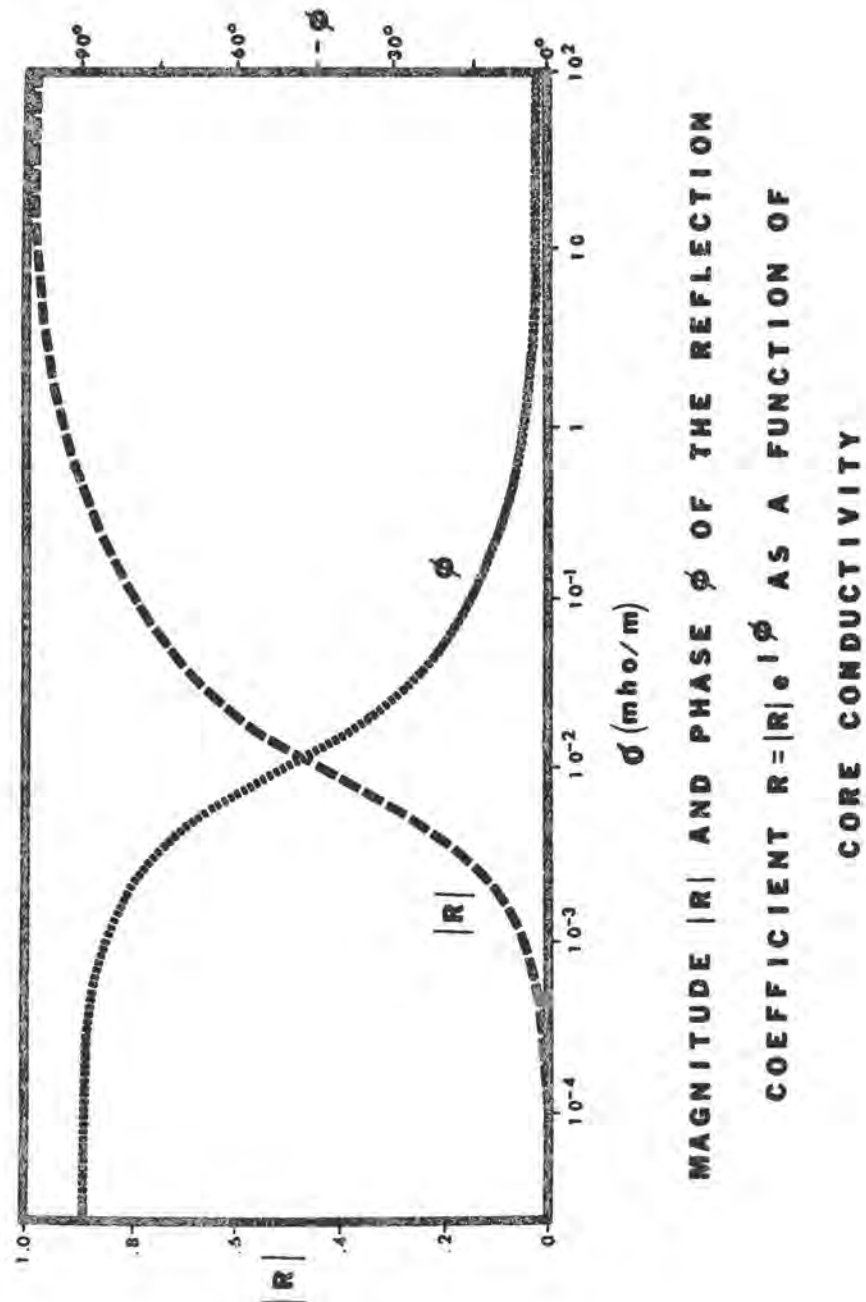


Figure 7

Reflection coefficient  $R$ , giving the ratio of the induced field to the inducing field  $B_0$ , is plotted against core conductivity. The induced dipole moment is proportional to  $R$  and reaches a maximum of  $B_0 a^3/2$ , where  $a$  is the core radius, when the conductivity is very large. This figure is derived from Sill and Blank (1969).

conductivity is less than this, the magnetic moment is very much smaller, and the model is not relevant as an Io-effect mechanism.

#### 7.4 APPLICATION TO IO

The very slow variation of the magnetic moment of Io as it moves from one quadrant of its orbit to the next is negligible in calculating the power that it radiates. We may therefore take the magnetic moment given by 7.4 where  $B_0$  is the time-varying component of the magnetic field as seen by Io. The behavior of the power radiated is very simple for the case of a centered dipole. In that case, Equation 7.2 shows that the magnetic moment rotates at exactly twice the rate that Jupiter rotates beneath Io. The moments due to the tilt of the field, parallel and perpendicular to Io's velocity are:

$$M_{\parallel}^T = -R \frac{a^3}{2} \cdot \frac{3}{2} \frac{M}{R_J^3} \sin \alpha \sin \phi$$

$$M_{\perp}^T = R \frac{a^3}{2} \cdot \frac{3}{2} \frac{M}{R_J^3} \sin \alpha \cos \phi$$
(7.6)

In this case the magnitude of the moment remains constant in time, while the direction rotates around Io.

A displacement of Jupiter's dipole along the z axis adds the following moments to the above:

$$M_{\perp}^D = 0$$

$$M_{\perp}^D = R \frac{a^3}{2} \frac{3}{2} \frac{M}{R_I^3} \sin \beta \quad (7.7)$$

Thus the displacement along the  $z$  axis contributes only (in first order) to the transverse magnetic moment. The quantity  $M/R_I^3$  in Equations 7.6 and 7.7 is the ambient magnetic field strength in the equatorial plane.

Figure 8 shows the relative shear Alfvén power radiated by Io as a function of Io's azimuth from the plane of Jupiter's dipole ( $\lambda_{III} 198^\circ$ ) for five different displacements of the dipole from Jupiter's center. Note that when the dipole is displaced in the southern hemisphere, the energy flux peaks when the northern end of Jupiter's dipole points toward Io; on the other hand, when the dipole is displaced to the north, the peak power is  $180^\circ$  out of phase. Since Dulk's (1965) observations show that the northern end of Jupiter's dipole must lean toward Io for the main and early-source Io-related emission to occur, this mechanism for the Io-effect is inconsistent with a displacement of Jupiter's dipole to the north. If future high-resolution observations of the DIM emission indicate that the centroid of emission is north of Jupiter's center, then this model can be ruled out.

The width of the peaks in Figure 8 cannot be

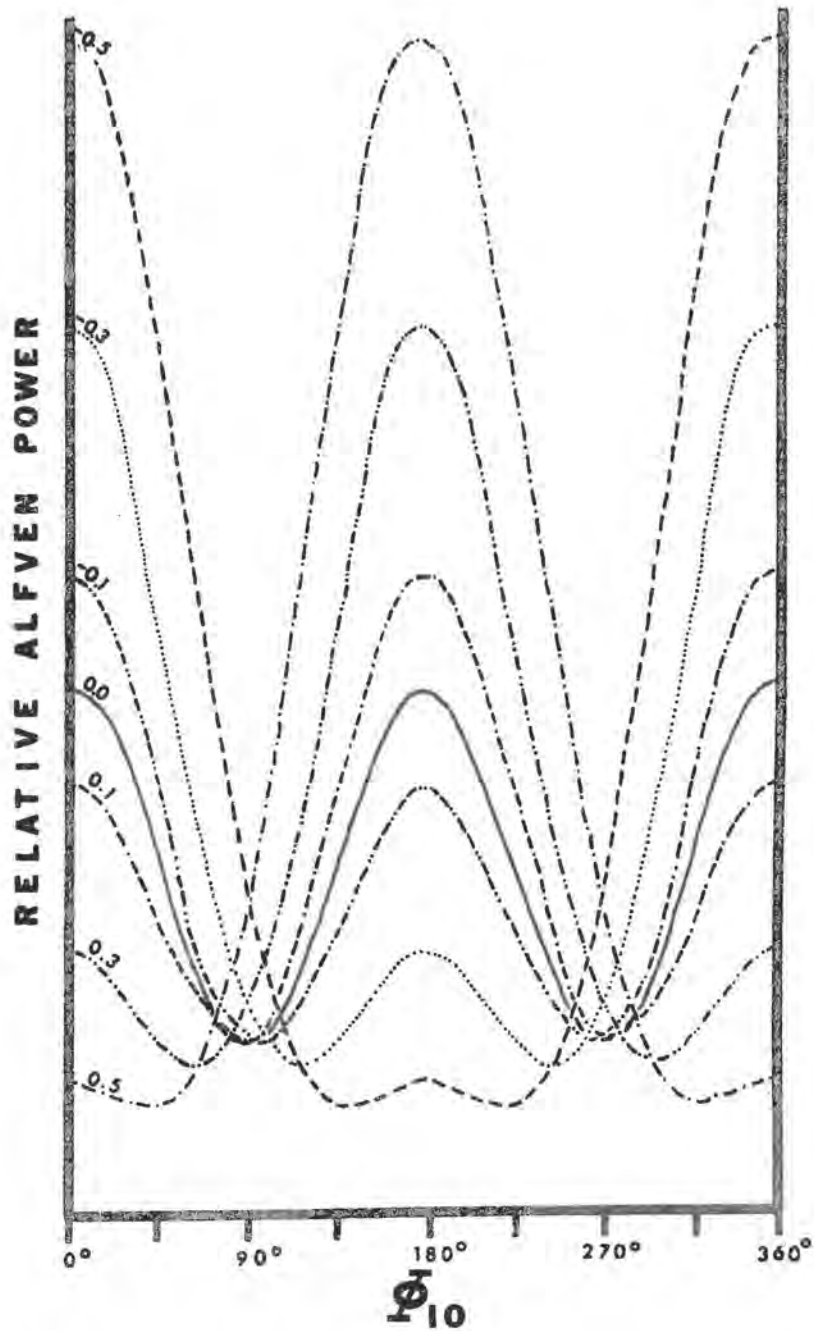


Figure 8

The relative flux of energy in shear Alfvén waves for seven different axial displacements of Jupiter's dipole from its center. The displacements are labeled (in units of Jupiter's radius) next to the left axis. The horizontal coordinate is the zenomagnetic longitude of Io, measured from the longitude of the northern end of Jupiter's tilted dipole.

related to the width of the peaks in a plot of DAM emission probability against Io azimuth, since those widths are much smaller and have been attributed to beaming effects (Dulk, 1965).

This model does not easily account for the  $15^\circ$  asymmetry in the Io azimuths during the Io-related emission. In their model, Goldreich and Lynden-Bell argue that the flux tube connecting Io to the ionosphere is dragged back relative to Io by  $15^\circ$ , but no such distortion is likely to result from the flow of Alfvén waves. If the Alfvén waves reach the DAM emission region at the time a flux tube has moved  $15^\circ$  in longitude, the mean Alfvén speed would have to be extremely low, about 400 km/s--much too low for the possible ranges of density and field shown in Figure 6. Perhaps a local inhomogeneity like that associated with the longitude dependence of the Io-unrelated DAM emission is an explanation of the asymmetry.

CHAPTER VIII  
TRANSPORT ALONG FIELD LINES

8.1 DAMPING OF HIGH WAVENUMBERS

The terms of the dielectric tensor that lead to collisionless damping were first investigated by Landau (1946) in the case of no magnetic field. The waves that were damped were electrostatic and longitudinal in nature. However even transverse waves can be damped by collisionless processes. This is shown by the dispersion relation for shear Alfvén waves including thermal effects at frequencies low compared to the electron gyrofrequency.

$$k_z^2 = \frac{\omega^2}{c^2} K_{11}(k_z, \omega) \quad (8.1)$$

where 
$$K_{11} = 1 + i \frac{\pi n_i^2}{\omega \Omega_i} \left[ i - a F(a) \right] \quad (8.2)$$

and 
$$F(a) = \frac{-i}{\sqrt{\pi}} \oint \frac{e^{-z^2}}{z-a} dz \quad (8.3)$$

The contour of integration must be that chosen by Landau (1946), i.e., the contour is deformed to encircle the singularity from below (above) for propagation in the plus (minus) Z direction. F is an entire function of its complex argument a.

$$a = -\sqrt{\frac{M}{2KT}} \frac{\Omega_i}{k_z} \quad (8.4)$$

This is the reciprocal of the product of wavenumber and

the ion gyroradius.  $\pi_i$  is the ion plasma frequency and  $\Omega_i$  is the ion gyrofrequency.

Generally  $a$  is very large and  $F$  assumes its asymptotic form:

$$F(a) \rightarrow \sqrt{\pi} \operatorname{sgn} k_z e^{-a^2} + \frac{i}{a} \approx \frac{i}{a} \quad (8.5)$$

In that case  $K_{11}$  is purely real and simply the ratio  $c^2/u^2$ , where  $u$  is the Alfvén speed. But at high temperatures or large wavenumbers, 8.5 is not a good approximation. The first term of 8.5 leads to damping. This damping is equivalent to a limit on the magnitude of  $k_z$  in the complex plane satisfying Equation 8.1. Wavelengths smaller than a certain value cannot even exist. This follows from the fact that  $F$  is an entire function and has its maximum magnitude of  $\sqrt{\pi}/2$  at the origin. Thus 8.1 and 8.2 imply that:

$$\begin{aligned} \sqrt{\frac{2kT}{M}} \frac{c^2}{\pi_i^2 \omega} \left| k_z^3 + k_z \frac{\omega^2}{c^2} \left( \frac{\pi_i^2}{\omega \Omega_i} - 1 \right) \right| \\ = |i F(a)| < \sqrt{\pi}/2 \end{aligned} \quad (8.6)$$

When  $\omega/\Omega_i < (\pi_i/\Omega_i)^2 = 4\pi M N c^2/B^2$  (which is very well satisfied for our problem), the left hand side is greater than the cubic term alone. Thus

$$|k_z|^3 < \frac{\omega \pi_i^2}{c^2} \frac{\sqrt{\pi}}{2} \sqrt{\frac{M}{2kT}} = \frac{\sqrt{\pi \omega}}{2\pi_i} \left( \frac{v_i}{c} \right)^2 \frac{1}{D^3}, \quad (8.7)$$

where  $V_i$  is the ion thermal speed, and  $D$  is the Debye length. Therefore all wavelengths at low frequencies must be much greater than a Debye length. Inserting  $\omega \sim 10^{-1}$ ,  $kT = 10$  ev,  $N = 1 \text{ cm}^{-3}$  into the right hand side of 8.7 we find that the minimum wavelength is on the order of a kilometer. All disturbances on this scale are heavily damped, but waves of much larger length are unaffected.

These arguments show that if the damping terms are dropped by letting the temperature vanish in the equations, there is nothing to restrict high wavenumbers produced by a source. This throws into question the results of Sundaram (1969) and Arbell, et al. (1963) who have calculated the waves generated by a source in a zero-temperature plasma. Their calculations involve Fourier transforms in wavenumber space that give finite contributions from infinitely distant contours. But if there is even an infinitesimal temperature, the large wavenumbers will be exponentially damped, so their Fourier transforms will not be valid, even approximately, for a finite temperature plasma. This thesis has avoided the difficulty by keeping a non-zero temperature and then letting the frequency be small.

The damping rate  $k_i$  is obtained from Equation 8.1 with the asymptotic form 8.5 of  $F(a)$ . Let  $k_i$  be the imaginary part of  $k_z$  and assume  $|k_i| \ll |k_z|$ . The low frequency limit of  $k_i$  is (Stix, 1960):

$$k_i = \frac{\sqrt{\pi}}{2} \frac{\pi_i}{c} (1 + \Omega_i^2 / \pi_i^2)^{-1/2} a e^{-a^2} \quad (8.8)$$

For a density of  $1 \text{ cm}^{-3}$ , a field of .05 gauss, and a temperature of 10 ev,  $\pi_i \sim 10^3$ ,  $\Omega_i \sim 5 \times 10^2$ . At a frequency  $\omega \sim 10^{-1} \text{ sec}^{-1}$ , the Alfvén wavenumber is  $10^{-11} \text{ cm}^{-1}$  and  $|a| \sim 10^7$ . Thus  $k_i \sim \exp(-10^{14}) \text{ cm}^{-1}$ , and collisionless damping of the shear Alfvén waves is completely negligible.

## 8.2 FIELD CURVATURE

The calculations of Chapters V and VI assumed that the ambient magnetic field lines were straight. It is important to consider whether the Alfvén waves generated by  $I_0$  will travel around the curved lines of force. To do this it is necessary to formulate the problem in curvilinear coordinates which match the external, curl-free field. This has been in considerable generality by Bajwa and Srivastava (1969) and in somewhat less generality by Parker (1955). Let  $s$  be a coordinate along the field lines. Then if we ignore the dependence on the other coordinates and say that the density is independent of position we obtain Bajwa and Srivastava's equation for velocity perturbations  $v_3$  perpendicular to the field and to the field normal:

$$\frac{d^2 v_3}{ds^2} + \frac{1}{u} \frac{du}{ds} \frac{dv_3}{ds} + \frac{\omega^2}{u^2} v_3 = 0, \quad (8.9)$$

where  $u$  is the Alfvén speed and  $\omega$  is the wave frequency. Let  $W = \sqrt{u}$ . Then 8.9 can be written as:

$$\frac{d^2}{ds^2} (Wv_3) + \left( \frac{\omega^2}{u^2} - \frac{W''(s)}{W(s)} \right) (Wv_3) = 0 \quad (8.10)$$

This form shows that travelling wave solutions exist only if

$$K_{\text{WKB}}^2 \equiv \frac{\omega^2}{u^2} - u^{-1/2} \frac{d^2}{ds^2} u^{1/2} > 0 \quad (8.11)$$

The critical frequency  $\omega_c$ , below which waves will not carry energy around the curvature of the field is

$$\omega_c = \left( u^{3/2} \frac{d^2}{ds^2} u^{1/2} \right)^{1/2} \quad (8.12)$$

The behavior of this derivative depends on the latitude in the dipole field at which the source is radiating. Appendix IX shows that near the maximum extent  $L$  of a field line, the critical frequency is given by

$$\omega_c = \frac{u}{L} (1 - u^2/c^2)^{1/2} \frac{3}{\sqrt{2}} \left\{ \left( 1 - \frac{5}{6} \frac{s^2}{L^2} \right) - 5 \frac{u^2}{c^2} \cdot \frac{9}{2} \frac{s^2}{L^2} \right\}^{1/2} \quad (8.13)$$

The coordinate  $s$  is measured from the maximum extent of the line either northward or southward. Terms of order  $(s/L)^4$  have been neglected. When  $s = 0$  the critical frequency is  $0.5s^{-1}$  for a density of  $1 \text{ cm}^{-3}$  and field of .05 gauss. Waves of much lower frequency will not propagate beyond the bend of the field line, but

will be reflected partially and perhaps set up a standing oscillation in the outer portion of the flux tube. Eventually, however the energy will either be dissipated or be transmitted down the flux tube. Note that as  $I_0$  moves to higher geomagnetic latitudes in its orbit,  $\omega_c$  will decrease, perhaps allowing a larger flux of energy to flow down the field lines.

These calculations are very crude and not meant to give anything but order of magnitude estimates of the effects of curvature. The equations are derived from the WKB approximation, which is only accurate for wavelengths much smaller than the scale of the system. Thus these results can only give the trend of the critical frequency versus field and position. Accurate information on the critical frequency  $\omega_c$  for the Alfvén waves would require at least a numerical solution of the three dimensional system of equations derived by Bajwa and Srivastava (1969) for a point source of waves. Other effects, such as dispersion in shape of the wave pulse due to the finite size of the source will not even be discussed.

### 8.3 DENSITY EFFECTS

Parker (1955) has estimated the effect of density variations on Alfvén waves by using a WKB approach. (He takes  $u \ll c$  so that  $U = B (4\pi\rho)^{1/2}$ . For  $u \sim c$ , density effects will be less important.) For slowly

varying density, the WKB solutions for velocity and field perturbations are:

$$\begin{bmatrix} \mathbf{v} \\ \mathbf{B} \end{bmatrix} = \text{const} \times \begin{bmatrix} \rho^{-1/4} \\ \rho^{1/4} \end{bmatrix} \exp \left[ i\omega(t \pm \int \frac{ds}{u}) \right] \quad (8.14)$$

Even when the field varies with  $s$ , to this approximation, the wave amplitudes depend only on the density but weakly so. The density of Jupiter's magnetosphere probably does not vary so rapidly in the vicinity of Io's orbit that the wave amplitudes will be modified drastically by the effects included in Equation 8.14. Only if the density nearly vanishes somewhere along the field line would the Alfvén waves be greatly affected. This is conceivable if the trapped particles of the magnetosphere fall into outer and inner families as Melrose (1967) has suggested. In that case,  $v$  would increase without limit and the wave would become nonlinear or be modified or reflected. We will not speculate any further on this.

#### 8.4 ROTATIONAL EFFECTS

Kendall and Plumpton (1964) have shown the effects of rotation on MHD waves in a perfectly conducting fluid. The addition of the Coriolis acceleration to the momentum equation yields a new dispersion relation for the shear Alfvén waves. Let  $\omega_0$  be the rotation rate of the fluid, with rotation vector at an angle  $\theta$  to the uniform magnetic field. Then the frequency satisfies either of

two equations:

$$\omega^2 \pm 2\omega \omega_0 \cos \Upsilon - k_z^2 u^2 = 0$$

For Jupiter,  $\omega_0 \approx 2 \times 10^{-4} \text{ s}^{-1}$ , while  $\omega \approx 10^{-1} \text{ s}^{-1}$  so the rotational term is very small, and the phase velocity is:

$$\frac{\omega}{k_z} = u \left( 1 \pm \frac{\omega}{\omega_0} \cos \Upsilon \right)$$

Thus the shear Alfvén waves are split up into two modes of slightly different group velocity, but the same direction since  $\omega$  is still only a function of  $k_z$ . The relative change is only of order  $10^{-3}$  and negligible.

## CHAPTER IX DISCUSSION

### 9.1 ALFVEN WAVES INTO ELECTROMAGNETIC WAVES

It is not the purpose of this thesis to calculate the generation of DAM radiation from the interactions of the Alfvén disturbance with the plasma medium. However we will suggest a few avenues of approach to the problem.

The amplitude of the Alfvén waves becomes relatively smaller compared to the local field as the waves propagate down toward Jupiter, but the waves tend to steepen because the Alfvén speed is larger in the wave. Thus the waves may steepen into shocks (Warwick, 1967) and therefore nonlinear effects will play a role in their interaction with the plasma.

If the shear Alfvén waves propagate along the field lines, they are not likely to encounter high energy particles unless Io is in a radiation belt. If we consider the compressional waves, which start out radiating spherically from Io, or if the shear waves are deflected by curvature or rotational effects into lower L shells, then the Alfvén waves generated by Io may interact with the high energy belts. If so, then there are two types of cyclotron overstabilities that it might excite (Stix, 1962). The first depends on a pitch angle (or temperature) anisotropy which feeds on the wave. The power absorption is small unless the wave frequency is comparable to the

gyrofrequency. Such a case is possible if the wave steepening drastically shifts the frequency spectrum of the wave to peak at much higher values, (e.g. from  $10^{-1}$  to  $10^5$  Hz). The second instability depends on the Doppler-shifted frequency of the wave matching the gyrofrequency for a group of drifting electrons. The electrons absorb energy from the wave strongly only if their velocities are highly relativistic. There is a large amount of energy available in the radiation belts, up to a maximum on the order of  $4 \times 10^{-2}$  erg/cm<sup>3</sup>, according to equation 2.3. An Alfvén wave traveling through these belts may tap some of this energy, which may be radiated or dumped into the ionosphere, where reflection, mode conversion, and/or re-radiation may occur.

A large amplitude Alfvén wave will tend to drive gyrating charged particles before it if their transverse velocity (and therefore their magnetic moment) is small because the magnetic moment is an adiabatic invariant. This is the Fermi mechanism for particle acceleration, but its effects should be weak because particles of small magnetic moment will be few in number, most having leaked through the loss cone of Jupiter's dipole field. If the Alfvén waves accelerate particles by one means or another, there is a wealth of mechanisms by which electromagnetic radiation can be produced. For example, coherent-electron bunching (Goldreich and Lynden-Bell,

1969; Ellis and McCulloch, 1963; or Cerenkov emission (Warwick, 1963a).

Marshall and Libby (1967) have suggested that a disturbance might trigger spin-flip transitions in molecules of the ionosphere. Perhaps a propagating distortion of the magnetic field would be a suitable disturbance.

## 9.2 MODEL-TESTING AND OBSERVATIONS

It is important that many models of the Io-effect be presented and their consequences carried out as far as possible, so that there be adequate hypotheses to be compared with observations. The dynamo model of Goldreich and Lynden-Bell (1969) and the Alfvén-Generation model presented in this thesis might be tested indirectly by close observation of large earth satellites. The forthcoming space stations may be adequately large that the relevant dimensionless ratios are scaled properly. If these satellites cause dynamo currents or Alfvén waves, then the theories may be at least partially justified. The absence of such effects might only suggest that the properties of Io and Jupiter's magnetosphere are too different from those of earth satellites and earth's magnetosphere for similar effects to be produced.

A 10 eV proton will have an average gyro-radius of roughly 100 meters; thus for the small Larmor radius

approximation used in Chapter VII to be valid, the satellite must be on the order of 100 meters in diameter, unless the thermal energy is much smaller than 10 ev. The existence or non-existence of Alfvén waves generated by such a satellite could be tested by magnetometer observations near the feet of the magnetic lines of force which connect the satellite to the ionosphere. If dynamo currents are generated, there should be electron enhancements and perhaps electron auroras at the feet of the satellites' flux tube. Tiuri (1965) and Tiuri and Kraus (1965) have received radar reflections from electron enhancements in the ionosphere in the magnetic shell occupied by small earth satellites. Whether these enhancements are caused by waves or currents is unknown. To determine which is involved in the disturbance would probably require in situ measurements of the flux tube electric and magnetic fields by a second satellite. An Alfvén wave will have no longitudinal currents or fields, while an electron current should be associated with a longitudinal electric field. Since a satellite measuring such effects will be moving rapidly with respect to the flux tube connected to a larger, outer satellite, these phenomena may be difficult to observe.

Direct tests of the beaming hypothesis (Dulk, 1965) and the Alfvén-wave and dynamo models of the Io-effect could be made with a satellite-borne radio telescope at a distance on the order of one A.U. or more.

In the dynamo model the DAM emission occurs at all longitudes of Io except when Io is in the shadow of Jupiter. The beaming effect postulated by Dulk causes the radiation to be observed only when the emission cone passes through the radio telescope. When Io is in shadow no DAM bursts should be observed even when the telescope is in this emission cone because no photoelectrons can be liberated from Io's surface to produce dynamo currents. The emission should also be reduced steadily as Io's flux tube moves from the sunset to the sunrise zone of Jupiter's ionosphere, since the conductivity of the ionosphere should decrease as Jupiter's night progresses. It will probably be impossible to have a telescope in the cone at such times except on a Jupiter fly-by, but a Mars or Venus mission may provide sufficiently large angular separation from earth to observe some of these effects.

In the Alfvén-wave model, the radiation of the Io-related into the early and main sources should only be a function of the longitude of Io measured from  $\lambda_{III} 200^\circ$ , the plane of Jupiter's magnetic dipole moment. The emission should peak when this longitude is zero, and it should be one-third of this or less when the longitude is near  $= 90^\circ$ , assuming that the dipole of Jupiter is centered or displaced southward.

Suppose that it is shown that Jupiter's dipole is displaced southward slightly, and further suppose that a satellite telescope moves south of the ecliptic plane and

observes an emission cone directed from Jupiter's southern hemisphere. (Sulk, 1965, suggests that this cone does not intersect the ecliptic plane.) In this Alfvén wave model, the ratio of the strengths of the emission when the northern end and the southern end of Jupiter's dipole are tilted toward Io should be:

$$\frac{P_n}{P_s} = \frac{[M_{11}^2 + 3M_I^2]_{\phi=0}}{[M_{11}^2 + 3M_I^2]_{\phi=\pi}} = \left( \frac{\sin \alpha + \sin \beta}{\sin \alpha - \sin \beta} \right)^2 \quad (9.1)$$

(See equations 7.6 and 7.7). For a tilt angle of  $10^\circ$  and southward displacements of the dipole by 0.1, 0.2, 0.3, and 0.4 Jupiter radii, the ratio above would equal 1.5, 2.2, 3.4, and 5.2, respectively. If a ratio inconsistent with equation 9.1 is not found, then the model presented in this thesis may be ruled out. This assumes that the foot of Io's flux tube will excite all longitudes of Jupiter equally well, which may only be approximately true.

As yet there is no direct observational evidence that the feet of Io's flux tube are in any way different in character than the feet of the rest of the flux tubes. Although the size of the Io-related DAM source has been delimited, its position is unknown. In principle this position could be determined by careful radio interferometry. Such an observation would give a clear victory to Dulk's hypothesis that the Io-related emission comes from one particular flux tube. It is also possible that the foot of Io's flux tube would stand out against its

background at other wavelengths. Particular attention should be directed to this region in future high-resolution ultraviolet and infrared observations of Jupiter. Auroras may be produced preferentially by the disturbance in that tube, and these may be visible in Lyman-alpha or forbidden molecular lines in the U.V. Heating effects may also make this region radiate in the far infrared. It may be worthwhile attempting a ground-based infrared observation with high resolution in one of the atmospheric IR windows, say at 10 or 22 microns.

Future high resolution photographs of Jupiter should check Lyot's observation (Dollfus, 1961) that the Galilean satellites rotate synchronously. If a satellite has even small librations it should generate Alfvén waves which may well be stronger than the waves calculated in this thesis.

### 9.3 LIMITATIONS OF THIS MODEL

The major limitation of the calculations of Chapter VIII is that the source currents cannot be calculated exactly. It is possible only to calculate the currents inside  $I_0$  that are caused by induction effects. Currents in the plasma generated by the flow around  $I_0$  or particle collisions with  $I_0$  have not been calculated, and can only be determined by a fully nonlinear model. Such currents will also generate Alfvén waves.

Another limitation of the calculations is the neglect of high wavenumbers and the consequent lack of information about the waves in the close vicinity of the source. Inclusions of high wavenumber effects would almost certainly have to be obtained by use of a high speed computer to sum series of Bessel functions multiplied by plasma dispersion functions. The solution for transverse Alfvén waves that has been obtained is an asymptotic one, valid only far from the source where compressional wave effects have decayed away. If the compressional waves were calculated in detail it might be found that the disturbance near the source has magnetic moments of its own. If that were the case, then the waves could be found as functionals of arbitrary magnetic moment densities and the complete solution determined by iteration or invariant imbedding. Such computation is far beyond the scope of this thesis. However, it is plausible that the resultant Alfvén power in such a computation will be larger than we have calculated. The reasoning is as follows. A plasma is diamagnetic and generally acts such as to cancel out variations in the magnetic field. If the compressional waves alter the local source, they should act in such a way as to tend to cancel out the "external" field of the source inside of  $I_0$ . Such cancellation is equivalent to a current loop outside of  $I_0$  which is opposite to the interior loop. Thus the field lines which pass from the undisturbed

region into the disturbed region will undergo new bends or twists in addition to those already computed. The interior bends will not be altered by the external currents so the Alfvén waves can only be increased. The mathematics of the problem agrees with these qualitative arguments. An "image" current outside of  $I_0$  will make the magnetic moment density more like the limiting case of a spherical shell of Dirac delta magnetic moments, and for that case the Alfvén power diverges. Thus our neglect of any such moment density produced by the compressional waves yields a smaller radiated power than actually will exist.

Perhaps the most stringent limitation of our model is the neglect of global effects. In principle it is possible to calculate the generation of Alfvén waves by a current source in an arbitrary magnetosphere. However it is unclear how dependent on the properties of the magnetosphere the solution would be. The generation of shear Alfvén waves will be modified in some way by the inclusion of curved field lines and variable density. The compressional Alfvén waves which are generated may not be entirely attenuated by geometry, since as Parker (1955) has suggested, focussing effects can conceivably occur when the Alfvén speed is a function of position.

There are two major limitations on the extent to which the model presented here fits the observations. First is its inability to explain the asymmetry in the

position angles at which Io excites DAM emission. (See the discussion at the end of Chapter VII.) Second is the lack of explanation of the third and fourth sources which appear in the regions near  $\phi = -70^\circ$  and  $+60^\circ$  respectively. ( $\phi$  is the azimuth of Io measured from the longitude of Jupiter's north magnetic pole.) These sources, however, occur with frequency less by a factor of five or more than the early and main sources.

#### 9.4 OTHER SATELLITE EFFECTS?

The theory given in Chapters VI and VII would apply equally well to the other satellites of Jupiter, provided that the plasma density and field strengths are such that the medium is collisionless, and the rate of flow past the satellite is much lower than the plasma frequency and the ion gyrofrequency. The ion gyrofrequency at Callisto's orbit may be too low for this to be true.

Let  $a$  be the radius of the induced magnetic dipole in each satellite, and let the moment  $m \sim f B_J R_J^3 a^3 / r^3$ , where  $B_J$  is Jupiter's surface field,  $R_J$  is its equatorial radius, and  $r$  is the orbital radius of the satellite.  $f$  is some fraction of unity determined by the efficiency of the source. Then equation 6.21 gives for the Alfvén power generated by the satellite:

$$P \sim \frac{v^2}{u} f^2 (B_J R_J^3)^2 a^2 / r^6 \quad (9.2)$$

The Alfven speed  $u$  depends on the model of the magnetosphere. If we assume Melrose's (1967) equation for density determined by centrifugally dominated interchange instabilities (see equation 2.10) and a density of  $1 \text{ cm}^{-3}$  at Io's orbit,  $u$  will be roughly proportional to  $r^{-3}$ . For the moment we identify  $r$  with the satellite radius. Then for Io, Europa, Ganymede and Callisto, the values of  $r$ ,  $v$ ,  $u$ ,  $a$  lie in the proportions:

Distance	$r$	1 : 1.6 : 2.5 : 4.5
Velocity	$v$	1 : 2.0 : 3.2 : 5.7
Alfven Speed	$u$	1 : 1/4 : 1/16 : 1/90
Radius	$a$	1 : 0.86 : 1.48 : 1.40

Thus the power given by equation (9.1) gives the proportions for Io, Europa, Ganymede, and Callisto to be:

Alfven Power:	1 : 0.7 : 1.5 : 0.7
---------------	---------------------

These figures are no more than order of magnitude estimates. As stated in Chapter VIII the formula for power is an overestimate when  $v$  approaches  $u$ , which might be true for Ganymede and Callisto. The unknown factor  $f$  may be highly different for the four satellites. However these figures indicate that the other satellites may generate Alfven waves as well. The feet of their flux tubes will be at higher latitudes of Jupiter, so their emission cones in Dulk's (1965) theory will not intersect the ecliptic plane. It would therefore be highly profitable for satellite-based radio telescopes

to look for such emission out of the ecliptic plane.

The radiated power for Jupiter V will be very small because of its very small radius (estimated from its albedo to be only on the order of 100 km) and its nearly synchronous motion.

## 9.5 CONCLUSIONS

We have shown, under very weak assumptions about the nature of Io and its environment, that Io will have an induced dipole moment and will continuously generate transverse Alfvén waves which can carry energy of at least  $10^9$  watt into each flux tube down to the surface of Jupiter.

There is a variety of ways by which satellite radio telescopes can distinguish between this model and Goldreich and Lynden Bell's (1969) model of the Io effect, assuming that Dulk's hypothesis (1965) about the beaming of the radiation is correct.

When suitable models of Jupiter's magnetosphere become available, ray tracing effects should be considered in the propagation of compressional Alfvén waves to see if focussing effects can cause them to be of appreciable amplitude close to Jupiter's magnetosphere.

Much more work needs to be done on the interaction of large satellites with a magnetoactive plasma medium. There should be constant interplay between observational results of earth satellites and theoretical computations.

The problem of the Io-effect is far from closed. The wake problem, wave propagation, current generation, and particularly conversion of waves and currents into electromagnetic radiation will remain intriguing fields of research for years to come.

## BIBLIOGRAPHY

- Al'pert, Ya. L. 1965, *Space Sci. Rev.*, 4, 375.
- Al'pert, Ya. L. Gurevich, A.V., and Pitayevsky, L.P., 1963, *Space Sci. Rev.*, 2, 680.
- Arkel, E., Felsen, L.B., 1963, *Electromagnetic Theory and Antennas*, ed. E.C. Jordan, The Macmillan Co., N. Y., 391.
- Axford, W. I., 1964, *Plan. Spa. Sci.*, 12, 45.
- Bajwa, G.S., Srivastava, K.M. 1969, *Canadian Journal of Physics*, 47, 1001.
- Barker, D. 1966, *M. N.*, 133, 285.
- Barnes, A. 1966, *The Physics of Fluids*, 9, 1483.
- Barrow, C.H. 1964, *Icarus*, 3, 66.
- Berge, G.L. 1965, *Radio Science*, 69D, 1552.
- \_\_\_\_\_ 1966, *Astrophys. J.*, 42, 737.
- Bernstein, I.B., Trehan, S.K. 1960, *Nuclear Fusion*, 1, 3.
- Bigg, E.K. 1964, *Nature*, 203, 1008.
- Binder, A.B., Cruikshank, D.P., 1964, *Icarus*, 3, 299.
- Branson, N.J.B.A. 1968, *MNRAS*, 139, 155.
- Brice, N., Ioannidis, G. 1970, submitted to *Icarus*.
- Briggs, R.J. 1964, *Electron Stream Interactions with Plasmas*, MIT Press, Cambridge, Mass.
- Brouwer, D., Clemence G. 1961, *The Sun*, Vol. 3, ed. G.P. Kuiper, The University of Chicago Press, Chicago, Ill.
- Burke, B.F., Franklin, K.L. 1955, *J.G.R.*, 60, 213.
- Burns, J.A. 1968, *Science*, 139, 971.
- Carr, T.D., Gulkis, S. 1969, *Ann. Rev. of Ast. and Sp.*, 7, 577.

- Chandrasekhar, S., Kaufman, A.N., and Watson, K.M., 1957, Annals of Physics, 2, 435.
- Chapman, S. 1964, Solar Plasma, Geomagnetism, and Aurora, Gordon and Breach, N.Y.
- Chew, G.F., Goldburg, M.L., and Low, F.E. 1956, Proc. Roy. Soc., London, A 236, 112.
- Chopra, K. P. 1961, Planet. Spa. Sci., 5, 288.
- Cole, K.D. 1966, Space Sci. Rev., 5, 699.
- Cowling, T.G. 1957, Magnetohydrodynamics, Interscience Publishers, N.Y.
- Denisse, J.F., Delcroix, J.L. 1963, Plasma Waves, Interscience Publishers, N.Y.
- deSitter, W. 1931, Mon. Not. Roy. Astron. Soc., 91, 706.
- Dickel, J.R., Degioanni, J.J., and Goodman, G.C. 1970, Radio Sci., 5, No. 2, 517.
- Dollfus, A. 1961, The Sun, Vol. 3, ed. G.P. Kuiper, The University of Chicago Press, Chicago, Ill.
- Douglas, J.N. 1964, IEEE Trans. AP-12, 839.
- Drell, S.D., Foley, H.M., and Cuderman, M.A. 1965, J. Geophys. Res., 70, 3131.
- Dulk, G.A. 1965a, Io-Related Radio Emission from Jupiter (Ph.D. Thesis, Astro-Geophysics Dept., U. of Colorado, Boulder, Colo.).
- \_\_\_\_\_ 1965b, Science, 148, 1585.
- \_\_\_\_\_ 1965c, Astron. J., 70, 137.
- \_\_\_\_\_ 1967, Icarus, 7, 173.
- \_\_\_\_\_ 1970, The Astrophysical Journal, 159, No. 2, 671.
- Duncan, R.A. 1966, Plan. Spa. Sci., 14, 173.
- Dungey, J.W. 1961, Phys. Rev. Lett., 6, 47.
- Ellis, G.R.A. 1965, Radio Science, 69D, 1513.
- England, A.W., Simmons, G., and Strangway, D. 1968, J. Geophys. R., 73, 3219.

- Franklin, K.L., Burke, B.F. 1958, *J. Geophys. Res.*, 63, 807.
- Fried, B.D., Gould, R.W. 1961, *The Physics of Fluids*, 4, 139.
- Ginzberg, V.L. 1964, *The Propagation of Electromagnetic Waves in Plasmas*, Addison-Wesley Pub. Co. Inc., Reading, Mass.
- Ginzburg, V.L., Syrovntskii, S. 1965, *Ann. Rev. Astron. Ap.*, 3, 297.
- \_\_\_\_\_ 1969, *Ann. Rev. Astron. Ap.*, 7, 375.
- Gledhill, J.A. 1967, *Ionospheric Physics Preprint Series*, Goddard Space Flight Center, *Jupiter's Magnetosphere*, X-615-67-47.
- Goldreich, P., Lynden-Bell, D. 1969, *Ap. J.*, 156, 59.
- Gordon, M.A. 1966, Thesis, *The Polarization and Spectral Dependence of Fine Structure in Jupiter Radio Bursts* University of Colorado, Boulder, Colo.
- Gordon, M.A., Warwick, J.W. 1967, *Astrophys. J.*, 148, 511.
- Gringauz, K.I., et al. 1963, *Plan. Sp. Sci.*, 9, 21.
- Gurevich, A.V., Pitaevskii, C.P., and Smirnova, V.V. 1969, *Spa. Sci. Rev.*, 9, 805.
- Guthart, H. 1964, Stanford Research Institute, Menlo Park, Calif., (cited by Hutquist, 1966).
- Hones, Jr., E.W., Bergeson, J.E. 1965, *J.G.R.*, 70, 4051.
- Hultquist, B. 1966, *Spa. Sci. Rev.*, 5, 599.
- Ioannidis, G.A. 1970, *Electron Density Distribution in Jupiter's Magnetosphere and Radio Wave Measurements*, Master's Thesis, Cornell University.
- Ioannidis, G.A., Brice, N.M. 1970, *Plasma Densities in the Jovian Magnetosphere*, in preparation, 1970.
- Jackson, J.D. 1963, *Classical Electrodynamics*, John Wiley & Sons, Inc., N.Y.
- Kendall, P.C., Plumpton, C. 1964, *Magnetohydrodynamics*, Vol. 1, The Macmillan Co., N. Y.
- Komesaroff, N.M., McCulloch, P.M. 1967, *Ap. Letters*, 1, 9.

- Kovnlevsky, J. 1967, I.A. U. Transactions.
- Kozlovskaya, S.V. 1963, Bulletin of the Institute of Theoretical Astronomy, IX, no. 5, 330 (in Russian).
- Kristofesson, L. 1969, J.G.R., 74, 3, 906.
- Kuperus, M. 1965, Recherches Astronomiques de L'Observatoire D'Utrecht, XVII.
- Landua, L. 1946, Journal of Physics USSR, X, No. 1.
- Laplace P. (1805), Mécanique, Céleste, 4, 1, cited by Marsden, 1966.
- Lebo, G.R., Smith, A.G., and Carr, T.D. 1965, Science, 148, 1724.
- Legg, M.P.C., Westfold, K.C. 1968, Ap. J., 154, 499.
- Liemohn, H.B., Scarf, F.L. 1962, J.G.R., 67, 1785.
- Lighthill, M.J. 1960, Philosophical Trans. of Royal Society of London, 252, 49.
- Liu, V.C. 1969, Spa. Sci. Rev., 9, 423.
- Marsden, B.G. 1966, The Motions of the Galilean Satellites of Jupiter, Ph.D. Thesis, Yale University.
- Marshall, L., Libby, W.F. 1967, Nature, 214, 126.
- Mayer, C.H., McCullough, T.P., Sloanaker, R.M. 1958, Ap. J., 127, 11.
- Melrose, D.B. 1967, Planet. Spa. Sci. 15, 381.
- McCune, J.E., Resler, Jr., E.L. 1960, Journal of the Aero Space Sciences, 493.
- McDonough, T., Brice, N.M. 1970, Termination of the Solar Wind, in Preparation. (see Brice and Ioannidis.)
- Morris, D., Berge, G.L. 1962, Astrophys. J., 136, 276.
- Moroz, V.I., 1966, Sov. Astr. 9, 999.
- Ness, N.F., Behannon, K.W., Taylor, H.E., and Whang, Y.C. 1968, J.G.R., 73, No. 11, 3421.
- Parker, E.N. 1955, Phys. Rev., 99, No. 1, 241.
- Parker, G.O., Dulk, G.A., and Warwick, J.W. 1969. Astrophys. J., 157, 439.

- Patel, V.L. 1964, *Phys. Rev. Litt.*, 12, 213.
- Petschek, H.E. 1966, *The Mechanism for Recombination of Geometric and Interplanetary Field Lines*, The Solar Wind, ed. Robert J. Mackin, Jr., and M. Nevyekaver, J.P.L., C.I.T., Pasadena, California.
- Piddington, J.H., Hobart, J. 1969, Cosmic Electrodynamics, Wiley, N.Y.
- Piddington, J.H., Drake, J.L. 1968, *Nature*, 217, 935.
- Rather, J.D.G., Witting, J.M., unpublished, reported by Warwick, 1967.
- Richardson, P.D., Shum, Y.M., 1968, *Nature*, 220, 897.
- Roberts, J.A. 1965, *Radio Sci.*, 69D, 1543.
- Roberts, J.A., Ekers, R.D. 1966, *Icarus*, 5, 149.
- Roberts, J.A., Ekers, R.D. 1968, *Icarus*, 8, 160.
- Roberts, J.A., Komesaroff, M.M. 1965, *Icarus*, 4, 127.
- Sagalyn, R.C., Smiddy, M. 1965, cited by Cole (1966).
- Sears, W.R. 1960, *Reviews of Modern Physics*, 32, No. 1, 701.
- Sears, W.R., Resler, E.L. 1958, *J. Fluid Mech.*, 5, 257.
- Shain, C.A. 1956, *Aust. J. of Phys.*, 9, 61.
- Sherril, W.M. 1965, *Astroph. J.*, 142, 1171.
- Sill, W.R., Blank, J.L. 1969, *J.G.R.*, 74, 736.
- Slonaker, R.M. 1959, *Astrom. J.*, 64, 346.
- Solomon, S.C., Töksoz, M.N., 1968, *Phys. Earth Planet. Int.* 1, 475.
- Stepanov, K.N. 1958, *Soviet Physics JETP*, 34(7), No. 5, 892.
- Stix, T.H. 1962, The Theory of Plasma Waves, McGraw-Hill Books Co. Inc., N.Y.
- Sundaram, A.K. 1969, *Canadian Journal of Physics*, 47, 1.
- Taji, M. 1967, *Journal of the Physical Society of Japan*, 22, No. 6, 1482.

- Tiuri, M.E. 1965, *Nature*, 207, 1075.
- Tiuri, M.E., Kraus, J.D. 1965, *Astron. J.*, 70, 695.
- Ward, S.H. 1969, *Radio Science*, 4, No. 2, 117.
- Warwick, J.W. 1967, *Spa. Sci. Rev.*, 6, 841.
- \_\_\_\_\_ 1963a, *Astrophys. J.*, 137, 41.
- \_\_\_\_\_ 1963b, *Astrophys. J.*, 137, 1317.
- \_\_\_\_\_ 1963c, *Radio Astronomical Techniques for the Study of Planetary Atmospheres in Radio Astronomical and Satellite Studies of the Atmosphere*, ed. J. Aarons, North-Holland Pub. Co., Amsterdam, p. 400.
- Warwick, J.W., Dulk, G.A. 1964, *Science*, 145, 380.
- Warwick, J.W., Dulk, G.A. 1968, *World Data Center A, Report UAG-3*.
- Warwick, J.W., Gordon, M.A. 1965, *Radio Science*, 69D, 1537.
- Williams, D.J., Mead, G.D. 1965, *J.G.R.* 70, 3017.
- Wilson, R.G., Warwick, J.W., and Libby, W.F. 1968, *Nature*, 22D, 1215.
- Witting, J.M. 1966, *Astrophys. J.*, 71, 187, (abstract).

## APPENDIX I

Stix (1960) shows that the dielectric tensor is given by:

$$K_{ij} = S_{ij} + 4\pi i \frac{Nec}{\omega B_0} \sum_k z_k M_{ij}^k, \quad (1)$$

where  $k$  is the species index,  $z_k$  is the species charge, and  $M$  is the "mobility tensor" given below. It is assumed that the zero order distribution function for each species is a two-temperature Maxwellian with zero mean velocities. (The effect of introducing drift velocities is simply to Doppler-shift some of the frequency terms of  $K_{ij}$ . For phase velocities much larger than the drift velocities, the drifts are negligible.)

Let the parallel and perpendicular temperatures be  $T_{||}$  and  $T_{\perp}$  respectively. Let  $\tau = T_{||}/T_{\perp}$ . The coordinate system is rotated such that the propagation vector lies in the  $xz$  plane;  $\Omega$  is gyrofrequency;  $K$  is the Boltzmann constant;  $m$  is the particle mass, and  $\lambda = k_x^2 K T_{\perp} / m \Omega^2$ . We suppress species subscripts in the expansion of  $M_{ij}$ .

$$M_{11} = \sum_{n=-\infty}^{\infty} n^2 \frac{I_n(\lambda)}{\lambda} e^{-\lambda} A_n$$

$$M_{12} = -M_{21} = iz \sum_{n=-\infty}^{\infty} n (I_n(\lambda) - I_n'(\lambda)) e^{-\lambda} A_n$$

$$M_{22} = \sum_{n=-\infty}^{\infty} \left( n^2 \frac{I_n(\lambda)}{\lambda} + 2\lambda (I_n(\lambda) - I_n'(\lambda)) \right) e^{-\lambda} A_n$$

$$M_{13} = M_{31} = \sum_{n=-\infty}^{\infty} n I_n(\lambda) e^{-\lambda} C_n$$

$$M_{23} = -M_{32} = z \sum_{n=-\infty}^{\infty} (I_n(\lambda) - I_n'(\lambda)) e^{-\lambda} C_n$$

$$M_{33} = (k_x/k_z) \sum_{n=-\infty}^{\infty} \frac{I_n(\lambda)}{\lambda} e^{-\lambda} (1 + n\Omega/\omega) C_n$$

$I_n(\lambda)$  is the modified Bessel function of the first kind of degree  $n$ .

$$A_n = (\Omega z/k_z \tau) \left( \tau \sqrt{\frac{m}{2KT_{11}}} F(a_n) - \frac{1}{2} (1-\tau) \frac{k_z}{\omega} F'(a_n) \right)$$

$$C_n = (k_x z/2k_z \tau) (1 + (1-\tau) n\Omega/\omega) F'(a_n)$$

$$a_n = \sqrt{\frac{m}{2KT_{11}}} (\omega + n\Omega)/k_z$$

$$F(a_n) = -\frac{j}{\sqrt{\pi}} \oint \frac{e^{-z^2}}{z-a_n} dz,$$

where the contour of integration extends from  $z = -\infty$  to  $z = +\infty$  and encircles from below if

$\text{Re} k_z < 0$  and from above if  $\text{Re} k_z < 0$ . For the former contour,  $F$  is related to other tabulated functions  $w$  and  $Z$ :

$$\pi^{-1/2} F(z) = w(z) = e^{-z^2} \text{erfc}(-iz),$$

(Fadeeva and Terent'ev, (1954)

$$iF(z) = Z(z) \quad (\text{Fried and Conte, 1961}).$$

The long-wavelength, low frequency approximation to the dielectric tensor is obtained by expanding the Bessel functions in powers of  $\lambda$ :

$$I_n(\lambda) = (\lambda/2)^n (1/n! + \lambda^2/4(n+1)! + \dots) \text{ for } n \geq 0$$

$$I_n(\lambda) = I_{-n}(\lambda), \text{ } n \text{ integral.}$$

The first terms in the expansion of the  $M_{ij}$  are:

$$M_{11} = (A_1 + A_{-1})/2$$

$$M_{12} = -M_{21} = iz(A_{-1} - A_1)/2$$

$$M_{22} = (A_1 + A_{-1})/2$$

$$M_{13} = M_{31} = \frac{1}{2}\lambda (C_1 - C_{-1})$$

$$M_{23} = -M_{32} = z C_0$$

$$M_{33} = (k_x/k_z \lambda) C_0$$

The required combinations of A's and C's are, explicitly:

$$\frac{1}{2} (A_1 \pm A_{-1}) = \frac{z}{2} \left\{ \frac{\Omega}{k_z V_{||}} \left[ F \left( \frac{\omega + \Omega}{k_z V_{||}} \right) \pm F \left( \frac{\omega - \Omega}{k_z V_{||}} \right) \right] - \frac{\Omega}{\omega} \frac{1 - \tau}{2\tau} \left[ F' \left( \frac{\omega + \Omega}{k_z V_{||}} \right) \pm F' \left( \frac{\omega - \Omega}{k_z V_{||}} \right) \right] \right\}$$

$$\frac{\lambda}{2} (C_1 - C_{-1}) = \frac{z k_x^3 K T}{4 k_z m \Omega^2 \tau} \left\{ \left[ F' \left( \frac{\omega + \Omega}{k_z V_{||}} \right) - F' \left( \frac{\omega - \Omega}{k_z V_{||}} \right) \right] + \frac{\Omega}{\omega} (1 - \tau) \left[ F' \left( \frac{\omega + \Omega}{k_z V_{||}} \right) + F' \left( \frac{\omega - \Omega}{k_z V_{||}} \right) \right] \right\}$$

$$C_0 = \frac{k_x}{2 k_z \tau} F' \left( \frac{\omega}{k_z V_{||}} \right)$$

We have utilized the thermal velocity,  $V_{||} \equiv (2KT_{||}/m)^{1/2}$  for simplicity. At this point it becomes necessary to make a further approximation. Assume that  $\Omega/k_z V_{||} \gg 1$ . This is equivalent to requiring that the wavelength be much greater than the gyroradius. Couple this to the assumption that  $\omega \ll \Omega$  and we are able to use the asymptotic form of F:

$$F(x) \rightarrow \sqrt{\pi} \frac{k_z}{|k_z|} e^{-x^2} + i \left( \frac{1}{x} + \frac{1}{2x^3} + \dots \right) \approx \frac{i}{x}$$

$$\text{Thus } F \left( \frac{\omega + \Omega}{k_z V_{||}} \right) + F \left( \frac{\omega - \Omega}{k_z V_{||}} \right) \approx -2ik_z V_{||} \omega / \Omega^2$$

$$\text{and } F\left(\frac{\omega+\Omega}{k_z V_{||}}\right) - F\left(\frac{\omega-\Omega}{k_z V_{||}}\right) \approx 2ik_z V_{||}/\Omega$$

$$F'\left(\frac{\omega+\Omega}{k_z V_{||}}\right) + F'\left(\frac{\omega-\Omega}{k_z V_{||}}\right) \approx -2ik_z^2 V_{||}^2/\Omega^2$$

$$F'\left(\frac{\omega+\Omega}{k_z V_{||}}\right) - F'\left(\frac{\omega-\Omega}{k_z V_{||}}\right) \approx -2i(k_z^2 V_{||}^2/\Omega^2)(2\omega/\Omega)$$

$$\frac{1}{2}(A_1 + A_{-1}) = iz\frac{\omega}{\Omega} \left[ 1 - \frac{1-\tau}{2\tau} \frac{k_z^2 V_{||}^2}{\omega^2} \right]$$

$$\frac{1}{2}(A_1 - A_{-1}) = iz \left[ 1 + \frac{1-\tau}{\tau} \frac{k_z^2 V_{||}^2}{\Omega^2} \right]$$

$$\frac{\lambda}{2}(C_1 - C_{-1}) = -iz\frac{k_z}{k_x} \left(\frac{k_x V_{||}}{\Omega}\right)^4 \frac{\omega}{\Omega} \left[ 1 + \frac{\Omega^2}{2\omega^2} (1-\tau) \right]$$

The expression for  $C_0$  cannot be simplified by this technique, since  $\omega/k_z V_{||}$  is not necessarily very large. In fact it can be of the order of unity.

We may now insert the above expressions into equation (1) to obtain:

$$K_{11} \approx K_{22} \approx 1 + 4\pi i \frac{Nec}{\omega B_0} \sum_k \left( -i\frac{\omega}{\Omega} \left[ 1 - \frac{1-\tau}{2\tau} \frac{k_z^2 V_{||}^2}{\omega^2} \right] \right)$$

$$K_{12} = -K_{21} \approx 4\pi i \frac{Nec}{B_0} \sum_k \left( -z \left[ 1 + \frac{1-\tau}{\tau} \frac{k_z^2 V_{||}^2}{\Omega^2} \right] \right)$$

$$K_{13} = K_{31} \approx 4\pi i \frac{Nec}{\omega B_0} \sum_k \left( -i \frac{k_z}{k_x} \left( \frac{k_x V_{||}}{\Omega} \right)^4 \frac{\omega}{\Omega} \right) \left( 1 + \frac{\Omega^2}{2\omega^2} (1-\tau) \right)$$

$$K_{23} = -K_{32} \approx 4\pi i \frac{Nec}{\omega B_0} \sum_k z \frac{k_x}{k_z} \frac{1}{2\tau} F' \left( \frac{\omega}{k_z V_{||}} \right)$$

$$K_{33} \approx 1 + 4\pi i \frac{Nec}{\omega B_0} \sum_k \frac{1}{\tau} \left( \frac{\Omega}{k_z V_{||}} \right)^2 F' \left( \frac{\omega}{k_z V_{||}} \right)$$

Evaluating the sums over species, the low-frequency, long-wavelength approximation to the dielectric tensor may be found. Let  $\sigma_{||} = T_{||}^{(i)}/T_{||}^{(e)}$ ;  $n_z = k_z c/\omega$ ;  $n_x = k_x c/\omega$ ;  $m$  and  $M$  are the electron and proton masses, respectively, and  $k_D = \sqrt{4\pi N e^2 / 2KT_{||} e}$  is the Debye wavenumber.

Then:

$$K_{11} \approx K_{22} \approx 1 + \frac{4\pi NMC^2}{B_0^2} \left[ 1 + \frac{m}{M} + \frac{1}{2} (\sigma_{||} (1-1/\tau_i) + 1-1/\tau_e) \left( \frac{V_{||}^e}{c} \right)^2 n_z^2 \right]$$

$$K_{12} = -K_{21} \approx i \frac{\omega}{\Omega_i} \left( \frac{4\pi NMC^2}{B_0^2} \right) \left( \frac{V_{||}^e}{c} \right)^2 n_z^2 [\sigma_{||} (1-1/\tau_i) - (1-1/\tau_e)]$$

$$K_{13} = K_{31} \approx \left( \frac{\omega}{\Omega_i} \right)^2 \frac{4\pi NMC^2}{B_0^2} \left( \frac{V_{||}^e}{c} \right)^4 n_z n_x^3 \sigma_{||}^2 (1-\tau_i)/2$$

$$K_{23} = -K_{32} \approx \frac{\Omega_i}{\omega} \frac{4\pi NMC^2}{B_0^2} \frac{1}{2} [F'(\omega/k_z V_{||}^i)/\tau_i - F'(\omega/k_z V_{||}^e)/\tau_e]$$

$$K_{33} \approx 1 + i \frac{\Omega_e}{\omega} \frac{k_D^2}{k_z^2} [F'(\omega/k_z V_{||}^e)/\tau_e + \frac{m}{M} F'(\omega/k_z V_{||}^i)/\tau_i]$$

It terms of order  $\omega/\Omega_i$  are neglected in the above expressions, and if we let  $\tau_i = \tau_e = 1$ , there is complete agreement with the low frequency limit of the dielectric tensor calculated by Stepanov (1958). The above form of  $K_{ij}$  is far too complicated for our purposes, so we make the further approximation that terms of order  $(V_{||}^e/c)^2$  are negligible. The neglect of such terms is legitimate, provided that  $n_z$  is not extremely large. This will be found to follow from the solution to the dispersion relation for shear Alfvén waves. In this approximation, we have:

$$K_{11} \approx K_{22} \approx 1 + \frac{4\pi N M C^2}{B_0^2} (1+m/M)$$

$$K_{12} = -K_{21} \approx 0$$

$$K_{13} = K_{31} \approx 0$$

and  $K_{23}$ ,  $K_{32}$ , and  $K_{33}$  are unchanged. Note that in this limit, temperature anisotropies play a role only in the latter three tensor elements. Since these are the only elements left which are related to the plasma analogue of sound waves, while the others are related to the magnetically dominated Alfvén waves, this result is not unexpected.

## APPENDIX II

To the approximation of Appendix I, the wave operator in the sourceless plasma wave equation can be written as:

$$\bar{\mathbf{k}} \times \bar{\mathbf{K}} \times \bar{\mathbf{E}} + \frac{\omega^2}{c^2} \bar{\mathbf{K}} \cdot \bar{\mathbf{E}} = \frac{\omega^2}{c^2} \bar{\mathbf{L}} \cdot \bar{\mathbf{E}},$$

where  $\bar{\mathbf{L}}$  is the matrix:

$$\bar{\mathbf{L}} = \begin{bmatrix} K_{11} - n_z^2 & 0 & n_x n_z \\ 0 & K_{11} - n^2 & K_{23} \\ n_x n_z & K_{32} & K_{33} - n_x^2 \end{bmatrix}$$

We have taken the propagation vector  $\bar{\mathbf{k}}$  to lie in the xz plane. The general form of  $\bar{\mathbf{L}}$  is obtained by a simple rotation in k space. The inverse of  $\bar{\mathbf{L}}$  is given by:

$$\bar{\mathbf{L}}^{-1} = \frac{1}{\phi(\bar{\mathbf{k}}, \omega)} \begin{bmatrix} L_{22}L_{33} + L_{23}^2 & -L_{13}L_{23} & -L_{13}L_{22} \\ L_{13}L_{23} & L_{11}L_{33} - L_{13}^2 & -L_{11}L_{23} \\ -L_{13}L_{22} & L_{11}L_{23} & L_{11}L_{22} \end{bmatrix}$$

where  $\phi(\bar{k}, \omega) = L_{11} L_{22} L_{33} + L_{11} L_{23}^2 - L_{22} L_{13}^2$ .

Now it is appropriate to look at the relative ratios of the elements of these tensors.  $K_{11}$  is of order  $4\pi NMc^2/B_0^2$ , while  $|K_{23}|$  is of order  $\Omega_1/\omega$  times this, and  $|K_{33}|$  is of order  $M\Omega_1^2/k_z^2 (V_{1i})^2$  times the latter. Thus at low frequencies and long wavelengths,

$$K_{11} \ll |K_{23}| \ll |K_{33}|.$$

These inequalities are not always true, since at isolated points in the complex  $\omega$  plane  $K_{23}$  and  $K_{33}$  vanish. However, Barnes (1967) showed in his calculations of Landau damping effects in hydromagnetic waves, that the transverse Alfvén wave is unaffected by the zeros of these quantities. Thus we may legitimately expand our expressions in powers of  $1/K_{33}$  and obtain an approximate solution by neglecting high powers.

It will be shown that  $n_z^2$  is of order  $K_{11}$  for the Alfvén waves. The determinant  $\phi$  of matrix  $L$  is given by:

$$\begin{aligned} \phi(\bar{k}, \omega) = & K_{33} (K_{11} - n_z^2) (K_{11} - n^2) [1 + K_{33}^{-1} (K_{23}^2 / (K_{11} - n^2) \\ & - n_x^2 (1 + n_z^2) / (K_{11} - n_z^2))] \end{aligned}$$

Therefore it is, approximately:

$$\phi(\bar{k}, \omega) \approx K_{33} (K_{11} - n_z^2) (K_{11} - n^2)$$

This vanishes when  $K_{33} = 0$ ,  $n_z^2 = K_{11}$ , or  $n^2 = K_{11}$ . The first zero is associated with the longitudinal ion sound

waves, the second and third zeros are associated with transverse and compressional Alfvén waves.

To the same order of approximation then,

$$\vec{L}^{-1} = \begin{bmatrix} \frac{1}{K_{11} - n_x^2} & 0 & \frac{-n_x n_z}{K_{33} (K_{11} - n_z^2)} \\ 0 & \frac{1}{K_{11} - n^2} & 0 \\ \frac{-n_x n_z}{K_{33} (K_{11} - n_z^2)} & 0 & \frac{1}{K_{33}} \end{bmatrix}$$

### APPENDIX III

The waves produced by the  $K_{33}$  element of the dielectric tensor are heavily dampened by collisionless effects. This is as true in a magnetic field as without one, since  $K_{33}$  depends only on  $k_z$  and does not involve  $B_0$  explicitly. If the collisionless damping effects were neglected, these electrostatic modes would propagate as sound waves along the magnetic field lines.

We may simplify the equations by neglecting temperature anisotropies, which cause negligible effect if they are small. Then in Fried and Gould's (1958) notation,  $K_{33}$  is given by:

$$K_{33} = 1 - \frac{1}{2} \frac{k_d^2}{k_z^2} [Z'(z_i) + Z'(z_e)],$$

where  $Z$  is the plasma dispersion function, and  $z_i$  and  $z_e$  are the phase velocity divided by the ion and electron thermal velocities.

The portion of the wave equation with source,

$$S(\bar{x}, t) = S_0 \delta(\bar{x} - \bar{x}') \delta(t - t'),$$

yielding electrostatic modes  $E$ , is simply:

$$K_{33} E(\bar{k}, \omega) = S_0 e^{-i\bar{k} \cdot \bar{x}' + i\omega t'}$$

Thus the electrostatic wave has the field:

$$E(\bar{x}, t) = \frac{S_0}{(2\pi)^2} \int d^3k \int d\omega \frac{e^{i\bar{k} \cdot (\bar{x} - \bar{x}') - i\omega(t-t')}}{K_{33}(\bar{k}, \omega)}$$

The contour of integration in  $\omega$  is chosen to satisfy causality. No waves can be produced before  $t=t'$ , so for  $t < t'$  the contour is considered to encircle the half-plane containing no zeroes of  $K_{33}$ , and for  $t > t'$ , the contour is altered to encircle all of the poles.

Fried and Gould show that the zeroes of  $K_{33}$  are at points  $\omega_n = z_n |k_z| V_{ii}^i$ ,  $n = 1, 2, 3, \dots$ , where  $\{z_n\}$  is a set of complex numbers in the lower half plane. Thus for  $t > t'$ ,

$$E(\bar{x}, t) = \frac{S_0}{(2\pi)^2} \int d^3k e^{-i\bar{k} \cdot (\bar{x} - \bar{x}')} \frac{1}{2\pi i} \sum_{n=1}^{\infty} \frac{e^{iz_n |k_z| V_{ii}^i (t-t')}}{K'_{33}(\omega_n)}$$

where

$$K'_{33}(\omega_n) = -\frac{1}{2} (k_d^2 / k_z^3 V_{ii}^i) (z''(z_n) + \epsilon z''(\epsilon z_n)),$$

and  $\epsilon$  is the ratio of the ion to the electron thermal speeds.

Note that  $K'_{33}(\omega_n) = 1/c_n k_z^3$  where  $c_n$  is a constant for each  $n$ . Thus we may evaluate  $E$  in terms of these constants:

$$E(\bar{x}, t) = 2\pi i S_0 \delta(x-x') \delta(y-y') X \sum_{n=1}^{\infty} c_n \int_{-\infty}^{\infty} k_z^3 e^{(iz_n |k_z| V_{ii}^i (t-t') - ik_z(z-z'))} dk_z$$

$$= 2\pi i S_0 \delta(x-x') \delta(y-y') \sum_{n=1}^{\infty} 6c_n [S_1^{-4} - S_2^{-4}]$$

where

$$S_{\frac{1}{2}} = -iz_n V_{11}^i (t-t') \pm i(z-z')$$

Thus the electrostatic field drops off in distance as  $(z-z')^{-4}$  and in time as  $(t-t')^{-4}$ . We may therefore neglect the electrostatic waves at large distances from the source even if  $K_{33}$  were not small compared to  $K_{11}$ .

#### APPENDIX IV

When  $K_{23}^{-1}$  and  $K_{33}^{-1}$  are negligible compared to  $K_{11}^{-1}$ , and the propagation vector is in the  $xz$  plane, the wave electric field is given formally by the equation (see Appendices I and II):

$$\bar{E}(\bar{k}, \omega) = \frac{4\pi ic}{\omega} \begin{bmatrix} \frac{1}{K_{11}^{-1} - n_z^2} & 0 & 0 \\ 0 & \frac{1}{K_{11}^{-1} - n^2} & 0 \\ 0 & 0 & 0 \end{bmatrix} \bar{j}_s(\bar{k}, \omega).$$

In order to determine the electric field for an arbitrary  $k$  vector, the matrix must be rotated by means of the rotation matrix  $R(\alpha)$ :

$$R(\alpha) = \begin{pmatrix} \cos \alpha & \sin \alpha & 0 \\ -\sin \alpha & \cos \alpha & 0 \\ 0 & 0 & 1 \end{pmatrix}$$

The quantity  $\alpha$  is the azimuthal angle of the  $k$  vector measured from the  $x$  axis. Let the matrix for  $\alpha = 0$  be  $L(0)$ , and the matrix for arbitrary  $\alpha$  be  $L(\alpha)$ . Then

$$L(\alpha) = R(-\alpha)L(0)R(\alpha),$$

where juxtaposition indicates matrix multiplication.

The resulting expression for  $\bar{E}$  is:

$$\bar{E}(\bar{k}, \omega) = \frac{-4\pi ic}{\omega} \left\{ \frac{1}{2} \frac{1}{K_{11}^{-n_z}{}^2} \begin{pmatrix} \cos^2 \alpha & \sin \alpha \cos \alpha & 0 \\ \sin \alpha \cos \alpha & \sin^2 \alpha & 0 \\ 0 & 0 & 0 \end{pmatrix} \right. \\ \left. + \frac{1}{2} \frac{1}{K_{11}^{-n_z}{}^2} \begin{pmatrix} \sin^2 \alpha & -\sin \alpha \cos \alpha & 0 \\ -\sin \alpha \cos \alpha & \cos^2 \alpha & 0 \\ 0 & 0 & 0 \end{pmatrix} \right\} \bar{j}_s$$

If we write  $\cos \alpha = k_x/k_r$  and  $\sin \alpha = k_y/k_r$ , where  $k_r$  is the radial component of  $\bar{k}$ , the above equation assumes the form:

$$\bar{E}(\bar{k}, \omega) = \frac{-4\pi ic}{\omega k_r^2} \left\{ \frac{1}{2} \frac{1}{K_{11}^{-n_z}{}^2} \begin{pmatrix} k_x^2 & k_x k_y & 0 \\ k_x k_y & k_y^2 & 0 \\ 0 & 0 & 0 \end{pmatrix} \right. \\ \left. + \frac{1}{2} \frac{1}{K_{11}^{-n_z}{}^2} \begin{pmatrix} k_y^2 & -k_x k_y & 0 \\ -k_x k_y & k_x^2 & 0 \\ 0 & 0 & 0 \end{pmatrix} \right\} \bar{j}_s$$

Obviously, the first matrix on the right hand side refers to the shear Alfvén mode which propagates along the field, and the second refers to the compressional mode, which propagates almost spherically. Care must be used in using the second matrix for propagation directions where

$k_z$  is small, since some of the assumptions made in computing this form of the equations would break down in that case. Such problems, however, do not arise in the case of the first matrix.

## APPENDIX V

The wave equation for shear Alfvén waves with a steady, translating current source of magnetic moment  $m$  is

$$\left( \frac{K_{11}}{c^2} \frac{\partial^2}{\partial t^2} - \frac{\partial^2}{\partial z^2} \right) \nabla_T^2 \phi = \frac{4\pi}{c} \frac{\partial}{\partial z} \left( -m_x \frac{\partial}{\partial y} + m_y \frac{\partial}{\partial x} \right) \delta(\bar{x} - \bar{v}t)$$

Let  $\bar{v} = (v, 0, 0)$  so that  $\delta(\bar{x} - \bar{v}t) = \delta(x - vt) \delta(y) \delta(z)$ . The solution to this may be obtained from the Green's functions  $g_1$  and  $g_2$  for the one-dimensional wave equation and the two-dimensional Laplace equation. Let  $g_1$  be the solution to:

$$\left( \frac{1}{u^2} \frac{\partial^2}{\partial t^2} - \frac{\partial^2}{\partial z^2} \right) g_1(z, t; z', t') = \delta(z - z') \delta(t - t').$$

Clearly we have taken  $u^2 = c^2/K_{11}$ .

Let  $g_2$  be the solution to:

$$\left( \frac{\partial^2}{\partial x^2} + \frac{\partial^2}{\partial y^2} \right) g_2(x, y; x', y') = \delta(x - x') \delta(y - y').$$

Then the well-known solutions for  $g_1$  and  $g_2$  are:

$$g_1(z, t; z', t') = \frac{1}{2} u H(-|z-z'| + u(t-t')),$$

$$g_2(x, y; x', y') = \frac{1}{4} \log \left[ (x-x')^2 + (y-y')^2 \right].$$

The function  $H$  is one when its argument is positive and zero when its argument is negative or zero. The solution to the equation

$$\left( \frac{1}{u^2} \frac{\partial^2}{\partial t^2} - \frac{\partial^2}{\partial z^2} \right) G = F(x, y, z, t)$$

is clearly

$$G = \int dz' \int dt' F \cdot g_1.$$

Thus for  $F = \delta(x-vt) \delta(z) \delta(y)$ ,

$$G = \frac{1}{2} \frac{u}{v} \delta(y) H(-|z| + u(t-x/v)).$$

Therefore the function  $\phi$  is obtained from the particular solution to:

$$\left( \frac{\partial^2}{\partial x^2} + \frac{\partial^2}{\partial y^2} \right) \phi = \frac{4\pi}{c} \frac{\partial}{\partial z} \left( -m_x \frac{\partial}{\partial y} + m_y \frac{\partial}{\partial x} \right) G$$

And this is obviously:

$$\phi = \int dx' \int dy' g_2 \cdot \frac{4\pi}{c} \frac{\partial}{\partial z} \left( -m_x \frac{\partial}{\partial y} + m_y \frac{\partial}{\partial x} \right) G$$

From the theory of generalized functions, (Lighthill, 1958),

$$\frac{\partial}{\partial z} H(-|z|+u(t-x/v)) = -\text{sgn}(z) \delta(-|z|+u(t-x/v)).$$

In generalized function theory, integration and differentiation may be interchanged with considerable arbitrariness.

Thus we obtain  $\phi$  in the form:

$$\begin{aligned} \phi(x, y, z, t) &= -\frac{4\pi}{c} \left( -m_x \frac{\partial}{\partial y} + m_y \frac{\partial}{\partial x} \right) \int dx' \int dy' \\ &\quad \frac{1}{4\pi} \log \left[ (x-x')^2 + (y-y')^2 \right] (-u/2v) \text{sgn}(z) \\ &\quad \delta(y') \delta(-|z| + u(t-x'/v)) \\ &= \frac{1}{2c} \text{sgn}(z) \left( -m_x \frac{\partial}{\partial y} + m_y \frac{\partial}{\partial x} \right) \log \left( (x-(ut-|z|)v/u)^2 + y^2 \right) \end{aligned}$$

Applying the  $x$  and  $y$  differential operators, we find the solution for  $\phi$ :

$$\phi = \frac{1}{c} \text{sgn}(z) \frac{-m_x y + m_y (x-vt + v|z|/u)}{(x-vt + v|z|/u)^2 + y^2}$$

## APPENDIX VI

The Alfven wave vector potential is given by:

$$\mathbf{A}_F = \frac{v}{u} \left( -m_x \frac{\partial}{\partial y} + m_y \frac{\partial}{\partial x} \right) F$$

where

$$F = \int d^3 x^1 M(\bar{x}^1) \frac{x-x^1}{(x-x^1)^2 + (y-y^1)^2} / \int d^3 x M(\bar{x})$$

and

$$X = x - vt + v|z|/u$$

$$X^1 = x^1 + vz^1/u$$

The integration is limited to the region  $|\bar{x}^1| < R$  so that  $X^1 \approx x^1$  when  $v \ll u$ . We therefore change to cylindrical coordinates:

$$X = r \cos w,$$

$$y = r \sin w,$$

and similarly for the primed coordinates. We assume that  $M$  is a function only of  $\sqrt{r^2 + z^2}$ , the spherical radius.

Then:

$$F \approx \left( \int r^1 dr^1 \int dz^1 M(r^1, z^1) \int_0^{2\pi} dw^1 \frac{r \cos w - r^1 \cos w^1}{r^2 - 2rr^1 \cos(w-w^1) + (r^1)^2} \right) \\ \div (4\pi \int s^2 M(s) ds)$$

The integral over azimuth  $w^1$  can readily be shown to be:

$$\begin{cases} \frac{2\pi}{r} \cos w & \text{if } r^1 < r \\ 0 & \text{if } r^1 > r \end{cases}$$

Converting  $r^1 dr^1 dz^1$  to spherical coordinates and integrating over co-latitude, we find that:

$$\int r^1 dr^1 dz^1 M(s) \begin{cases} 1, r^1 < r \\ 0, r^1 > r \end{cases} = 2 \int_0^R s^2 ds M(s) \begin{cases} 1 - \sqrt{1 - r^2/s^2}, s > r \\ 1, s < r \end{cases}$$

Therefore

$$F = \frac{\cos w}{r} \begin{cases} 1 - \frac{\int_0^R M(s) s \sqrt{s^2 - r^2} ds}{R} & , r \leq R \\ \int_0^r M(s) s^2 ds & \\ 1 & , r \geq R \end{cases}$$

Letting

$$F = \frac{\cos w}{R} G(r), \text{ we have, finally:}$$

$$A_F = \frac{1}{R} \frac{v}{u} \left( -m_x \frac{\partial}{\partial y} + m_y \frac{\partial}{\partial x} \right) \cos w G(r).$$

where

$$\cos w = \frac{x}{(x^2 + y^2)^{1/2}}$$

## APPENDIX VII

Let

$$A_1 = \frac{\partial}{\partial y} \left( \cos w G(r) \right)$$

$$A_2 = \frac{\partial}{\partial x} \left( \cos w G(r) \right)$$

Then

$$A_F = \frac{1}{R} \frac{v}{u} (-m_x A_1 + m_y A_2).$$

Since the Poynting vector is proportional to  $|\nabla A_F|^2$ , where  $\nabla$  is the two-dimensional gradient, we consider the integrals

$$P_{ij} = \int \nabla A_i \cdot \nabla A_j \, dx dy, \quad i, j = 1, 2.$$

The integral  $P_{12}$  vanishes because  $\nabla A_1$  is a y derivative and  $\nabla A_2$  is an x derivative and integration yields their values at infinity, which are zero.  $P_{11}$  and  $P_{22}$  are another matter. Convert  $\partial/\partial x$  and  $\partial/\partial y$  to cylindrical coordinates  $(r, w)$ . (Note that  $\partial/\partial x = \partial/\partial X$ , so the conversion is legitimate.)

$$\frac{\partial}{\partial x} = -\frac{1}{r} \sin w \frac{\partial}{\partial w} + \cos w \frac{\partial}{\partial r}$$

$$\frac{\partial}{\partial y} = \frac{1}{r} \cos w \frac{\partial}{\partial w} + \sin w \frac{\partial}{\partial r}$$

Then evaluate the quantities:

$$\int_0^{2\pi} dw \left( \left( \frac{\partial A_i}{\partial r} \right)^2 + \frac{1}{r^2} \left( \frac{\partial A_i}{\partial w} \right)^2 \right), \quad i = 1, 2,$$

using the integrals:  $\int \sin^2 w dw = \int \cos^2 w dw =$

$$4 \int \sin^2 w \cos^2 w dw = \frac{4}{3} \int \cos^4 w dw = \frac{4}{3} \int \sin^4 w dw = \pi$$

The results are:

$$\int_0^{2\pi} dw (\nabla A_1)^2 = \frac{\pi}{4} \left( 7 \left[ \left( \frac{G}{r} \right)' \right]^2 + 3 (G'')^2 + 2 \left( \frac{G}{r} \right)' G'' \right)$$

$$\int_0^{2\pi} dw (\nabla A_2)^2 = \frac{\pi}{4} \left( 5 \left[ \left( \frac{G}{r} \right)' \right]^2 + (G'')^2 - 2 \left( \frac{G}{r} \right)' G'' \right)$$

These must be integrated over  $r$  to obtain  $P_{11}$  and  $P_{22}$ .

But first we note that a linear combination of the above forms is a perfect derivative when multiplied by  $r$ .

$$\int_0^{\infty} dr r \int_0^{2\pi} dw \left( 3 (\nabla A_2)^2 - (\nabla A_1)^2 \right) = -\pi \int_0^{\infty} \frac{\partial}{\partial r} (G/r - G')^2 dr$$

It is easily shown that  $G/r - G'$  vanishes at zero and infinity. Thus the radial integral above vanishes. So we have the quite general result.

$$P_{11} = 3 P_{22} = \frac{3\pi}{4} \int_0^{\infty} r dr \left( 5 \left[ \left( \frac{G}{r} \right)' \right]^2 + (G'')^2 - 2 \left( \frac{G}{r} \right)' G'' \right)$$

That is, the moment directed transverse to the direction of motion is three times as effective in generating waves as is the moment directed parallel to the velocity. This integral can be simplified by observing the identity:

$$5r \left( \left( \frac{G}{r} \right)' \right)^2 + r \left( G'' \right)^2 - 2r \left( \frac{G}{r} \right)' G'' =$$

$$r \left\{ 3 \left[ \left( \frac{G}{r} \right)' \right]^2 + r^2 \left[ \left( \frac{G}{r} \right)'' \right]^2 \right\} + \frac{\partial}{\partial r} \left\{ r^2 \left[ \left( \frac{G}{r} \right)' \right]^2 \right\}$$

The argument of the derivative on the right hand side vanishes at zero and infinity. This is easily seen from the integral expression for  $G(r)$ . Thus the expressions for  $P_{11}$  and  $P_{22}$  reduce to:

$$P_{11} = 3 P_{22} = \frac{3\pi}{4} \int_0^{\infty} r dr \left\{ 3 \left[ \left( \frac{G}{r} \right)' \right]^2 + r^2 \left[ \left( \frac{G}{r} \right)'' \right]^2 \right\}$$

Non-dimensionalize by letting  $s = r/R$  and let  $f(s) = R^2(G/r)'$ . Then

$$P_{11} = 3 P_{22} = \frac{3}{4} \frac{1}{R^2} \int_0^{\infty} s ds \left( 3f^2 + s^2(f')^2 \right)$$

This form is particularly suitable for application of the Calculus of variations to find the minimum value of the integral. First of all note that  $G(s)$  (and hence  $f$ ) is known for  $s \geq 1$ .  $G(s) = 1/s$  so  $f(s) = -2/s^3$ . Continuity requires that  $f(1) = -2$ . Also the behavior of  $G$  at  $s = 0$

implies that  $f(0) = 0$ . These two conditions are needed as boundary conditions for determination of the minimum of the above integral. The extremum of this integral is obtained from the Euler equation:

$$\frac{d}{ds} \left( s^3 \frac{df}{ds} \right) - 3sf = 0$$

The solution is

$$f(s) = c_1 s + c_2 s^{-3}$$

Clearly for  $s < 1$ ,  $c_2 = 0$  and for  $s > 1$ ,  $c_1 = 0$ . (Note that this gives the function  $f(s)$  for  $s > 1$  as it actually is.  $Gr(s)$  for  $s > 1$  is of the form that minimizes the portion of the integral for  $s > 1$ .) When we match the boundary condition at  $s = 1$ ,  $f(s) = -2s$ . Inserting this function into the integral yields the extremum (which obviously is a minimum):

$$P_{11} = P_{22} \geq 6\pi/R^2$$

It is instructive to compute  $Gr(s)$  and its derivatives for examples of  $M(r)$ .

$$\text{Case (a) Let } M(s) = \begin{cases} 1-s^2 & s < 1 \\ 0 & s > 1 \end{cases}$$

$$\begin{aligned} \text{Then } Gr(s) &= \frac{1}{s} \begin{cases} 1 - \frac{\int_s^1 (1-r^2)r(r^2 - s^2)^{1/2} dr}{\int_0^1 (1-r^2)r^2 dr} & , s < 1 \\ 1 & , s > 1 \end{cases} \\ &= \begin{cases} \left[ 1 - (1-s^2)^{5/2} \right] / s & , s < 1 \\ 1/s & , s > 1 \end{cases} \end{aligned}$$

For  $s < 1$  the first and second derivatives are:

$$G^{\prime}(s) = - \left( 1 - (1-s^2)^{3/2} (1 + 4s^2) \right) / s^2$$

$$G^{\prime\prime}(s) = 2 \left( 1 - (1-s^2)^{1/2} \left( 1 + \frac{1}{2}s^2 + 6s^2 \right) \right) / s^3$$

Note that  $G$ ,  $G^{\prime}$  and  $G^{\prime\prime}$  are finite at  $s = 0$  and continuous with the corresponding derivatives of  $1/s$  at  $s = 1$ .

$$\text{Case (b) Let } M(s) = \begin{cases} 1-s^6 & s < 1 \\ 0 & s > 1 \end{cases}$$

$$\begin{aligned} \text{Then } Gr(s) &= \frac{1}{s} \begin{cases} 1 - \frac{\int_0^1 (1-r^6) r (r^2-s^2)^{1/2} dr}{\int_0^1 (1-r^6) r^2 dr} & , s < 1 \\ 1 & , s > 1 \end{cases} \\ &= \begin{cases} \left( 1 - (1-s^2)^{5/2} \left( 1 + \frac{4}{7}s^2 + \frac{8}{35}s^4 \right) \right) / s & , s < 1 \\ 1/s & , s > 1 \end{cases} \end{aligned}$$

The first and second derivatives are:

$$G^{\prime}(s) = - \left( 1 - (1-s^2)^{3/2} \left( 1 + \frac{8}{7}s^2 + \frac{12}{5}s^2 + \frac{8}{5}s^4 \right) \right) / s^2$$

$$G^{\prime\prime}(s) = 2 \left( 1 - (1-s^2)^{1/2} \left( 1 + \frac{1}{2}s^2 + \frac{83}{70}s^4 + \frac{163}{70}s^6 + \frac{192}{35}s^8 \right) \right) / s^3$$

Again,  $G$ ,  $G^{\prime}$ , and  $G^{\prime\prime}$  are finite at the origin and continuous with  $1/s$  and its derivatives at  $s = 1$ .

These functions have been coded and integrated on the Olivetti Programma 101, yielding for the integral

$$\int_0^1 s \, ds \left( 3 \left( \frac{G}{s} \right)' \right)^2 + s^2 \left( \frac{G}{s} \right)''^2$$

the values:

$$\text{Case (a)} \quad 14.540$$

$$\text{Case (b)} \quad 7.071$$

These are, respectively, 7.27 and 3.13 times the theoretical minimum value of 4 for the integral.

The final form for the Alfvén power is

$$P = \frac{u}{4\pi} \left( \frac{1}{R} \frac{v}{u} \right)^2 \int dx \int dy \left( m_x^2 (\nabla A_1)^2 + m_y^2 (\nabla A_2)^2 \right)$$

$$= \frac{1}{4\pi} \frac{v^2}{u} \frac{1}{R^2} (3m_x^2 + m_y^2) P_{22}$$

$$P = \frac{1}{16} \frac{v^2}{u} \frac{1}{R^4} (3m_x^2 + m_y^2) \int_0^\infty s \, ds (3f^2 + s^2 (f')^2)$$

$$\text{where} \quad f(s) = (G(s)/s)'$$

## APPENDIX VIII

Let a magnetic dipole lie at the origin of a Cartesian coordinate system with its moment  $M$  lying in the  $xz$  plane, tilted at an angle  $\alpha$  with respect to the  $z$  axis. The components of the magnetic field are:

$$B_x = \frac{M}{r^5} \left( 3 \cos\alpha (x \cos\alpha - z \sin\alpha) (z \cos\alpha + x \sin\alpha) + (3(z \cos\alpha + x \sin\alpha)^2 - r^2) \sin\alpha \right)$$

$$B_y = \frac{M}{r^5} 3y(z \cos\alpha + x \sin\alpha)$$

$$B_z = \frac{M}{r^5} \left[ \left( 3(z \cos\alpha + x \sin\alpha)^2 - r^2 \right) \cos\alpha - 3(z \cos\alpha + x \sin\alpha)(x \cos\alpha - z \sin\alpha) \sin\alpha \right]$$

where  $r^2 = x^2 + y^2 + z^2$ .

Consider the field components measured on a circle centered at  $(x, y, z) = (-x_N, -y_N, -z_N)$ , lying parallel to the  $xy$  plane, and having radius  $R$ .

The locus of that circle in terms of parameter  $\phi$ , which corresponds to the azimuth measured from the  $xz$  plane, is given by:

$$x = -x_N + R \cos\psi$$

$$y = -y_N + R \sin\psi$$

$$z = -z_N$$

$$\text{and } r^2 = R^2 + 2R(x_N \cos\psi + y_N \sin\psi) + r_N^2$$

$$\text{where } r_N^2 = x_N^2 + y_N^2 + z_N^2$$

If we assume that  $|\sin\alpha| \ll 1$  and  $r_N \ll R$ , we may neglect terms of second order in these quantities. Convert to spherical polar coordinates with  $z$  the polar axis  $\theta = 0$ , and azimuth  $\phi$  is measured from the  $x$  axis.

$$B_x = \frac{M}{r^3} \left[ 3 \cos\phi (\cos\theta + \cos\phi \sin\alpha) - \sin\alpha \right]$$

$$B_y = \frac{M}{r^3} \left[ 3 \sin\phi (\cos\theta + \cos\phi \sin\alpha) \right]$$

$$B_z = \frac{-M}{r^3}$$

where  $r = R - (x_N \cos\psi + y_N \sin\psi)$  to first order.

Expand  $r^{-3}$  to first order in  $x_N$  and  $y_N$ , and let  $R_N$  be the distance of the dipole from the  $z$  axis.

$$R_N^2 = x_N^2 + y_N^2$$

Then to first order,  $\psi = \phi$ , and the fields are:

$$B_x = \frac{M}{R^3} \left[ (3 \cos^2\phi - 1) \sin\alpha - 3 \frac{z_N}{R} \cos\phi \right]$$

$$B_y = \frac{M}{R^3} \left[ 3 \sin\phi \cos\phi \sin\alpha - 3 \frac{z_N}{R} \sin\phi \right]$$

$$B_z = \frac{-M}{R^3} \left[ 1 + 3 (x_N \cos\phi + y_N \sin\phi) / R \right]$$

The mean values of these quantities over  $0 < \phi \leq 2\pi$  are:

$$\langle B_x \rangle = \frac{1}{2} \frac{M}{R^3} \sin\alpha$$

$$\langle B_y \rangle = 0$$

$$\langle B_z \rangle = \frac{-M}{R^3}$$

Therefore the fluctuating parts of the field are:

$$\delta B_x \equiv B_x - \langle B_x \rangle = \frac{3M}{R^3} \left[ \frac{-z_N}{R} \cos\phi + \frac{1}{2} \sin\alpha \cos 2\phi \right]$$

$$\delta B_y \equiv B_y - \langle B_y \rangle = \frac{3M}{R^3} \left[ \frac{-z_N}{R} \sin\phi + \frac{1}{2} \sin\alpha \sin 2\phi \right]$$

$$\delta B_z \equiv B_z - \langle B_z \rangle = \frac{-3M}{R^3} \left[ \frac{x_N}{R} \cos\phi + \frac{y_N}{R} \sin\phi \right]$$

The azimuthal ( $\phi$ ) and radial (R) components of these fluctuating parts are:

$$\delta B_\phi = \delta B_x \cos\phi + \delta B_y \sin\phi,$$

$$\delta B_R = -\delta B_x \sin\phi + \delta B_y \cos\phi.$$

Explicitly,

$$\delta B_{\phi} = \frac{3M}{R^3} \left( \frac{-z}{R} + \frac{1}{2} \sin \alpha \cos \phi \right),$$

$$\delta B_R = \frac{3}{2} \frac{M}{R^3} \sin \alpha \sin \phi.$$

## APPENDIX IX

In the following, let  $u_0 = B/(4\pi NM)^{1/2}$ .  $U_0$  is the Alfven speed in the limit of infinite light speed. We assume that density is constant and desire to calculate the quantities

$$K_1 = u_0^{-1/2} \frac{d}{ds}(u_0^{1/2}) = B^{-1/2} \frac{d}{ds} B^{1/2}$$

and

$$K_2 = u_0^{-1/2} \frac{d^2}{ds^2}(u_0^{1/2}) = B^{-1/2} \frac{d^2}{ds^2} B^{1/2}$$

where  $s$  is arc length measured along a field line. For convenience we parametrize spherical coordinates as follows:

$$r = L(1-t^2)$$

$$\sin \theta = (1-t^2)^{1/2}$$

Then the dipole field is given by:

$$B_r = 2 B_1 t(1-t^2)^{-3}$$

$$B_\theta = B_1 (1-t^2)^{-5/2},$$

where  $B_1$  is constant on a field line. The line element is given by:

$$(ds)^2 = (dr)^2 + r^2(d\theta)^2 = L^2(1 + 3t^2)dt$$

For small departures from the magnetic equatorial plane,

$$s = L(t + 1/2 t^3 + \dots)$$

The exact forms of  $K_1$  and  $K_2$  turn out to be:

$$K_1 = \frac{-9}{2} \frac{t}{L} (1 + \frac{5}{3}t^2) (1 + 3t^2)^{-3/2} (1-t^2)^{-1}$$

and

$$K_2 = \frac{9}{2} \frac{1}{L^2} (1 + \frac{37}{6}t^2 + \frac{118}{9}t^4 + \frac{45}{2}t^6) (1 + 3t^2)^{-3} (1-t^2)^{-2}$$

The critical frequency was obtained from the WKB form of the Alfvén wave equation for curved lines of force:

$$\omega_c = u^{-1} \left( u^{-1/2} \frac{d^2 u^{1/2}}{ds^2} \right)^{1/2},$$

where  $u$  is the Alfvén velocity equal to  $c/(1+c^2/u_0^2)^{1/2}$ .

By differentiating we find:

$$u^{-1/2} \frac{d^2 u^{1/2}}{ds^2} = (u/u_0)^2 (K_2 - 5u^2 K_1^2/c^2)$$

If we expand  $K_1$  and  $K_2$  to order  $t^2$  and substitute  $s$  to order  $s^2$ , we find:

$$u^{-1/2} \frac{d^2 u^{1/2}}{ds^2} = (u/u_0)^2 \left( \frac{9}{2} \frac{1}{L^2} (1 - \frac{5}{6}t^2) - \frac{5u^2}{c^2} \left( \frac{81}{4} \frac{t^2}{L^2} \right) \right)$$

Therefore

$$\omega_c = \frac{1}{u_0} u^2 \frac{3}{2L} \left( 1 - \frac{5}{6} \frac{s^2}{L^2} - \frac{45}{2} \frac{u^2}{c^2} \frac{s^2}{L^2} \right)^{1/2}$$

This equation is approximately true for  $s < L/4$ . This covers the range of the field lines where the curvature is greatest.